University University

Thermofisher Scientific

INNER SHELL SPECTROSCOPY AND RELATIVISTIC ATOM IONIZATION CROSS SECTION BY ELECTRON IMPACT

Author:
Valerii Brudanin

July, 2023

Abstract

The elemental composition of materials in the Transmission Electron Microscope is probed by inner shell ionization of atoms by a high energetic electron beam. Proper elemental quantification of the material requires detailed knowledge of the electron-atom differential ionization cross section (DCS). In the current work, the cross section is calculated in the context of relativistic quantum mechanics. Relativistic effects become important due to the high energy of the electron beam. The atomic dynamics is calculated in a fully relativistic setting, using Dirac-Hartree-Fock (DHF) solutions for the atomic bound and continuum wavefunctions. The relaxation of the atom due to the ionization by the beam needs to be taken into account. To address this, a continuum wave is computed in a self-consistent field of an ion. Non-orthogonality between atomic and ionic wavefunctions leads to additional corrections. They are shown to be important at low energy of the ionized electron which is particularly interesting for materials with elements which have close ionization energies.

Acknowledgements

By the end of this project, which was, by no means, a simple task, I want to say several words of gratitude to people, whose presence allow me to keep pushing whatever it takes.

First, of no surprise, I am very grateful to my supervisor Ioannis Iatrakis, who consistently guided me to the proper direction. I appreciate very much the whole support I am getting from you, which goes far beyond the research. I would also like to thank my university advisor Umut Gursoy, who gave me this idea to do my thesis in a company.

Second, thanks to my colleges from the company for their participation. I got a lot of assistance with all kinds of formalities from my project manager Frederic Bernardo, and experimental data used in the project was provided by Christoph Mitterbauer.

Third, I am glad to have a family, that motivated me to go to Utrecht University and was always there to support me in heavy times.

Finally, I am happy to know my physicist friends, who, being scattered around the globe, stay in touch with me. I get most of my inspiration from your achievements. I know that we all are capable of fantastic things. Special gratitude to Daria Orekhova, Alexander Nikolaev, Timur Kadyrov and Anna Tsehanovich.

Contents

1 Introduction

Recent technological achievements in material science and engineering allow for a creation of more and more sophisticated devices, designated for material analysis. One such a device is a transmission electron microscope, which makes it possible to obtain atomic resolution images of the investigated sample, using the diffraction of electrons on atoms. Moreover, studying other types of electron-atom interactions, it is possible to probe chemical properties of the material [5, 7, 6].

One of the most intriguing possibilities is to obtain quantitative information about the amount of a particular chemical element within a chosen area of the sample. This opens possibilities for research in various areas, such as sciences and semiconductor industry. However, to conduct such a quantification, it is necessary to process advanced theoretical models for the analysis of particular processes, occurring while electron passes through the material. A powerful source of information about the composition of a sample is a spectrum of energy loss of incoming electrons [7]. Inelastic scattering of the electron with the material leads to some energy loss which does not always contain tractable physical information about the material structure. However, the incoming electron transfers sufficient amount of energy to ionize an inner shell of the atom [16, 25, 13].

The probability of the process is element specific and depends on the wavefunctions of atomic electrons, as well as the interaction with of incoming beam electrons. The computation of atomic wavefunctions is analytically impossible due to the electron-electron interaction and requires heavy numerical procedures to be involved [14, 3, 10]. Atomic wavefunctions can be approximated by a calculation of an one electron problem in some effective central potentials [4, 15]. Nevertheless, there exists a method to obtain more reliable atomic wavefunctions using the Dirac-Hartree-Fock(DHF) method [14]. In principle, extensions of this method, that include multiple configurations or many body perturbative corrections allow to obtain atomic wavefunctions with higher precision [4, 3, 14, 12]. Nowadays, it is computationally feasible to obtain DHF solutions for all the elements even on a personal computer and longer computations for corrections can, if necessarily, be performed on clusters.

This work is devoted to improving the theoretical calculation of differential ionization cross section which can be used for elemental quantification of materials in TEM. Cross sections are obtained within framework of Dirac-Hartree-Fock with relaxation, which accounts for the changes of electron structure of the atom after the ionization, [2, 11, 9]. Ab initio calculations allow us to have controled framework for those calcualtions and determine the range of applicability and . Many Body Perturbation theory and variational approach allow for the improvement of results in cases, where they are not sufficiently close to the experiment.

2 Spectroscopy in TEM

2.1 Transmission electron microscopy

Transmission electron microscopy (TEM) is a method for investigation materials using a high energy electron beam, which passes through the material, interacting with it [5, 7, 6]. There are two types of phenomena that can occur inside the electron microscope: elastic and inelastic scattering. Elastic scattering can first of all be used to obtain high resolution images of the sample up to atomic scales. As an electron De Broglie wave length is much less than that of the visible light, it is possible to achieve much higher image detailing resolution. Inelastic scattering in contrast allows to obtain the information about the chemical composition of the sample, measuring the excitations of the system as a result of inelastic interactions: atomic excitation and relaxation. Two main kinds of spectroscopy are used in TEM, the X-ray energy-dispersive spectroscopy (XEDS or just EDS) and electron energy loss spectroscopy (EELS). They will be both discussed in details below.

The electron microscope can be operated in two essential modes: the TEM mode and the STEM mode. In the first case, the sample is illuminated with a broad parallel electron beam and observe the diffraction pattern of all the scattered electrons. This is a direct analog of the visible light or X-ray microscopy due to the wave nature of electron. Another mode is called scanning transmission electron microscopy (STEM). In this mode the electron beam is focused on a small area of the sample and then is moved over the surface, allowing for scanning the specimen point by point, hence the naming. This mode is particularly useful as it allows to investigate local properties of the sample. Recovering the distribution of the elemental composition of the sample. With the usage of EDS or EELS it becomes possible to create an elemental map of the sample, examples are in a figure below.

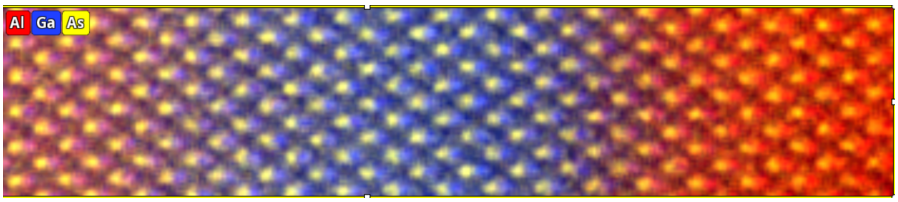

Figure 1: Elemental map of AlGaAs. Internal ThermoFisher Scientific Data

2.2 Motivation to use electrons

There are several reasons that using electrons turn out to be more and more beneficial than using light. Using high energy X-rays we can also achieve very high resolution. In principle X-ray crystallography is still the most common way to determine protein structures. However, X-rays are much harder to manipulate and we need synchrotrons to produce them. Moreover, there are no good X-ray lenses, so such techniques as STEM are impossible with X-rays. Another point is that interaction of light with matter is much weaker than that of electrons. In some cases this can even be beneficial, for example for studying of biological samples, which are easily damaged with high energy electrons. The disadvantage is that to obtain a clear picture there is a need in a significant amount of a specimen under investigation in a crystallized form - only then we have enough scattering to get a good diffraction

pattern. Growing crystals of big molecules, such as proteins, is an extremely complicated and time consuming task, so there is a tendency to use TEMs more and more even in biological studies. Finally, with TEMs we can exploit some unique spectroscopic techniques. While EDS is a direct analog of X-ray absorbion spectroscopy (XAS), there is no X-ray technique similar to EELS. Overall, electron microscopes win due to their relatively small sizes, universality and easiness to control.

2.3 Composition of the electron microscope

Transmission electron microscope is an extremely complex and expensive device [5]. The main components of each electron microscope are source of fast electrons, directing electromagnetic lenses, sample holder and spectrometers or screens to gather electrons.The composition of the microscope, as well as various processes that occur during the electron interaction with a specimen, are shown in the Figure 2

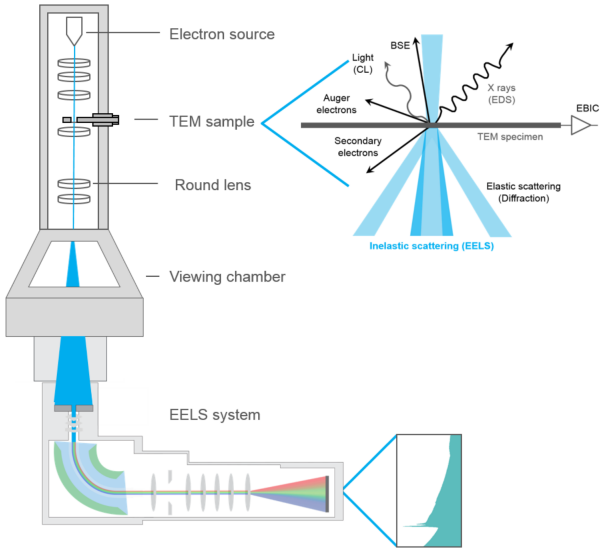

Figure 2: Principal scheme of the microscope and electron-sample interaction https://eels.info/about/overview

2.3.1 Electron source

There are two possible kinds of sources used in TEM - thermoionic sources and and field-emission sources (FEG). The first emit electrons under the heating up to high temperatures, while the second exploit the phenomenon of quantum tunneling of electrons exposed to high electric fields. To achieve necessarily high fields, needles of FEGs are done as thin as possible, up to a single atom on the tip.

2.3.2 Electromagnetic lenses

To focus the electron beam, electrostatic and magnetic lenses are used. Electrostatic lenses rely on the creating of the inhomogeneous electric field. In practice, magnetic lenses are much more widespread. Their simple configuration is shown in the picture below.
The idea of magnetic lenses is the following: initial deviation of the electron velocity from the parallel to the optical axis makes it accelerate in the magnetic field in the plane perpendicular to the optical axis. This velocity in the perpendicular plane then creates Lorentz force, which pushes electron back to the axis. As a result electron moves in a spiral close to the axis. Despite many analogies being made between optical and electromagnetic lenses, due to the complex paths of the electrons in the latest, they are far more subjected to aberrations. Spherical aberration is the main limiting factor of the TEM resolution, making it to become two orders of magnitude less than limited by diffraction.

2.3.3 Spectrometers

A detector for X-rays in TEM is mainly composed of a semiconductor diode (typically silicon). High-energy X-rays excite multiple electron-hole pairs while passing through the medium. The electrons and holes can be separated by applying a voltage between the cathode and anode, which results in the current flowing through the detector. The number of electron-hole pairs excited is proportional to the energy of the incoming X-ray, as well as to the full charge flowed thorough the circuit. So, measuring the charge, we can obtain information about the incoming x-ray.

X-ray detectors though highly efficient have a number of flaws. They can not operate equally efficiently in the whole energy range. There are two major reasons for this. The first is absorption of low-energy X-rays in the dead layer (areas near electrodes, where electron-holes recombine faster than separated) or in the protective window (thin layers of materials, sealing the entrance to the detector and preventing it from chemical contamination). The second is that cross section of the medium becomes smaller with the growth of X-ray energy and eventually stops capturing all the entering X-rays. Typical detector efficiency is plotted in the figure below.

The way of detection of X-ray generating electron-holes is very fast, allowing for measuring thousands of electrons per second. For the X-ray spectroscopy this is of crucial importance, as there are not so many X-rays generated for small atoms due to the low fluorescence yield and for heavy atoms due to the low differential cross sections of inner shells excitation. Also detector takes only a part of the full solid angle X-ray radiation, what aggravates the problem of low counts. However, significant drawbacks of silicon detectors is that generation and detection of electron-holes is a stochastic process, with a sufficiently big dispersion. The energy resolution of silicon detectors is of order of 100 eV, which makes it almost impossible to separate close peaks. This is known to be the biggest limitation of XEDS.

Electron spectrometer in EELS is just a magnetic lens. It focuses electrons of the same energy to the same point on the detector independently of their initial direction (up to aberrations), while electrons with different energies are focused to the different points of the detector. Resolution of EELS spectrometers is about 1 eV.

2.4 Inelastic scattering

Main scattering processes that account for the electron energy loss are low energy excitation of outer electrons - intraband transitions and plasmons, collective excitation of atoms - phonons and inner electrons transitions to the conduction band or the continuum (i.e. ionization). Another reason for energy loss, which contributes significantly, is the emission of electromagnetic waves by an accelerated electron, so-called bremsstrahlung radiation. As plasmons and intraband transitions have small energies of order $< 50eV$. They constitute the so-called low loss part of the spectra. Another process, which is central for the material quantification and which is this whole work about, is an excitation or ionization of inner atomic electrons. This process is orders of magnitude less probable than low loss excitations.

2.5 X-ray energy-dispersive spectroscopy

One of the processes, which occurs in the sample while being hit by beam electrons is an excitation of inner atomic electrons to higher energy levels or to the continuum. Excited atom can then relax by filling the hole with an electron from a higher level. This process frees energy, which can escape from the atom with an X-ray [6] or another electron from higher level (so-called Auger electron). XEDS is based on measuring of the energy of the characteristic X-rays. A scheme of X-ray emission and an example of an XEDS spectrum are shown in the Figures 3 and 4

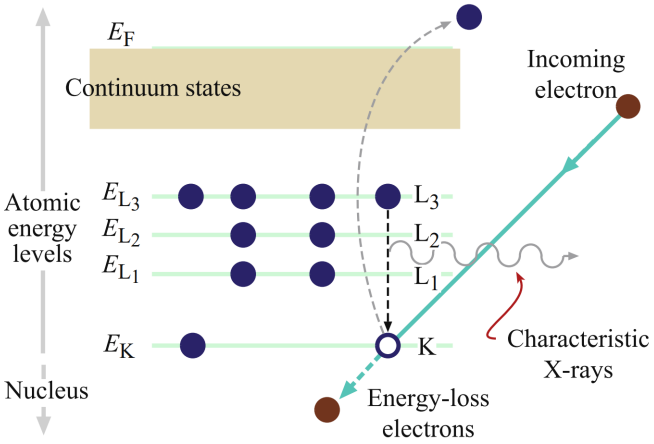

Figure 3: X-ray emission in atomic systems
Transmission Electron Microscopy, D. B. Williams, C. B. Carter

Due to the simplicity of X-ray detection and their relatively straightforward correspondence to the particular atomic processes XEDS was historically the first spectroscopic method implemented in TEM, and now it is built-in in every standard electron microscope. Measuring and characterisation of outgoing Auger electrons is also possible but significantly more involved, so such experiments are only conducted on the specific devices in academia.

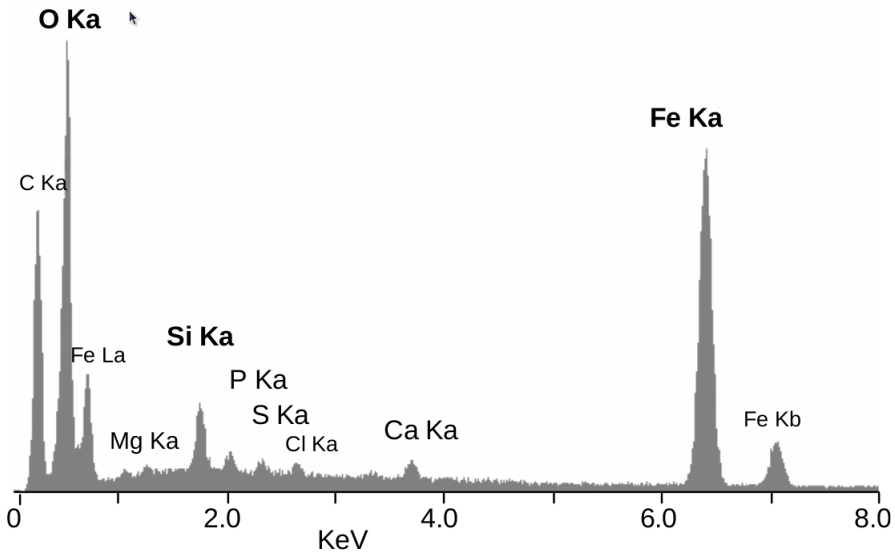

Figure 4: Elemental Energy dispersive X-Ray microanalyses of the mineral crust of Rimicaris exoculata. Lauri Corbari and others, 2008

$1s_{1/2}$	$2s_{1/2}$	$2p_{1/2}$	$2p_{3/2}$	$3s_{1/2}$	$3p_{1/2}$	$3p_{3/2}$	$3d_{3/2}$	$3d_{5/2}$
K	L_1	L_2	L_3	M_1	M_2	M_3	M_4	M_5

Table 1: Correspondence between atomic and spectroscopic notation.

In contrast to the common notation among physicists, that is based on the electron quantum numbers such as $1s_{1/2}$ or $3d_{5/2}$ in a spectroscopic community atomic levels are historically enumerated in a different way. Principal quantum numbers are in one-to-one correspondence with Latin letters such as $1-K$, $2-L$, $3-M$, etc. Atomic subshells are labeled with numbers, with 1 for s subshell, $2, 3$ for $2p_{1/2,3/2}$ subshells, $4, 5$ for $d_{3/2,5/2}$ and so on. The correspondence between first several levels given in atomic and spectroscopic notation are given in the following table.

The principal formula of the X-ray quantification [5] is

$$\frac{C_A}{C_B} = k_{AB}\frac{I_A}{I_B} \tag{2.1}$$

where C_A and C_B are weight or atom number fractions of elements A and B, I_A and I_B are their intensities on the EDS spectra, and k_{AB} is a so-called sensitivity factor.

The sensitivity factor can be determined experimentally from comparison of intensities of samples of the known composition under specified conditions. In such a case it is called a Cliff-Lorimer method. The advantage is a high precision, while the disadvantage is the dependence of k_{AB} on multiple parameters of the experiment. Theoretical treatment, on the other hand, can provide a universal way to determine the k_{AB}. The formula for the

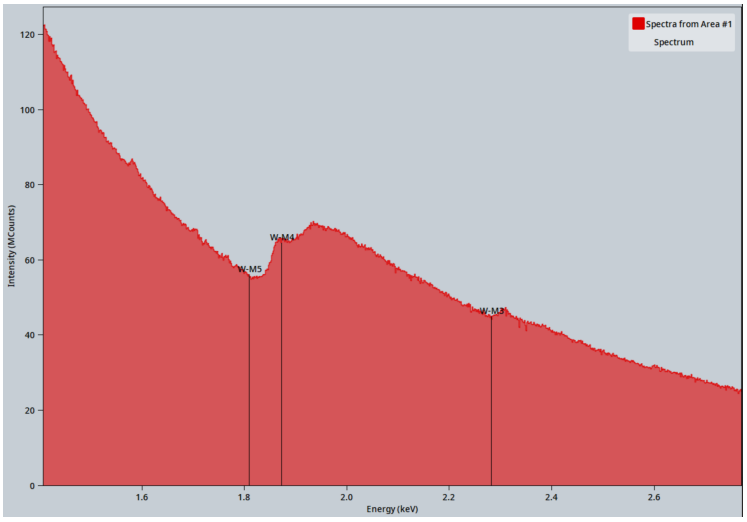

Figure 5: Example EELS spectrum. Internal ThermoFisher Scientific data

ratio of the atom numbers in a unit of volume is

$$k_{AB} = \frac{(\sigma\omega a\epsilon)_B}{(\sigma\omega a\epsilon)_A} \tag{2.2}$$

Here σ is a total cross section, i.e., the probability to excite the atom. ω is a fluorescent yield, that is equal to the ratio of atoms, relaxed through the X-ray emission to the amount of excited atoms. a is a relative probability of a transition though the process corresponding to the given peak (i.e K, L, M and other transitions). Finally, ϵ is the efficiency of a detector for an incident X-ray as discussed above.

2.6 Electron energy loss spectroscopy

Another widespread spectroscopy method in TEM is electron energy loss spectroscopy. With the help of spectrometer, located beyond the sample, it becomes possible to separate electrons according to their final energy. Subtracting this energy from the initial energy of the electron we obtain the energy lost by an electron in the sample. Being plotted against the number of electrons, it gives us an electron energy loss spectrum.
EELS possesses a number of advantages over the XEDS. First, it allows for much better spectral energy resolution as modern spectrometers allow for a separation of electrons with much lesst than $1eV$ difference (while their kinetic energy can be up to $300keV$). This allows for a close peaks separation and an observation of such fine effects as difference in chemical composition or a phase of the sample. Another advantage is that each atomic excitation is accompanied with the energy loss of a beam electron, while not every excited atom relaxes through X-ray photoemission. That is why we need not worry about the fluorescence yield. This means that EELS is by far more applicable for the investigation of light atoms, which typically can not be studied with EDS because of their low fluorescence yield. We also do not have any relative transitions probabilities to carry about. Finally, detector efficiency can be considered to be 1 in the whole range of incoming electron energies, as

they are relatively close to each other. This is why elemental quantification now depends on a, basically, single parameter - cross sections. The major disadvantage of EELS, though, that experimental spectra are much harder to interpret and process. While in principle low energy loss is even more useful than high energy loss, as it very sensitive to any changes in the sample and allows to distinguish different phases such as vitreous and hexagonal ice, it is also very hard to predict theoretically. Collective effects can be only computed via effective field models and there is no unique way to choose model parameters the best for all kinds of materials and structures. For this reason, high energy loss is a much more reliable instrument for elemental quantification, and it forms the base of the whole TEM spectroscopy.

To carefully process high-energy EELS spectra following considerations must be taken into account. Background in EELS is more complicated then in the case of XEDS. For a given edge it builds up predominantly from electrons, that lost energy on bremsstrahlung radiation and electrons, lost energy on shallower edges. Subtraction of the background can only be done effectively [7] and sometimes brings errors. Another factor is that we must take multiple collisions into account. To avoid electron be multiply scattered, which would significantly disturb a spectrum shape, EELS samples should be made extremely thin, of order several nanometers. This ensures that the mean free path of the electron inside the material is much longer than sample length and makes a probability of multiple collisions small. However, probability of low-loss interactions is many orders of magnitude higher than high-loss. That is why high-loss spectrum always contains some admixture of low-loss. It can be purified by a procedure of deconvolution.

3 Angular momentum

3.1 Spherical harmonics

The orbital angular momentum operators are defined as $\boldsymbol{L} = \boldsymbol{r} \times \boldsymbol{p}$. The components L_x, L_y and L_z do not commute, however the operator L^2 commutes with any of the components. The simultaneous eigenfunctions of L^2 and L_z in real space are called spherical harmonics Y_{lm}. They can be written in coordinates as

$$Y_{lm}(\theta, \phi) = P_l^m(cos(\theta))\Phi_m(\phi) \tag{3.1}$$

where P_l^m are associated Legendre polynomials

$$P_l^m = (1 - x^2)^{m/2} \frac{d^m}{dx^m} \frac{1}{2^l l!} \frac{d^l}{dx^l}(x^2 - 1)^l \tag{3.2}$$

and

$$\Phi_m(\phi) = \frac{1}{\sqrt{2\pi}} e^{im\phi} \tag{3.3}$$

$Y_{lm}(\theta, \phi)$ are normalized on unity.

3.2 Addition of two angular momenta

If we have two states that are eigenstates of angular momenta

$$\boldsymbol{j_1}|\psi_1\rangle = j_1|\psi_1\rangle$$
$$\boldsymbol{j_2}|\psi_2\rangle = j_2|\psi_2\rangle$$

then we often need to express eigenstates of the full angular momentum $J = j_1 + j_2$ of a two particle system in a basis of one particle wavefunctions. We write

$$|J, M\rangle = \sum_{m_1, m_2} C(j_1, j_2, J; m_1, m_2, M)|j_1, m_1\rangle|j_2, m_2\rangle \tag{3.4}$$

where $C(j_1, j_2, J; m_1, m_2, M) = \langle j_1, m_1, j_2, m_2|J, M\rangle$ are called Clebsh-Gordan coupling coefficients [14, 4, 12]. They satisfy several conditions, which are derived at any textbook on quantum mechanics.

$$C(j_1, j_2, J; m_1, m_2, M) \neq 0 \qquad \text{only if} \quad m_1 + m2 = m$$
$$\sum_{m_1, m_2} C(j_1, j_2, J'; m_1, m_2, M')C(j_1, j_2, J; m_1, m_2, M) = \delta_{J'J}\delta_{M'M}$$
$$\sum j, mC(j_1, j_2, J; m_1', m_2', m_2', M)C(j_1, j_2, J, m_1, m_2, M) = \delta_{m_1', m_1}\delta_{m_2', m_2}$$
$$J_{max} = j_1 + j_2, \qquad J_{min} = |j_1 - j_2| \tag{3.5}$$

They also satisfy following permutation properties

$$C(j_1, j_2, J; -m_1, -m_2, -M) = (-1)^{j_1 + j_2 - J} C(j_1, j_2, J; m_1, m_2, M) \tag{3.6}$$
$$C(j_2, j_1, J; m_2, m_1, M) = (-1)^{j_1 + j_2 - J} C(j_1, j_2, J; m_1, m_2, M) \tag{3.7}$$

$$C(j_1, J, j_2; m_1, -M, -m_2) = (-1)^{j_1 - m_1}\sqrt{\frac{2j_2+1}{2J+1}}C(j_1, j_2, J, m_1, m_2, M) \tag{3.8}$$

In practice it is more convenient to work with the so-called Wigner 3j Symbols defined by:

$$\begin{pmatrix} j_1 & j_2 & j_3 \\ m_1 & m_2 & m_3 \end{pmatrix} = \frac{(-1)^{j_1 - j_2 - m_3}}{\sqrt{2j_3+1}} C(j_1, j_2, j_3; m_1, m_2, -m3) \tag{3.9}$$

From properties of Glebsh-Gordan coefficients it follows that

$$\begin{pmatrix} j_1 & j_2 & j_3 \\ m_1 & m_2 & m_3 \end{pmatrix} = \begin{pmatrix} j_2 & j_3 & j_1 \\ m_2 & m_3 & m_1 \end{pmatrix} = \begin{pmatrix} j_3 & j_1 & j_2 \\ m_3 & m_1 & m_2 \end{pmatrix}$$

$$\begin{pmatrix} j_1 & j_2 & j_3 \\ m_1 & m_2 & m_3 \end{pmatrix} = (-1)^{j_1+j_2+j_3}\begin{pmatrix} j_2 & j_1 & j_3 \\ m_2 & m_1 & m_3 \end{pmatrix} = (-1)^{j_1+j_2+j_3}\begin{pmatrix} j_1 & j_2 & j_3 \\ -m_1 & -m_2 & -m_3 \end{pmatrix}$$

$$\sum_{m_1,m_2}\begin{pmatrix} j_1 & j_2 & j_3' \\ m_1 & m_2 & m_3 \end{pmatrix}\begin{pmatrix} j_1 & j_2 & j_3 \\ m_1 & m_2 & m_3 \end{pmatrix} = \frac{1}{2j_3+1}\delta_{j_3' j_3}\delta_{m_3' m_3}$$

$$\sum_{j_3,m_3}(2j_3+1)\begin{pmatrix} j_1 & j_2 & j_3 \\ m_1 & m_2 & m_3 \end{pmatrix}\begin{pmatrix} j_1 & j_2 & j_3 \\ m_1' & m_2' & m_3 \end{pmatrix} = \delta_{m_1,m_1'}\delta_{m_2 m_2'}$$

$$\begin{pmatrix} j & j & 0 \\ m & -m & 0 \end{pmatrix} = \frac{(-1)^{j-m}}{\sqrt{2j+1}}$$

$$\begin{pmatrix} j_1 & j_2 & j_3 \\ 0 & 0 & 0 \end{pmatrix} = 0 \qquad \text{if} \quad j_1 + j_2 + j3 \quad \text{is odd} \tag{3.10}$$

3.3 Irreducible tensor operators

We call an operator "irreducible tensor operator" if it satisfies following relations

$$\begin{aligned} [J_z, T_q^k] &= qT_q^k \\ [J_\pm, T_q^k] &= \sqrt{(k \pm q + 1)(k \mp q)}T_{q\pm 1}^k \end{aligned} \tag{3.11}$$

with $J_\pm = J_x \pm iJ_y$. Tensor operators satisfy the Wigner-Eckart theorem

$$\langle j_1, m_1 | T_q^k | j_2, m_2 \rangle = (-1)^{j_1 - m_1}\begin{pmatrix} j_1 & k & j_2 \\ -m_1 & q & m_2 \end{pmatrix}\langle j_1 || T^k || j_2 \rangle \tag{3.12}$$

where $\langle j_1 || T^k || j_2 \rangle$ is called the reduced matrix element and depends only on k. It is straightforward to show, that spherical harmonics satisfy properties of tensor operators. We will use following tensor operators through derivations of several equations

$$C_q^k = \sqrt{\frac{4\pi}{2k+1}}Y_{kq}(\theta, \phi) \tag{3.13}$$

3.4 Graphical representation of angular momentum

In analogy with Feynman diagrams, angular momentum graphs allow to substitute clumsy and hard-to-remember operation with Wigner symbols with an intuitive visual representation [14, 12]. The main rules are following

$$\underline{j_1, m_1 \qquad j_2, m_2} = \delta_{j_1,j_2}\delta_{m_1,m_2} \tag{3.14}$$

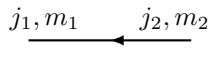

$$= (-1)^{j_1 - m_1} \delta_{j_1, j_2} \delta_{m_1, -m_2} \tag{3.15}$$

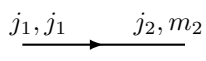

$$= (-1)^{j_1 + m_1} \delta_{j_1, j_2} \delta_{m_1, -m_2} \tag{3.16}$$

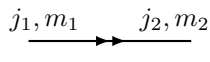

$$= (-1)^{2j_1} \delta_{j_1, j_2} \delta_{m_1, m_2} \tag{3.17}$$

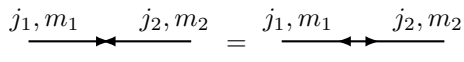

$$= \delta_{j_1, j_2} \delta m_1, m_2 \tag{3.18}$$

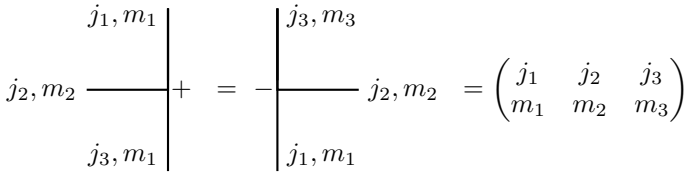

$$= \begin{pmatrix} j_1 & j_2 & j_3 \\ m_1 & m_2 & m_3 \end{pmatrix} \tag{3.19}$$

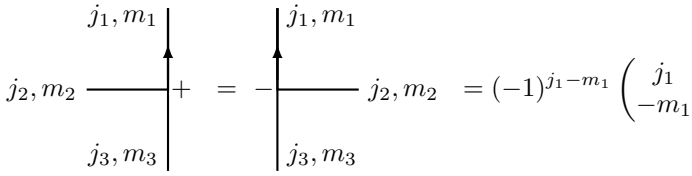

$$= (-1)^{j_1 - m_1} \begin{pmatrix} j_1 & j_2 & j_3 \\ -m_1 & m_2 & m_3 \end{pmatrix} \tag{3.20}$$

(3.21)

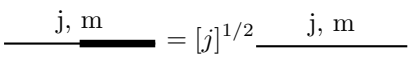

$$= [j]^{1/2} \tag{3.22}$$

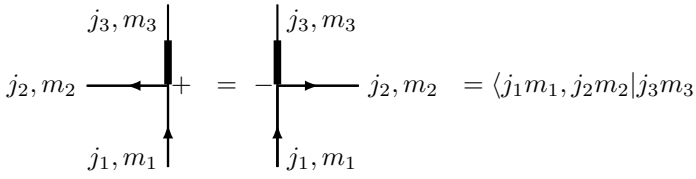

$$= \langle j_1 m_1, j_2 m_2 | j_3 m_3 \rangle \tag{3.23}$$

$$= (-1)^{j_1-j_2+m_3}\sqrt{(2j_3+1)}\begin{pmatrix} j_1 & j_2 & j_3 \\ m_1 & m_2 & m_3 \end{pmatrix} \tag{3.24}$$

$$\sum_{m_2} \underbrace{\qquad}_{j_1,m_1 \quad j_2,m_2} \times \underbrace{\qquad}_{j_2,m_2 \quad j_3,m_3} = \underbrace{\qquad}_{j_1,m_1 \quad j_3,m_3} \delta_{j_1,j_2} \tag{3.25}$$

Orthogonality relation for 3-j symbols in the graphical form is

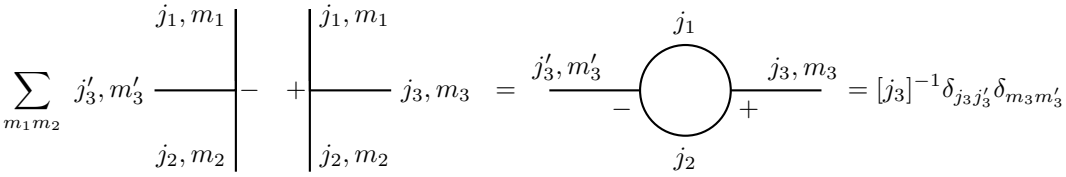

$$= [j_3]^{-1}\delta_{j_3j_3'}\delta_{m_3m_3'} \tag{3.26}$$

Among others graphical identities ones very useful are line elimination ones. Using

$$\begin{pmatrix} j_1 & j_2 & 0 \\ m_1 & m_2 & 0 \end{pmatrix} = \delta_{j_1,j_2}\delta(m_1,-m_2)(-1)^{j_1-m_1}[j_1]^{-1/2}$$

we can write

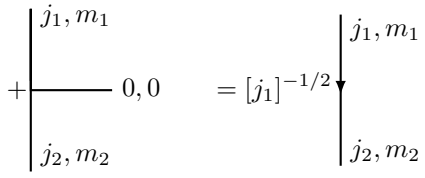

(3.27)

From 3.26 and 3.27 it follows that

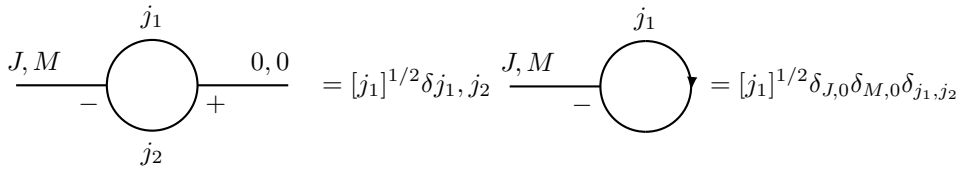

(3.28)

and

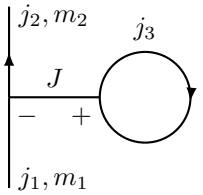

$$= \sqrt{\frac{[j_3]}{[j_1]}}\delta_{J,0}\delta_{j_1,j_2}\delta_{m_1,m_2} \tag{3.29}$$

3.5 Addition of three angular momenta

If we want to couple three angular momenta, then we can do it in three different ways.

$$\begin{aligned} &|(j_1j_2)J_{12}, j_3, JM\rangle \\ &|j_1, (j_2j_3)J_{23}, JM\rangle \\ &|(j_1j_3)J_{13}, j_2, JM\rangle \end{aligned} \tag{3.30}$$

We can express one set in terms of another as

$$|j_1, j_2j_3J_{23}, JM\rangle = \sum_{J_{12}} |(j_1j_2)J_{12}, j_3, JM\rangle\langle(j_1j_2)J_{12}, j_3, JM|j_1, (j_2j_3)J_{23}, JM\rangle \tag{3.31}$$

Using diagrammatic techniques we can evaluate

$\langle(j_1j_2)J_{12}, j_3, JM| =$

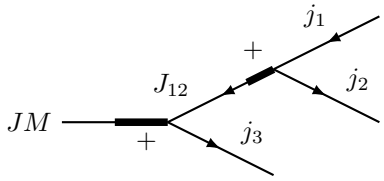

(3.32)

$|j_1(j_2j_3)J_{23}, JM\rangle =$

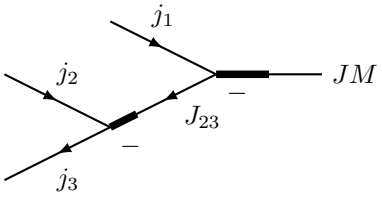

(3.33)

And consequentially,

$\langle(j_1j_2)J_{12}, j_3, JM|j_1(j_2j_3)J_{23}, JM\rangle =$

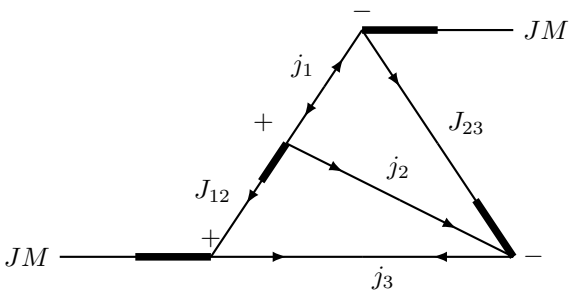

$= (-1)^{2j_2}[J_{12}, J_{23}]$

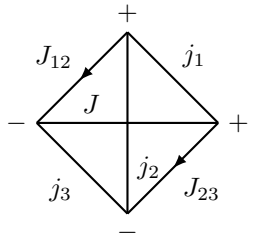

$$= (-1)^{j_1+j_2+j_3+J}[J_{12}, J_{23}] + \quad + \qquad = (-1)^{j_1+j_2+j_3+J}[J_{12}, J_{23}] \begin{Bmatrix} J_{12} & j_3 & J \\ J_{23} & j_1 & j_2 \end{Bmatrix}$$

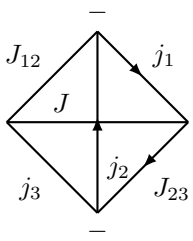

(3.34)

Where at the last equality a Wigner 6j symbol was introduced for the square diagram. It can also be written analytically as

$$\begin{Bmatrix} j_1 & j_2 & j_3 \\ j_4 & j_5 & j_6 \end{Bmatrix} = \sum_{m's} (-1)^{\sum_i [j_i - m_i]} \begin{pmatrix} j_1 & j_2 & j_3 \\ -m_1 & -m_2 & -m_3 \end{pmatrix} \begin{pmatrix} j_1 & j_5 & j_6 \\ m_1 & -m_5 & m_6 \end{pmatrix} \times \begin{pmatrix} j_2 & j_6 & j_4 \\ m_2 & -m_6 & m_4 \end{pmatrix} \begin{pmatrix} j_3 & j_4 & j_5 \\ m_3 & -m_4 & m_5 \end{pmatrix} \quad (3.35)$$

4 Central field Dirac equation

4.1 Separation of variables

Stationary Dirac equation for a one electron atom with a spherically symmetric nucleus potential [14] can be written as

$$h_D\varphi = E\varphi \tag{4.1}$$

$$h_D = (c\,\boldsymbol{\alpha}\cdot\boldsymbol{p} + \beta c^2 + V_{nuc}(r)) \tag{4.2}$$

It is not complicated to show (Appendix 2) that Dirac Hamiltonian commutes with an operator of full momentum. However, it does not commute with an operator of angular momentum. So, solutions to the Dirac equation should be eigenstates of j but not l. Therefore we will introduce operator $K = -1 - \boldsymbol{\sigma}\boldsymbol{L}$. Its eigenstates are

$$K\varphi = \kappa\varphi \tag{4.3}$$

and we are looking for the solution of the Dirac equation in the form

$$\varphi = \frac{1}{r}\begin{pmatrix} iP_\kappa(r)\Omega_{\kappa m}(\hat{r}) \\ Q_\kappa(r)\Omega_{-\kappa m}(\hat{r}) \end{pmatrix} \tag{4.4}$$

where Ω is a spherical spinor defined as

$$\Omega_{jlm} = \sum_\mu C(l, 1/2, j, m-\mu, \mu, m) Y_{l,m-\mu}(\theta,\varphi)\chi_\mu \tag{4.5}$$

$$\Omega_{l+\frac{1}{2}lm}(\theta,\varphi) = \begin{pmatrix} \sqrt{\frac{l+m+1/2}{2l+1}}Y_{l,m-1/2}(\theta,\varphi) \\ \sqrt{\frac{l-m+1/2}{2l+1}}Y_{l,m+1/2}(\theta,\varphi) \end{pmatrix} \tag{4.6}$$

$$\Omega_{l-\frac{1}{2}lm}(\theta,\varphi) = \begin{pmatrix} -\sqrt{\frac{l-m+1/2}{2l+1}}Y_{l,m-1/2}(\theta,\varphi) \\ \sqrt{\frac{l+m+1/2}{2l+1}}Y_{l,m+1/2}(\theta,\varphi) \end{pmatrix} \tag{4.7}$$

So it is possible to classify states by the value of an operator κ instead of j and l. This is so called "spectroscopic notation", which will be used further. From the definition of κ it follows that $\kappa = -l-1$ for $j = l+\frac{1}{2}$ and $\kappa = l$ for $j = l-\frac{1}{2}$. So, $j = |\kappa| - 1/2$ and we have that both components of φ are eigenstates of the same j but different l.
The following relations can be shown to hold (Appendix 2).

$$\boldsymbol{\sigma}\cdot\boldsymbol{p} = -i\boldsymbol{\sigma}\cdot\hat{\boldsymbol{r}}\left(i\hat{\boldsymbol{r}}\cdot\boldsymbol{p} - \frac{\boldsymbol{\sigma}[\boldsymbol{r}\times\boldsymbol{p}]}{r}\right) = -i\boldsymbol{\sigma}\cdot\hat{\boldsymbol{r}}\left(i\hat{\boldsymbol{r}}\cdot\boldsymbol{p} - \frac{\boldsymbol{\sigma}\cdot\boldsymbol{L}}{r}\right) \tag{4.8}$$

$$\boldsymbol{\sigma}\cdot\hat{\boldsymbol{r}}\;\Omega_{\kappa m} = -\Omega_{-\kappa m} \tag{4.9}$$

Then

$$\begin{aligned}\boldsymbol{\alpha}\cdot\boldsymbol{p}\begin{pmatrix} iP_\kappa(r)\Omega_{\kappa m}(\hat{r}) \\ Q_\kappa(r)\Omega_{-\kappa m}(\hat{r}) \end{pmatrix} = \begin{pmatrix} -i\boldsymbol{\sigma}\cdot\hat{\boldsymbol{r}}(\frac{\partial}{\partial r} + \frac{(-\kappa+1)}{r})\frac{Q_\kappa(r)}{r}\Omega(\hat{r})_{-\kappa m} \\ \boldsymbol{\sigma}\cdot\hat{\boldsymbol{r}}(\frac{\partial}{\partial r} + \frac{(\kappa+1)}{r})\frac{P_\kappa(r)}{r}\Omega(\hat{r})_{\kappa m} \end{pmatrix} = \\ -\frac{1}{r}\begin{pmatrix} -i(\frac{\partial}{\partial r} - \frac{\kappa}{r})Q_\kappa(r)\Omega(\hat{r})_{\kappa m} \\ (\frac{\partial}{\partial r} + \frac{\kappa}{r})P_\kappa(r)\Omega(\hat{r})_{-\kappa m} \end{pmatrix}\end{aligned} \tag{4.10}$$

And Dirac equation becomes

$$H_D\varphi = \frac{1}{r}\begin{pmatrix} \left(ic(\frac{\partial}{\partial r} - \frac{\kappa}{r})Q_\kappa + i(c^2 + V_{nuc})P_\kappa\right)\Omega_{\kappa m} \\ \left(c(\frac{\partial}{\partial r} + \frac{\kappa}{r})P_\kappa + (-c^2 + V_{nuc})Q_\kappa\right)\Omega_{-\kappa m} \end{pmatrix} = E\,\frac{1}{r}\begin{pmatrix} iP_\kappa\Omega_{\kappa m} \\ Q_\kappa\Omega_{-\kappa m} \end{pmatrix} \tag{4.11}$$

Angular part drops out, and we arrive to the system of the 1st order ODE

$$\begin{aligned} (c^2 + V_{nuc})P_\kappa + c\left(\frac{\partial}{\partial r} - \frac{\kappa}{r}\right)Q_\kappa &= EP_\kappa \\ -c\left(\frac{\partial}{\partial r} + \frac{\kappa}{r}\right)P_\kappa + (-c^2 + V_{nuc})Q_\kappa &= EQ_\kappa \end{aligned} \tag{4.12}$$

P_κ is so-called "big" component of the Dirac spinor, and Q_κ is a "small" component.

4.2 Pauli approximation

$E - V - c^2$ is a binding energy of the electron, and we expect it to be small, compared to its rest energy. So, we can neglect terms of the order $\frac{E-V-c^2}{c^2}$. Such an approximation is called Pauli approximation. If we rewrite the system as

$$\begin{aligned} c\left(\frac{\partial}{\partial r} - \frac{\kappa}{r}\right)Q_\kappa &= (E - c^2 - V_{nuc})P_\kappa \\ -c\left(\frac{\partial}{\partial r} + \frac{\kappa}{r}\right)P_\kappa &= (E + c^2 - V_{nuc})Q_\kappa \end{aligned} \tag{4.13}$$

And further elaborate on the second equation

$$-c\left(\frac{\partial}{\partial r} + \frac{\kappa}{r}\right)P_\kappa = (E + 2c^2 - c^2 - V_{nuc})Q_\kappa \tag{4.14}$$

Dividing it by $2c^2$ in Pauli approximation we obtain

$$-\frac{1}{2c}\left(\frac{\partial}{\partial r} + \frac{\kappa}{r}\right)P_\kappa = Q_\kappa \tag{4.15}$$

After the substitution of Q_κ to the first equation

$$-\frac{1}{2}\left(\frac{d^2}{dr^2} + \frac{\kappa(\kappa+1)}{r^2} + V_{nuc}\right)P_\kappa = (E - c^2)P_\kappa \tag{4.16}$$

Notating $E' = E - c^2$ and using the fact that $\kappa(\kappa+1) = l(l+1)$ independently of j value we arrive to a Schrodinger equation for the central field.

$$-\frac{1}{2}\left(\frac{d^2}{dr^2} + \frac{l(l+1)}{r^2} + V_{nuc}\right)\Psi = E'\Psi \tag{4.17}$$

This shows that the big component should of the Dirac spinor should be associated with the "usual" non-relativistic wavefunction. We can also estimate the order of the small component. It is roughly c times smaller than the big one. In atomic units $c \approx 137$, we can expect Q to be hundred times less then P. We can also estimate the range of validity of Pauli approximation. Binding energy should be much less than c^2. Non-relativistic energy of hydrogen-like ions are $\frac{Z^2}{2n^2}$, which for $n = 0$ means that $Z << c = 137$. In practice, relativistic corrections turn out to be important for inner shells already for $Z \approx 30$.

4.3 Solution for the Coulomb field

If we take V_{nuc} to be $-\frac{Z}{r}$ than it becomes possible to solve the Dirac equation analytically. First, we find asymptotic behaviour at infinity:

$$\begin{aligned} c\frac{dQ_\kappa}{dr} &= (E-c^2)P_\kappa \\ c\frac{dP_\kappa}{dr} &= -(E+c^2)Q_\kappa \end{aligned} \tag{4.18}$$

Substituting the second equation to the first

$$-\frac{c^2}{E+c^2}\frac{d^2P_\kappa}{dr^2} = (E-c^2)P_\kappa$$

or the same

$$c^2\frac{d^2P_\kappa}{dr^2} + (E^2-c^4)P_\kappa = 0 \tag{4.19}$$

This equation has trivial linearly independent solutions $P_\kappa = e^{\pm\lambda}$, $\lambda = \sqrt{c^2 - \frac{E^2}{c^2}}$ and $c^2 > E$, as E corresponds to the binding energy and hence less, than the rest mass. The solution must go to 0 at infinity, so we must choose a "-" sign. From the second equation on the system 4.11 we immediately get that

$$Q_\kappa = \sqrt{\frac{c^2-E}{c^2+E}}P_\kappa \tag{4.20}$$

Now we will seek for a general solutions in a form

$$\begin{aligned} P_\kappa &= \sqrt{1+E/c^2}e^{-\lambda r}(F_1+F_2) = a_+e^{-\lambda r}(F_1+F_2) \\ Q_\kappa &= \sqrt{1-E/c^2}e^{-\lambda r}(F_1-F_2) = a_-e^{-\lambda r}(F_1-F_2) \end{aligned} \tag{4.21}$$

Substitution into 4.18 gives

$$\begin{aligned} a_+(-\frac{Z}{r}+c^2)(F_1+F_2) + ca_-(\lambda-\frac{\kappa}{r})(F_1-F_2) + ca_-(F_1'-F_2') = Ea_+(F_1+F_2) \\ -ca_+(-\lambda+\frac{\kappa}{r})(F_1+F_2) - ca_+(F_1'+F_2') + a_-(-\frac{Z}{r}-c^2)(F_1-F_2) = Ea_-(F_1-F_2) \end{aligned}$$

Multiplying first equation with a_+, second with a_- and then adding and subtracting them, we obtain, noticing $\lambda = ca_+a_-$

$$\begin{aligned} a_+^2(V+c^2)(F_1+F_2) + \lambda[(-\lambda-\frac{\kappa}{r})(F_1-F_2) - (-\lambda+\frac{\kappa}{r})(F_1+F_2)] - 2\lambda F_2' + \\ +(V-c^2)a_-^2(F_1-F_2) = Ea_+^2(F_1+F_2) + Ea_-^2(F_1-F_2) \\ a_+^2(V+c^2)(F_1+F_2) + \lambda[(-\lambda-\frac{\kappa}{r})(F_1-F_2) + (\lambda+\frac{\kappa}{r})(F_1+F_2)] + 2\lambda F_1' - \\ -(V-c^2)a_-^2(F_1-F_2) = Ea_+^2(F_1+F_2) - Ea_-^2(F_1-F_2) \end{aligned}$$

Simple algebraic manipulations allows to find express F_1' and F_2'

$$\begin{aligned}\frac{dF_1}{dr} &= \frac{EZ}{c^2\lambda r}F_1 + (\frac{Z}{\lambda r} - \frac{\kappa}{r})F_2 \\ \frac{dF_2}{dr} &= -(\frac{Z}{\lambda r} + \frac{\kappa}{r})F_1 + \left(2\lambda - \frac{EZ}{\lambda c^2 r}\right)F_2\end{aligned} \tag{4.22}$$

Or, making a change of variable $x = 2\lambda r$

$$\begin{aligned}\frac{dF_1}{dx} &= \frac{EZ}{c^2\lambda x}F_1 + (\frac{Z}{\lambda x} - \frac{\kappa}{x})F_2 \\ \frac{dF_2}{dx} &= -(\frac{Z}{\lambda x} + \frac{\kappa}{x})F_1 + \left(1 - \frac{EZ}{\lambda c^2 x}\right)F_2\end{aligned} \tag{4.23}$$

Proposing solution near the origin is $F_1 = a_1 x^\gamma, F_2 = a_2 x^\gamma$,

$$\begin{aligned}a_1\gamma x^{\gamma-1} &= a_1\frac{EZ}{c^2\lambda}x^{\gamma-1} + a_2(\frac{Z}{\lambda} - \kappa)x^{\gamma-1} \\ a_2\gamma x^{\gamma-1} &= -a_1(\frac{Z}{\lambda} + \kappa)x^{\gamma-1} + a_2\left(\not{\gamma} - \frac{EZ}{\lambda c^2}\right)x^{\gamma-1}\end{aligned} \tag{4.24}$$

It gives as 2 conditions

$$\frac{a_1}{a_2} = \frac{(\frac{Z}{\lambda} - \kappa)}{(\gamma - \frac{EZ}{c^2\lambda})} = -\frac{\gamma + \frac{EZ}{c^2\lambda}}{\frac{Z}{\lambda} + \kappa} \tag{4.25}$$

which can be both satisfied only if

$$\gamma = \sqrt{\kappa^2 - \frac{Z^2}{c^2}} = \sqrt{\kappa^2 - \alpha^2 Z^2}$$

We can express F_2 through F_1 and obtain from 4.23 the second order ODE

$$F_2 = \frac{1}{-\kappa + \frac{Z}{\lambda}}\left(x\frac{dF_1}{dx} - \frac{EZ}{c^2\lambda}F_1\right) \tag{4.26}$$

$$\frac{1}{-\kappa + \frac{Z}{\lambda}}\frac{d\left(x\frac{dF_1}{dx} - \frac{EZ}{c^2\lambda}F_1\right)}{dx} = -(\frac{Z}{\lambda x} + \frac{\kappa}{x})F_1 + \left(1 - \frac{EZ}{\lambda c^2 x}\right)\left(\frac{1}{-\kappa + \frac{Z}{\lambda}}\left(x\frac{dF_1}{dx} - \frac{EZ}{c^2\lambda}F_1\right)\right) \tag{4.27}$$

Multiplying by $-\kappa + \frac{Z}{\lambda}$ and rearranging terms we obtain

$$\begin{aligned}xF'' + \left(1 - \frac{EZ}{c^2\lambda} - x + \frac{EZ}{\lambda c^2}\right)F' + \left(\frac{EZ}{C^2\lambda} - \frac{\frac{E^2Z^2}{c^4\lambda^2} - \kappa^2 - \frac{Z^2}{\lambda^2}}{x}\right)F = \\ = xF'' + (1-x)F' + \left(\frac{EZ}{c^2\lambda} - \frac{\gamma^2}{x}\right)F\end{aligned} \tag{4.28}$$

At the last step the definitions of κ, γ and λ were used to simplify the expression. Factoring the asymptotic at 0, $F = x^\gamma F_1$ this equation becomes

$$x[x^\gamma F'' + \gamma x^{\gamma-1}F' + \gamma(\gamma-1)x^{\gamma-2}F] + (1-x)[x^\gamma F' + \gamma x^{\gamma-1}F] - \left(\frac{\gamma^2}{x} - \frac{EZ}{c^2\lambda}\right)x^\gamma F = 0$$
$$xF'' + (2\gamma + 1 - x)F' + \left(\gamma - \frac{EZ}{c^2\lambda}\right)F = 0 \tag{4.29}$$

If we denote $b = 2\gamma + 1$ and $a = \gamma - \frac{EZ}{c^2\lambda}$ than we arrive to the so-called Kummer's equation

$$xF'' + (b-x)F' - aF = 0 \tag{4.30}$$

which has solutions in terms of hypergeometric functions (Appendix 3) $M(a,b,x)$ and $U(a,b,x)$. From physical reasons we need those regular at origin, i.e. $F(a,b,x) = M(a,b,x)$. From recurrent and differential formulas for $M(a,b,x)$ it can also be derived that $x\frac{dM(a,b,x,)}{dx} + aM(a,b,x) = aM(a+1,b,x)$. Using it in 4.26 we arrive to the system

$$F_1 = x^\gamma F(a,b,x)$$
$$F_2 = \frac{\gamma - \frac{EZ}{c^2\lambda}}{-\kappa + \frac{Z}{\lambda}}F(a+1,b,x) \tag{4.31}$$

From which we express solutions to the radial Dirac equation

$$P_\kappa(r) = A_{norm}\sqrt{1+E/c^2}e^{\lambda r}(2\lambda r)^\gamma\left[(-\kappa + \frac{Z}{\lambda})F(a,b,2\lambda r) + (\gamma - \frac{EZ}{c^2\lambda})F(a+1,b,2\lambda r)\right]$$
$$Q_\kappa(r) = A_{norm}\sqrt{1-E/c^2}e^{\lambda r}(2\lambda r)^\gamma\left[(-\kappa + \frac{Z}{\lambda})F(a,b,2\lambda r) - (\gamma - \frac{EZ}{c^2\lambda})F(a+1,b,2\lambda r)\right] \tag{4.32}$$

Asymptotic behaviour of $F(a,b,x)$ for large x is

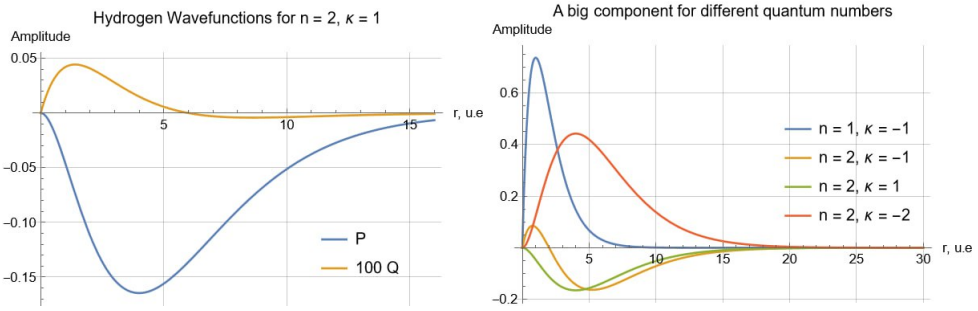

Figure 6: Dirac Hydrogen wavefunctions

$$F(a,b,x) \xrightarrow{x\to\infty} \frac{\Gamma(b)}{\Gamma(a)}e^x x^{a-b}[1 + O(x^{-1})]$$

which diverges unless $\Gamma(a) = \infty$. This happens when a is a non-positive integer n_r. Recalling $a = \gamma - \frac{EZ}{c^2\lambda}$, we can find eigenvalues from the equation

$$\frac{EZ}{c^2\lambda} = \frac{EZ}{c^2\sqrt{c^2 - E^2/c^2}} = \gamma + n_r \tag{4.33}$$

The solution is

$$E_\kappa = \frac{c^2}{\sqrt{1 + \frac{\alpha^2 Z^2}{(\gamma+n-k)^2}}} \tag{4.34}$$

Index κ here due to the fact that γ and hence E implicitly depend on κ, i.e full and angular momenta. However, $\gamma = \sqrt{\kappa^2 - Z/\lambda}$ depends only on $|\kappa| = k = j + 1/2$, so angular momentum dependency drops out.
For every κ there is infinite amount of eigenvalues, depending on n_r. So in analogy with the non-relativistic case we can denote $n_r = n - k$. Where n is principal quantum number and $n >= k >= 1$. Then each n corresponds to $2n$ possible values of κ. However, one eigenfunction, namely corresponding to $\kappa = n$ is identically zero which follows from $\gamma = \frac{EZ}{c^2\lambda}$, leading to $\lambda = \frac{Z}{\kappa}$, which gives 0 after the substitution to 4.32. So there is no true eigenvalue, corresponding to $\kappa = n$ and hence each n has only 2n - 1 corresponding κ.
Solution to the Dirac equation still miss a normalization. We should have $\langle\varphi|\varphi\rangle = 1$, which implies together with normalized to unity angular part that $\int(P^2(r) + Q^2(r))dr = 1$. The analytical integration of hypergeometric functions is cumbersome but feasible and leads to the result

$$A_{norm} = A_{n\kappa} = \frac{1}{N\Gamma(2\gamma+1)}\sqrt{\frac{Z\Gamma(2\gamma+1+n-k)}{2(n-k)!(N-\kappa)}} \tag{4.35}$$

where $N = \sqrt{n^2 - 2(n-k)(k-\gamma)}$ We can expand the Dirac eigenvalues in terms of αZ till the $\alpha^4 Z^4$, which turns out to be the first correction beyond non-relativistic eigenvalues and explains so-called "fine splitting" of energy levels.

$$\begin{aligned}
&\gamma = \sqrt{\kappa^2 - Z^2/c^2} = |\kappa|(1 - \frac{\alpha^2 Z^2}{2\kappa^2}) \\
&E_{n\kappa} = \frac{c^2}{1 + \frac{\alpha^2 Z^2}{(\gamma+n-k)^2}} = \frac{c^2}{\sqrt{1 + \frac{\alpha^2 Z^2}{(n-\frac{\alpha^2 Z^2}{2k})^2}}} = \frac{c^2}{1 + \frac{\alpha^2 Z^2}{2n^2} + \frac{\alpha^4 Z^4}{2n^3 k} - \frac{1}{8}\frac{\alpha^4 Z^4}{n^4}} \\
&= c^2(1 - \frac{\alpha^2 Z^2}{2n^2} - \frac{\alpha^4 Z^4}{2n^3 k} + \frac{\alpha^4 Z^4}{4n^4}) = c^2 - \frac{Z^2}{2n^2} - \frac{\alpha^2 Z^4}{2n^3}\left(\frac{1}{k} - \frac{3}{4n}\right)
\end{aligned} \tag{4.36}$$

c^2 term here is a rest mass of the electron, $\frac{Z^2}{2n^2}$ is a non-relativistic energy and $\frac{\alpha^2 Z^4}{2n^3}\left(\frac{1}{k} - \frac{3}{4n}\right)$ is a fine structure correction. We can see that it grows quite fast with the atomic number.

5 Mutli-electron atom

5.1 One-particle approximation

The stationary Dirac equation for a multi electron atom is

$$H(\boldsymbol{r}_1, \boldsymbol{r}_2, ..., \boldsymbol{r}_N)\Psi(\boldsymbol{r_1}, \boldsymbol{r_2}, ..., \boldsymbol{r_N}) = E\Psi(\boldsymbol{r}_1, \boldsymbol{r}_2, ..., \boldsymbol{r}_N) \tag{5.1}$$

where the Hamiltonian is

$$H = \sum_{i=1}^{N} \left(c\,\boldsymbol{\alpha} \cdot \boldsymbol{p_i} + \beta c^2 + V_{nuclear}(r_i) + \frac{1}{2} \sum_{\substack{j=1 \\ j \neq i}}^{N} \frac{1}{r_{ij}} \right) \tag{5.2}$$

This equation does not allow for a precise solution even with the help of a computer. To see it, let's notice that it depends on N radius-vectors. Therefore, it is 3N-dimensional equation. If we have a grid with a hundred points for each dimension, then, for instance, for iron we will have to store 10^{156} wavefunction values, which exceeds the number of atoms in the observable Universe. Even for the simplest multi electron atom - He, with only 2 electrons, we would have 10^{12} points, what is more than feasible for practical applications.

The solution to this problem is a so-called one electron approach, where we consider a multi electron wavefunction to factorize into a product of one electron wavefunctions [4, 14, 12, 3].

$$\Psi(\boldsymbol{r_1}, \boldsymbol{r_2}, ..., \boldsymbol{r_N}) = \psi_1(\boldsymbol{r_1})\psi_2(\boldsymbol{r_2})...\psi_N(\boldsymbol{r_N}) \tag{5.3}$$

Where we assume that every $\psi_i(r_i)$ is a solution of the one particle Dirac equation

$$h_D\psi_i(\boldsymbol{r}_i) = E\psi_i(\boldsymbol{r}_i) \tag{5.4}$$

in some potential $V(\boldsymbol{r}_i)$. Electrons are, however, fermions, so instead of a simple product of wavefunctions we must take an antisymmetrized one

$$\Psi(\boldsymbol{r}_1, \boldsymbol{r}_2, ..., \boldsymbol{r}_N) = \sum_{i_1, i_2, ... i_N} \epsilon_{i_1, i_2, ... i_N} \psi_1(\boldsymbol{r}_{i_1})\psi_2(\boldsymbol{r}_{i_2})...\psi_N(\boldsymbol{r}_{i_N}) \tag{5.5}$$

Which is canonically written in a determinantal form and called a Slater determinant

$$\Psi(\boldsymbol{r}_1, \boldsymbol{r}_2, ..., \boldsymbol{r}_N) = \frac{1}{\sqrt{N}} \begin{vmatrix} \psi_1(\boldsymbol{r}_1) & \psi_2(\boldsymbol{r}_1) & \cdots & \psi_N(\boldsymbol{r}_1) \\ \psi_1(\boldsymbol{r}_2) & \psi_2(\boldsymbol{r}_2) & \cdots & \psi_N(\boldsymbol{r}_2) \\ \vdots & & & \\ \psi_1(\boldsymbol{r}_N) & \psi_2(\boldsymbol{r}_N) & \cdots & \psi_N(\boldsymbol{r}_N) \end{vmatrix} \rangle \tag{5.6}$$

If $\{\psi_i(\boldsymbol{r})\}$ form a basis, then Slater determinants will form a basis in a 3N-dimensional configuration space of antisymmetric functions, so any $\Psi(\boldsymbol{r}_1, \boldsymbol{r}_2, ..., \boldsymbol{r}_N)$ can be approximated by a linear combination of Slater determinants arbitrarily well.

A Slater determinant is a synonym to a configuration wavefunction, as it describes a configuration of electrons with given atomic numbers: $\psi_i = \psi_{n_i, \kappa_i, m_i}$. In principle, one Slater determinant is not enough to describe the atomic wavefunction, as it does not have well-defined one electron quantum numbers. However, for closed subshells, i.e. those, which

have 2κ electrons, due to the Pauli principle, we have a uniquely defined set of quantum numbers. Of course, intershell correlations are still possible, but as shells are well separated in energy, with a good choice of one electron wavefunctions, a Slater determinant is usually a good approximation to the atomic wavefunction.
In this case the task becomes a search for "good" one electron wavefunctions. There are two possible ways to tract what "good" means. Either we can seek for those one electron wavefunctions, which give us best observables in a Coulomb Hamiltonian 5.1, or we can seek for a Hamiltonian, which can be written as a sum of one electron Hamiltonians

$$H(\boldsymbol{r}_1, \boldsymbol{r}_2, ..., \boldsymbol{r}_N)\Psi(\boldsymbol{r_1}, \boldsymbol{r_2}, ..., \boldsymbol{r_N}) = \sum_{i=1}^{N} h_i \tag{5.7}$$

and gives us such one-particle wavefunctions, that effectively reproduce observables of the original one. I.e., such a Hamiltonian must be close in the operator sense. Choice of such a Hamiltonian is a state of art, where some reasonable physical considerations are taken as guidelines (for example, it should give proper asymptotes, include correlations and take the Pauli principle into account). If we consider the full energy of the atom to be the most important observable, than the first method has a unique solution named Hartree-Fock (HF) after those sicentists who proposed this formalism (Name Dirac-Hartree-Fock (DHF) states for the relativistic case). The method with effective Hamiltonians include parametric potentials and effective potentials, obtained, predominantly from Density Functional Theory. The latest is named so because it operates with electron densities rather than wavefunctions. There are a lot of effective Hamiltonians designed suitable for different cases. In many cases approximate Hamiltonians turn out to be handier and much faster to compute. The drawback, however, is that effective methods is always based on some assumptions and often arbitrary fitted parameters and hence lacks universality and may give unpredictable results with some new or complicated types of calculations. Below several simple effective potentials are considered and then Dirac-Fock-Method is discussed in details.

5.2 Effective potenials

5.2.1 Parametric potentials

Parametric potential is just a potential, containing parameters defined not theoretically, but as a best fit to experiment [14]. An example of a simple parametric potential is

$$V_b(r) = V_{nuc}(r) + \frac{Z - N + 1}{r}(1 - e^{-r/b}) \tag{5.8}$$

With a proper choice of b it can give relatively good electron energies. However, if we need to adjust b for every new element (and probably a shell), then this method becomes useless for any new calculations. Moreover, true shapes of electron potentials in big atoms are rather complicated and we can not hope to reliably predict more sophisticated observables from a simple model. However, parametric potentials are still sometimes used in more involved effective theories as a global (unique for all atoms) adjustments to some theoretically motivated terms. An example will be given while discussing a Hartree-Exchange potential.

5.2.2 Thomas-Fermi potential

The first invented and the simplest DFT potential, which allows for ab-initio calculations of atomic structure (and widely used beyond it) is a non-relativistic free-electron functional,

named after its inventors L.H. Thomas and E. Fermi [14, 4]. Suppose that we have a box of a volume V, containing a gas of free electrons. Momentum of electrons is quantized and can take values $p_x = p_y = p_z = \frac{2\pi N}{V^{1/3}}$. Then the number of states in d^3p is

$$d^3N = 2\frac{V}{(2\pi)^3}d^3p \tag{5.9}$$

where a factor 2 accounts for spin states. If we now move to spherical coordinates then assuming all states up to a momentum p_f are filled, full number of possible states is

$$N = \frac{1}{\pi^2}\int_0^{p_f} p^2 dp = \frac{V}{3\pi^2}p_f^3 \tag{5.10}$$

which leads to the electron density

$$\rho = \frac{N}{V} \tag{5.11}$$

and kinetic energy density

$$\epsilon_k = \frac{1}{\pi^2}\int_0^{p_f}\frac{p^2}{2}p^2 dp = \frac{1}{10\pi^2}p_f^5 = \frac{3}{10}(3p^2)^{2/3}\rho^{5/3} \tag{5.12}$$

In the Thomas-Fermi theory the validity of the last equation also for particles in a non-uniform field (and hence non-uniform density) of an atom is assumed. Taking also a potential of electrons to be that from classical electrostatics

$$V_e(r) = \int_0^r \frac{1}{r_>}4\pi r'^2\rho(r')dr' \tag{5.13}$$

We obtain for the full energy of an atom

$$E = \int_0^{R_{max}} dr\left[\frac{3}{10}(3p^2)^{2/3}\rho^{5/3} + \frac{1}{2}\int_0^r \frac{1}{r_>}4\pi r'^2\rho(r')dr' - V_{nuc}(r)\right]4\pi r^2\rho(r)dr \tag{5.14}$$

with a constraint that integration over the density gives us the full number of electrons

$$\int_0^{R_{max}} 4\pi r'^2\rho(r')dr' = N \tag{5.15}$$

We want to find the minimum of the energy, so we need to vary $\frac{\delta}{\delta\rho}(E - \lambda N)$. Variation gives trivially

$$\frac{1}{2}(3\pi^2)^{2/3}\rho^{2/3} - V_{nuc} + \int_0^R \frac{1}{r_>}4\pi r'^2\rho(r')dr' = \lambda \tag{5.16}$$

We obtain λ by evaluating this expression at $r = R\,\mathrm{max}$

$$\lambda = -\frac{Z-N}{R} = V(R) \tag{5.17}$$

where $V(R)$ is a sum of the nucleus and electron potential. Expressing the electron density in terms of potential through the Laplace equation

$$\frac{1}{r}\frac{d^2}{dr^2}rV(r) = -4\pi\rho(r) \tag{5.18}$$

we obtain the following expression for the potential

$$\frac{d^2}{dr^2} r[V(R) - V(r)] = \frac{8\sqrt{2}}{3\pi} \frac{(r[V(R) - V(r)])^{3/2}}{r^{1/2}} \tag{5.19}$$

which can be solved numerically. An example of a Thomas-Fermi potential is shown in the Figure ??

The main drawback of the Thomas-Fermi model is that it clearly does not take into account the anti-fermionic nature of electrons. The exchange interaction, which will be discussed in details in the DHF chapter is completely omitted. For these reasons it does not good good results neither for atomic energies nor wavefunctions. However, modifications of this method allow to improve the results significantly.

5.2.3 Thomas-Fermi-Dirac potential

The first improvement over the Thomas-Fermi model is to include the exchange interaction of an electron gas. Through the lengthy derivation it is possible to obtain

$$\epsilon_{exc} = -\frac{3}{4} \left(\frac{3}{\pi}\right)^{1/3} \rho(r)^{4/3} \tag{5.20}$$

and leads for the equation for the potential [4]

$$\frac{d^2}{dr^2} \left[r \left(\frac{1}{\pi^2} + V(R) - V(r) \right) \right] = \frac{8\sqrt{2}}{3\pi r^{1/2}} \left[\frac{r^{1/2}}{\pi} + \left[r \left(\frac{1}{\pi^2} + V(R) - V(r) \right) \right]^{1/2} \right]^3 \tag{5.21}$$

In principle, however, exchange energy is non-local, so any local exchange energy density is just an approximation. Moreover, free gas approximation is not ideal. One of the most noticeable problems, is that both TF and TFD potentials contain self-interaction of electrons. This leads to the fact, that limiting value of $V_R = \frac{(Z-N)}{r}$, which should not be the case, because an electron far from the nucleus should feel a potential of only $N-1$ electrons.

5.2.4 Hybrid potentials

Hartree-Slater(HS), Hartree-Exchange(HX) and other most advanced effective methods use a combined scheme for the effective potential. It is partially determined self-consistently (typically the direct term) and partially from the DFT (exchange term). This means that we must solve a system of equations

$$(V_{kinetic} + V_{nuc} + V_H + V_{exc})|\psi_i\rangle = \epsilon_i |\psi_i\rangle \tag{5.22}$$

where V_H is a full electron density determined self-consistently as

$$V_H = \sum_{j \neq i} \int_0^{\inf} \frac{1}{r_>} P_j^2 dr \tag{5.23}$$

An example of a sophisticated and partially parametric potential used for the HX method [4] is

$$V_{HX} = -kf(r) \left[\frac{\rho'}{\rho' + 0.5/(n_i - l_i)} \right] \left(\frac{\rho'}{\rho} \right) \left(\frac{24\rho}{\pi} \right)^{1/3} \tag{5.24}$$

with k = 0.65 determined as a global parameter, and $f(r)$ is a function, which adjusts exchange for some particular cases. $\rho' = \rho - min(2, N_i)\rho_i$ is an adjusted density, accounting for the self-interaction and N_i is a number of electrons on a subshell which an i-th electron belongs to.

Hartree-Slater is in contrast non-parametric and also much simpler

$$V_{HS} = -\frac{3}{\pi}[\rho_s^{1/3} - (2\rho_i)^{1/3}] \tag{5.25}$$

with $\rho_s = \rho$ if $N_i \neq 1$ and $\rho_s = \rho + \rho_i$ otherwise. These potentials can be adjusted further to obtain either an analog of Dirac equation or take into account fine structure corrections (first of all spin interactions) effectively. Such sophisticated hybrid methods can produce very good ionization energies. However, they still do not fully capture complicated shapes of atomic wavefunctions. In this work it was confirmed that cross sections obtained from full self-consistent calculations are closer to experiments then effective ones as expected.

5.3 Determinantal matrix elements

Before the discussion of the Hartree-Fock method, some preliminary results should be established. We need to be able to calculate one and two particle matrix elements

$$\begin{aligned} &\langle F| \sum_i f(i) |I\rangle \\ &\langle F| \sum_{i,j} g(i,j) |I\rangle \end{aligned} \tag{5.26}$$

in the case when $\langle F|$ and $|G\rangle$ are represented by Slater determinants and $f(i)$ and $g(i,j)$ are one and two particle operators.

5.3.1 One- and two-electron operators in mutually orthogonal bases

In case if initial and final states are written in the same orthonormal basis and final and initial states are the same

$$\begin{aligned} &\langle F| \sum_i f(i) |G\rangle = \frac{1}{N!} \sum_i \sum_{\substack{a_1,\dots a_N \\ b_1,\dots,b_N}} \epsilon_{a_1,a_2,\dots a_N} \epsilon_{b_1,b_2,\dots,b_N} \times \\ &\times \int d\boldsymbol{r}_1 \dots d\boldsymbol{r}_N \psi_{a_1}(\boldsymbol{r}_1)\psi_{a_2}(\boldsymbol{r}_2)\dots\psi_{a_N}(\boldsymbol{r}_N)\psi_{b_1}(\boldsymbol{r}_1)\psi_{b_2}(\boldsymbol{r}_2)\dots\psi_{b_N}(\boldsymbol{r}_N) f(\boldsymbol{r}_i) = \\ &\frac{1}{N!} \sum_i \sum_{\substack{a_1,\dots a_N \\ b_1,\dots,b_N}} \epsilon_{a_1,a_2,\dots a_N} \epsilon_{b_1,b_2,\dots,b_N} \int d\boldsymbol{r}_i \psi_{a_i}(\boldsymbol{r}_i)\psi_{b_i}(\boldsymbol{r}_i) f(\boldsymbol{r}_i) \prod_{j!=i} \delta_{a_j,b_j} = \\ &\frac{1}{N!} \sum_i \sum_{a_1,\dots,a_N} \sum_{b_i} \epsilon_{a_1,\dots a_i,\dots a_N} \epsilon_{a_1,\dots b_i,\dots,a_N} \langle \psi_{a_i}|f(\boldsymbol{r})|\psi_{b_i}\rangle = \\ &\frac{1}{N} \sum_i \sum_{a_i,b_i} \delta_{a_i,b_i} \langle \psi_{a_i}|f(\boldsymbol{r})|\psi_{b_i}\rangle = \sum_{a_i} \langle \psi_{a_i}|f(\boldsymbol{r})|\psi_{a_i}\rangle = \sum_i f_i \end{aligned} \tag{5.27}$$

If one of the one electron wavefunctions ψ_k is different in the final state, then

$$\langle F|\sum_i f(i)|G\rangle = \frac{1}{N!}\sum_i \sum_{a_1,...a_N b_1,...,b_N} \epsilon_{a_1,a_2,...a_N}\epsilon_{b_1,b_2,...,b_N} \times$$
$$\times \int d\boldsymbol{r}_1...d\boldsymbol{r}_N \psi_{a_1}(\boldsymbol{r}_1)\psi_{a_2}(\boldsymbol{r}_2)...\psi_{a_N}(\boldsymbol{r}_N)\psi_{b_1}(\boldsymbol{r}_1)\psi_{b_2}(\boldsymbol{r}_2)...\psi_{b_N}(\boldsymbol{r}_N)f(\boldsymbol{r}_i) =$$
$$\frac{1}{N!}\sum_i \sum_{\substack{a_1,...a_N \\ b_1,...,b_N}} \epsilon_{a_1,a_2,...a_N}\epsilon_{b_1,b_2,...,b_N} \int d\boldsymbol{r}_i \psi_{a_i}(\boldsymbol{r}_i)\psi_{b_i}(\boldsymbol{r}_i)f(\boldsymbol{r}_i)\prod_{j!=i}\delta_{a_j,b_j}\delta_{b_i,k} =$$
$$\frac{1}{N!}\sum_i \sum_{a_1,...,a_N} \epsilon_{a_1,...a_i,...a_N}\epsilon_{a_1,...k,...,a_N}\langle\psi_{a_i}|f(\boldsymbol{r})|\psi_k\rangle =$$
$$\frac{1}{N}\sum_i\sum_{a_i}\delta_{a_i,k}\langle\psi_{a_i}|f(\boldsymbol{r})|\psi_{b_i}\rangle = \langle\psi_k|f(\boldsymbol{r})|\psi_k\rangle = f_{kk} \tag{5.28}$$

Finally, if there is more than one different one electron state, matrix element is identically 0.

In the same fashion, the two-electron matrix element can be derived and the result is

$$\begin{aligned}
\langle F|\frac{1}{2}\sum_{i\neq j} g(i,j)|G\rangle &= \frac{1}{2}\sum_{a_i,b_j}(\langle\psi_{a_i}\psi_{b_j}|g(\boldsymbol{r}_1,\boldsymbol{r}_2)|\psi_{a_i}\psi_{b_j}\rangle - \langle\psi_{a_i}\psi_{b_j}|g(\boldsymbol{r}_1,\boldsymbol{r}_2)|\psi_{b_j}\psi_{a_i}\rangle) \\
&= \frac{1}{2}\sum_{ij}(g_{ijij} - g_{ijji}) \text{ if all } a_i = b_i \\
\langle F|\frac{1}{2}\sum_{i\neq j} g(i,j)|G\rangle &= \sum_{a_i}(\langle\psi_{a_i}\psi_{b_k}|g(\boldsymbol{r}_1,\boldsymbol{r}_2)|\psi_{a_i}\psi_{b_k}\rangle - \langle\psi_{a_i}\psi_{b_k}|g(\boldsymbol{r}_1,\boldsymbol{r}_2)|\psi_{b_{k'}}\psi_{a_i}\rangle) = \\
&\sum_i g_{ikik'} - g_{ikk'i} \text{ if one } a_k \neq b_k \\
\langle F|\frac{1}{2}\sum_{i\neq j} g(i,j)|G\rangle &= \langle\psi_{a_l}\psi_{b_k}|g(\boldsymbol{r}_1,\boldsymbol{r}_2)|\psi_{a_{l'}}\psi_{b_{k'}}\rangle - \langle\psi_{a_l}\psi_{b_k}|g(\boldsymbol{r}_1,\boldsymbol{r}_2)|\psi_{b_k}\psi_{a_{l'}}\rangle = \\
&g_{lkl'k'} - g_{lkk'l} \text{ if } a_k \neq b_k, a_l \neq b_l
\end{aligned} \tag{5.29}$$

5.3.2 One electron matrix element between non-orthogonal one-electron wavefunctions

In case if $|F\rangle$ and $|I\rangle$ are expressed through two different non-orthonormal sets of wavefunctions, formulas becomes significantly more complicated [19]. Though there exist elegant ways to shorten the notation, explicit derivation in terms of determinants is presented below for the sake of clarity.

We start with the following lemma, proven in the Appendix 2

Lemma:

$$\langle\Psi_f|\sum_{i=1}^N f(i)|\Psi_i\rangle = \sqrt{N!}\langle\psi'_1(1)...\psi'_N(N)|\sum_{i=1}^N f(i)|\Psi_f\rangle \text{ where } \Psi_i = \{\psi_1(1)...\psi_N(N)\} \tag{5.30}$$

Using it we obtain

$$\langle\Psi_f|\sum_{i=1}^{N} f(i)|\Psi_i\rangle = \langle\{\chi(1)\psi_2'(2)...\psi_N'(N)\}|\sum_{i=1}^{N} f(i)|\{\psi_1(1)\psi_2(2)...\psi_N(N)\}\rangle$$

$$= \sqrt{N!}\langle\chi(1)\psi_2'(2)...\psi_N'(N)|\sum_{i=1}^{N} f(i)|\{\psi_1(1)...\psi_N(N)\}\rangle \tag{5.31}$$

$$= \langle\chi(1)\psi_2'(2)...\psi_N'(N)|\sum_{i=1}^{N} f(i)|\begin{vmatrix} \psi_1(1) & . & . & \psi_N(1) \\ . & . & & . \\ . & & . & . \\ \psi_1(N) & . & . & \psi_N(N) \end{vmatrix}\rangle = \sum_{i=1}^{N}\sum_{j=1}^{N}(-1)^{j+i}\times$$

$$\times\langle\chi(1)\psi_2'(2)...\psi_N'(N)|f(i)|\psi_j(i)\begin{vmatrix} \psi_1(1) & . & . & \psi_{j-1}(1) & \psi_{j+1}(1) & . & . & \psi_N(1) \\ . & . & & & & & & . \\ . & & & . & & & & . \\ \psi_1(i-1) & . & . & \psi_{j-1}(i-1) & \psi_{j+1}(i-1) & . & . & \psi_N(i-1) \\ \psi_1(i+1) & . & . & \psi_{j-1}(i+1) & \psi_{j+1}(i+1) & . & . & \psi_N(i+1) \\ . & & & & . & & & . \\ . & & & & & & . & . \\ \psi_1(N) & . & . & \psi_{j-1}(N) & \psi_{j+1}(N) & . & . & \psi_N(N) \end{vmatrix}\rangle =$$

$$= \sum_{i=1}^{N}\sum_{j=1}^{N}(-1)^{j+i}\langle\psi_i'|f(i)|\psi_j\rangle\begin{vmatrix} \langle 1'|1\rangle & . & . & \langle 1'|j-1\rangle & \langle 1'|j+1\rangle & . & . & \langle 1'|N\rangle \\ . & & & . & & & & . \\ . & & & . & & & & . \\ \langle i-1'|1\rangle & . & . & \langle i-1'|j-1\rangle & \langle i-1'|j+1\rangle & . & . & \langle i-1'|N\rangle \\ \langle i+1'|1\rangle & . & . & \langle i+1'|j-1\rangle & \langle i+1'|j+1\rangle & . & . & \langle i+1'|N\rangle \\ . & & & & . & & & . \\ . & & & & & & . & . \\ \langle N'|1\rangle & . & . & \langle N'|j-1\rangle & \langle N'|j+1\rangle & . & . & \langle N'|N\rangle \end{vmatrix}$$

Here $\langle i'|j\rangle$is a short notation for the $\langle\psi_i'|\psi_j\rangle$.

6 Dirac-Hartree-Fock solution

6.1 Closed-shell equations

The idea of this method is to find wavefunctions, which minimize the energy E of the Hamiltonian 5.1 on the space of one Slater determinant wavefunctions. In case if a linear combination of several determinants would be taken, the procedure generalizes to the so-called Multi-Configuration Dirac-Hartree-Fock (MCDHF) method.
With the help of identities from the previous section it is found

$$\langle\psi_1...\psi_N|\sum_i(c\boldsymbol{a}\cdot\boldsymbol{p_i}+\beta c^2+V_{nuclear}(\boldsymbol{r_i}))|\psi_1...\psi_N\rangle=\sum_i\langle\psi_i|c\boldsymbol{a}\cdot\boldsymbol{p}+\beta c^2+V_{nuclear}|\psi_i\rangle \tag{6.1}$$

The action of the one electron Dirac Hamiltonian was found in the Chapter 4 and with it we obtain

$$\begin{aligned}&\sum_i(\langle\psi_i|c\boldsymbol{a}\cdot\boldsymbol{p}+\beta c^2+V_{nuclear}|\psi_i\rangle=\\&\int drd\hat{r}\left(P_{n\kappa_i}\Omega^\dagger_{\kappa_i m},\ Q_{n\kappa_i}\Omega^\dagger_{-\kappa_i m}\right)\cdot\begin{pmatrix}\left((c^2+V_{nuc})P_{n\kappa_i}+c\left(\frac{\partial}{\partial r}-\frac{\kappa_i}{r}\right)Q_{n\kappa_i}\right)\Omega_{\kappa_i m}\\\left(-c\left(\frac{\partial}{\partial r}+\frac{\kappa}{r}\right)P_{n\kappa_i}+(-c^2+V_{nuc})Q_{n\kappa_i}\right)\Omega_{-\kappa_i m}\end{pmatrix}=\\&\int dr\Big(P_{n\kappa_i}(c^2+V_{nuc})P_{n\kappa_i}+cP_{n\kappa_i}\left(\frac{\partial}{\partial r}-\frac{\kappa_i}{r}\right)Q_{n\kappa_i}-cQ_{\kappa_i m}\left(\frac{\partial}{\partial r}+\frac{\kappa_i}{r}\right)P_{n\kappa_i}+\\&Q_{n\kappa_i}(-c^2+V_{nuc})Q_{n\kappa_i}\Big)=h_{ii}\end{aligned} \tag{6.2}$$

For the Coulomb repulsion

$$\langle\{\psi_1...\psi_N\}|\frac{1}{2}\sum_{i\neq j}r_{ij}^{-1}|\{\psi_1...\psi_N\}\rangle=\frac{1}{2}\sum_{ij}(\langle\psi_i\psi_j|r_{12}^{-1}|\psi_i\psi_j\rangle-\langle\psi_i\psi_j|r_{12}^{-1}|\psi_j\psi_i\rangle) \tag{6.3}$$

Let's do some transformations for the direct term. For exchange the derivation is identical. With the usage of the expansions

$$r_{12}^{-1}=\sum_{l=0}^{\infty}\frac{r_<^l}{r_>^{l+1}}P_l(cos\theta) \tag{6.4}$$

and

$$P_l(cos\theta)=\sum_{q=-l}^{l}(-1)^qC^l_{-q}(\hat{r}_1)C^l_q(\hat{r}_2) \tag{6.5}$$

it can be rewritten

$$\begin{aligned}&\langle\psi_i\psi_j|r_{12}^{-1}|\psi_i\psi_j\rangle=\sum_{l=0}^{\infty}\sum_{q=-l}^{l}\langle\psi_i\psi_j|\frac{r_<^l}{r_>^{l+1}}(-1)^qC^l_{-q}(\hat{r}_1)C^l_q(\hat{r}_2)|\psi_i\psi_j\rangle=\\&\sum_{l=0}^{\infty}\sum_{q=-l}^{l}(-1)^q\int dr_1dr_2\ \left((P^2_{n\kappa_i}(r_1)+Q^2_{n\kappa_i}(r_1))\frac{r_<^l}{r_>^{l+1}}(P^2_{n\kappa_j}(r_2)+Q^2_{n\kappa_j}(r_2))\right)\end{aligned}$$

$$\times \int d\hat{r}_1 \Omega^{\dagger}_{\kappa_i m_i}(\hat{r}_1) C^l_{-q}(\hat{r}_1) \Omega_{\kappa_i m_i}(\hat{r}_1) \int d\hat{r}_2 \Omega^{\dagger}_{\kappa_j m_j}(\hat{r}_2) C^l_q(\hat{r}_2) \Omega_{\kappa_j m_j}(\hat{r}_2) \tag{6.6}$$

Using the Wigner-Eckart theorem

$$\int d\hat{r} \Omega^{\dagger}_{\kappa_i m_i}(\hat{r}) C^l_q(\hat{r}) \Omega_{\kappa_J m_j}(\hat{r}) =$$

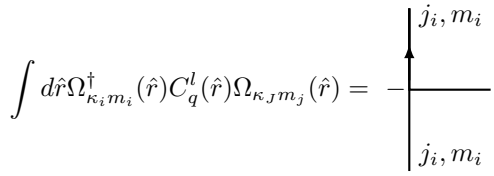

$$\langle \Omega_{\kappa_i m_i} || C^l || \Omega_{\kappa_j m_j} \rangle \tag{6.7}$$

We can work out the angular part

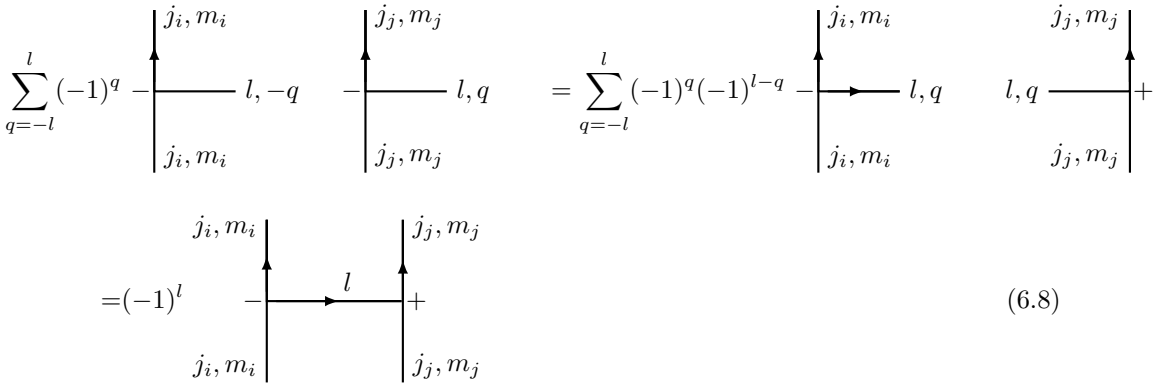

(6.8)

With a standard notation

$R^l_{iji'j'} = \int dr_1 dr_2 \; (P_{n_i\kappa_i}(r_1) P_{n_{i'}\kappa_{i'}}(r_1) + Q_{n_i\kappa_i}(r_1) Q_{n_{i'}\kappa_{i'}}(r_1)) \frac{r^l_<}{r^{l+1}_>} (P_{n_j\kappa_j}(r_1) P_{n_{j'}\kappa_{j'}}(r_1) + Q_{n_j\kappa_j}(r_1) Q_{n_{j'}\kappa_{j'}}(r_1))$

$X^l_{iji'j'} = (-1)^l R^l_{iji'j'} \langle \Omega_{\kappa_i m_i} || C^l || \Omega_{\kappa_{i'} m_{i'}} \rangle \langle \Omega_{\kappa_j m_j} || C^l || \Omega_{\kappa_{j'} m_{j'}} \rangle$

The reduced matrix element can be shown to be equal to (Appendix 2)

$$\langle \Omega_{\kappa_i m_i} || C^l || \Omega_{\kappa_j m_j} \rangle = (-1)^{j_i + 1/2} \sqrt{[j_i][j_j]} \begin{pmatrix} j_i & j_j & l \\ -1/2 & 1/2 & 0 \end{pmatrix} \prod (l_i + l_j + l) \tag{6.9}$$

We arrive to the following expression for the two-body Coulomb operator energy

$$\langle \{\psi_1 ... \psi_N\} | \frac{1}{2} \sum_{i \neq j} r^{-1}_{ij} | \{\psi_1 ... \psi_N\} \rangle =$$

$$= \frac{1}{2} \sum_{ij}$$

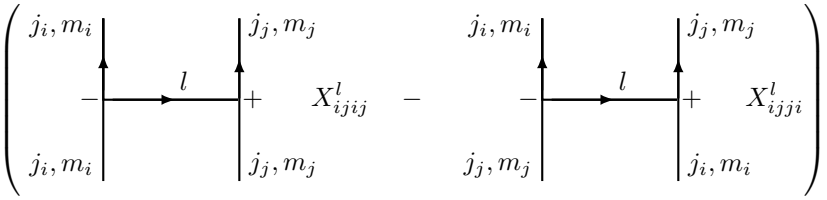

(6.10)

Till now all the derivations were exact and did not depend on which quantum numbers were used. Now we will assume that we consider a closed-shell atom. This allows to carry out the summation over all the full momenta projections. Using the fact that $X^l_i ji'j'$ does not depend on the projection of the momenta, we can sum over all m_j.

For direct term we obtain

$$\sum_{m_j}$$ 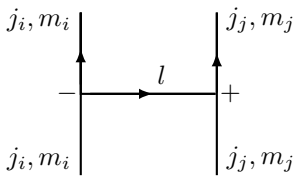

$$= \quad$$ 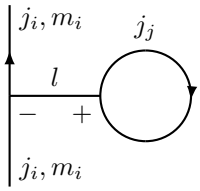

$$= \quad \delta_{l,0}\sqrt{\frac{[j_j]}{[j_i]}} \tag{6.11}$$

And for exchange

$$\sum_{m_j}$$ 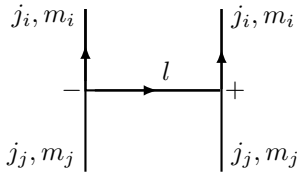

$$= \quad$$ 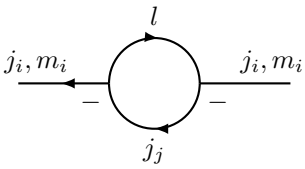

$$=$$

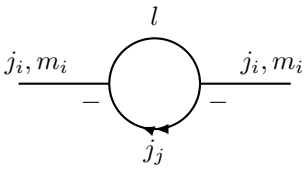

$$= (-1)^{-2j_j}(-1)^{l+j_i+j_j}$$ 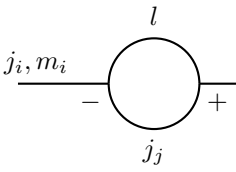

$$= (-1)^{j_i-j_j+l}\frac{1}{[j_i]} \tag{6.12}$$

Carefully gathering all the factors we get for the direct term

$$\sum_{l=0}^{\infty}\delta_{l,0}\sqrt{\frac{[j_j]}{[j_i]}}(-1)^l(-1)^{j_i-1/2}[j_i]\begin{pmatrix} j_i & j_i & 0 \\ -1/2 & 1/2 & 0\end{pmatrix}(-1)^{j_j+1/2}[j_j]\begin{pmatrix} j_j & j_j & 0 \\ -1/2 & 1/2 & 0\end{pmatrix}R^l_{ijij} = \tag{6.13}$$

$$= \sqrt{\frac{[j_j]}{[j_i]}}(-1)^l(-1)^{j_i+1/2}[j_i](-1)^{j_i+1/2}\frac{1}{[j_i]^{1/2}}(-1)^{j_j+1/2}[j_j](-1)^{j_j+1/2}\frac{1}{[j_j]^{1/2}}R^0_{ijij} = [j_j]R^0_{ijij} \tag{6.14}$$

And for the exchange

$$\sum_{l=0}^{\infty}(-1)^{j_i-j_j+l}\frac{1}{[j_i]}(-1)^l(-1)^{j_i+1/2}\sqrt{[j_i][j_j]}\begin{pmatrix} j_i & j_j & l \\ -1/2 & 1/2 & 0\end{pmatrix}(-1)^{j_j+1/2}\sqrt{[j_i][j_j]}\begin{pmatrix} j_j & j_i & l \\ -1/2 & 1/2 & 0\end{pmatrix}\times$$

$$\times\prod(l_i+l_j+l) = \sum_{l=0}^{\infty}(-1)^{2j_a+1}[j_j](-1)^{2(j_a+j_b+1)}[j_j]\begin{pmatrix} j_i & j_j & l \\ -1/2 & 1/2 & 0\end{pmatrix}^2\times$$

$$\times \prod (l_i + l_j + l) R^l_{ijji} = \sum_{l=|j_i - j_j|}^{j_i + j_j} [j_j] \begin{pmatrix} j_i & j_j & l \\ -1/2 & 1/2 & 0 \end{pmatrix}^2 \prod (l_i + l_j + l) R^l_{ijji} \tag{6.15}$$

So the final expression for the DHF energy is

$$\langle \{\psi_1 ... \psi_N\} | H | \{\psi_1 ... \psi_N\} \rangle = \sum_{n_i, \kappa_i} [j_i] \left(h_{ii} + \frac{1}{2} \sum_{n_j, \kappa_j} [j_j] \left(R^0_{ijij} - \sum_l \Lambda_{ijl} R^l_{ijji} \right) \right) \tag{6.16}$$

where the notation $\Lambda_{ijl} = \begin{pmatrix} j_i & j_j & l \\ -1/2 & 1/2 & 0 \end{pmatrix}^2 \prod (l_i + l_j + l)$ was introduced. The fact that neither one- nor two-body energy depends on m_i, so sum over the projections led to the prefactor $[j_i]$ in front of the brackets.

To complete the derivation of DHF equations, we need to find those one electron ψ_i that minimize the full energy. We want to obtain an orthonormal set, so we must impose constraints on the wavefunctions with the different principal quantum number, but the same angular part.

$$\int dr (P_{n_a, \kappa_a}(r) P_{n_b, \kappa_b}(r) + Q_{n_a, \kappa_a}(r) Q_{n_b, \kappa_b}(r)) = \delta_{n_a, n_b} \tag{6.17}$$

So we should solve a variation task

$$\delta (E_{DHF} - \sum_{i,j} \lambda_{i,j} \delta_{\kappa_i, \kappa_j} \int dr (P_{n_i, \kappa_j}(r) P_{n_i, \kappa_j}(r) + Q_{n_i, \kappa_a}(r) Q_{n_j, \kappa_j}(r)) = 0 \tag{6.18}$$

which is equivalent to the following system in terms of functional derivatives

$$\frac{\delta}{\delta P_k} (E_{DHF} - \sum_{i,j} \lambda_{i,j} \delta_{\kappa_i, \kappa_j} \int dr (P_{n_i, \kappa_j}(r) P_{n_i, \kappa_j}(r) + Q_{n_i, \kappa_a}(r) Q_{n_j, \kappa_j}(r)) = 0 \tag{6.19}$$

$$\frac{\delta}{\delta Q_k} (E_{DHF} - \sum_{i,j} \lambda_{i,j} \delta_{\kappa_i, \kappa_j} \int dr (P_{n_i, \kappa_j}(r) P_{n_i, \kappa_j}(r) + Q_{n_i, \kappa_a}(r) Q_{n_j, \kappa_j}(r)) = 0 \tag{6.20}$$

Let's vary this expression part by part. First, taking the derivative of one electron part w.r.t. P_k. As usual, we assume that variation vanishes on the boundaries.

$$\begin{aligned} &\frac{\delta}{\delta P_k} \sum_i [j_i] \int dr \left[P_i (V_{nuc} + c^2) P_i + c P_i \left(\frac{d}{dr} - \frac{\kappa}{r} \right) Q_i - c Q_i \left(\frac{d}{dr} + \frac{\kappa}{r} \right) P_i + Q_i \left(V_{nuc} - c^2 \right) Q_i \right] \\ &= [j_k] \left[2 P_k (V_{nuc} + c^2) + c \left(\frac{d}{dr} - \frac{\kappa}{r} \right) Q_k - c \left(-\frac{d}{dr} - \frac{\kappa}{r} \right) Q_c \right] \\ &= 2 [j_k] \left[P_k (V_{nuc} + c^2) + c \left(\frac{d}{dr} - \frac{\kappa}{r} \right) Q_k \right] \end{aligned} \tag{6.21}$$

Then we vary the two-electron part

$$\frac{\delta}{\delta P_k} \left(\frac{1}{2} \sum_{ij} [j_i][j_j] \int dr_1 dr_2 \Big[\left(P_i^2(r_1) + Q_i^2(r_1) \right) \frac{r_<^l}{r_>^{l+1}} \left(P_j^2(r_2) + Q_j^2(r_2) \right) -$$

$$- \sum_l -\Lambda_{ilj} \left(P_i(r_2)P_j(r_2) + Q_i(r_2)Q_j(r_2)\right) \frac{r_<^l}{r_>^{l+1}} \left(P_i(r_2)P_j(r_2) + Q_i(r_2)Q_j(r_2)\right) \Bigg] \Bigg)$$
$$= 2\sum_i [j_k][j_i] \Bigg[P_k \int dr \frac{r_<^l}{r_>^{l+1}} \left(P_i^2 + Q_i^2\right) - \sum_l \Lambda_{ilj} P_i \int dr \frac{r_<^l}{r_>^{l+1}} \left(P_i P_k + Q_i Q_k\right) \Bigg] \tag{6.22}$$

Finally, variation of the constraint gives us

$$\frac{\delta}{\delta P_k} \sum_{ij} \lambda_{ij} \delta_{\kappa_i,\kappa_j} \int dr (P_a P_b + Q_a Q_b) = 2 \sum_i \lambda_{ik} \delta_{\kappa_i,\kappa_k} P_i = 2(\lambda_{kk} P_k + \sum_{i \neq k} \lambda_{ik} \delta_{\kappa_i,\kappa_k} P_i) \tag{6.23}$$

Together with analogous derivatives for Q_k we arrive to the system of Dirac-Hartree-Fock equations

$$\begin{aligned}
&(V_{nuc} P_k + c^2) + c\left(\frac{d}{dr} - \frac{\kappa}{r}\right) Q_k + \sum_i [j_i](\nu_{0i} P_k - \sum_l \Lambda_{ilk} \nu_{lki} P_i) = \epsilon_k P_k + \sum_{i \neq k} \epsilon_{ik} \delta_{\kappa_i,\kappa_k} P_i \\
&(V_{nuc} - c^2) Q_k - c\left(\frac{d}{dr} + \frac{\kappa}{r}\right) P_k + \sum_i [j_i](\nu_{0i} Q_k - \sum_l \Lambda_{ilk} \nu_{lki} Q_i) = \epsilon_k Q_k + \sum_{i \neq k} \epsilon_{ik} \delta_{\kappa_i,\kappa_k} Q_i
\end{aligned} \tag{6.24}$$

Where the following notation was introduced

$\nu_{lki}(r) = \int dr' (P_k(r')P_i(r') + Q_k(r')Q_i(r')) \frac{r_<^l}{r_>^{l+1}}$ is a so-called screening potential
$\nu_{lii} = \nu_{li}$
$\epsilon_{ik} = \frac{\lambda_{ik}}{[j_k]}$
$\epsilon_k = \epsilon_{kk}$ will turn out to be a one electron-energy.

Another useful notation is
$V_{HF} P_k = \sum_i [j_i](\nu_{0i} P_k - \sum_l \Lambda_{ilk} \nu_{lki} P_i)$ With it we can rewrite 6.24 compactly as

$$\begin{aligned}
&(V_{nuc} + c^2 + V_{HF}) P_k + c\left(\frac{d}{dr} - \frac{\kappa}{r}\right) Q_k = \epsilon_k P_k + \sum_{i \neq k} \epsilon_{ik} \delta_{\kappa_i,\kappa_k} P_i \\
&(V_{nuc} - c^2 + V_{HF}) Q_k - c\left(\frac{d}{dr} + \frac{\kappa}{r}\right) P_k = \epsilon_k Q_k + \sum_{i \neq k} \epsilon_{ik} \delta_{\kappa_i,\kappa_k} Q_i
\end{aligned} \tag{6.25}$$

We still need to ensure the orthogonality of the wavefunctions, i.e., find the values of the Lagrangian multipliers and hence energies ϵ_{ik}.Let's consider equations for two subshells j and k and multiply P_j, Q_j equations with P_k, Q_k, P_k, Q_k equations with P_j, Q_j and integrate the resulting equations over r. We obtain

$$(1) \int dr P_j (V_{nuc} + c^2 + V_{HF}) P_k + c \int dr P_j \left(\frac{d}{dr} - \frac{\kappa}{r}\right) Q_k = \epsilon_k \int dr P_j P_k + \sum_{i \neq k} \epsilon_{ik} \delta_{\kappa_i,\kappa_k} \int dr P_j P_i$$

$$(2) \int dr Q_j (V_{nuc} - c^2 + V_{HF}) Q_k - c \int dr Q_j \left(\frac{d}{dr} + \frac{\kappa}{r}\right) P_k = \epsilon_k \int dr Q_j Q_k + \sum_{i \neq k} \epsilon_{ik} \delta_{\kappa_i,\kappa_k} \int dr Q_j Q_i$$

$$(3)\ \int drP_k(V_{nuc}+c^2+V_{HF})P_j + c\int drP_k\left(\frac{d}{dr}-\frac{\kappa}{r}\right)Q_j = \epsilon_j\int drP_kP_j + \sum_{i\neq j}\epsilon_{ij}\delta_{\kappa_i,\kappa_j}\int drP_jP_i$$

$$(4)\ \int drQ_k(V_{nuc}-c^2+V_{HF})Q_j - c\int drQ_k\left(\frac{d}{dr}+\frac{\kappa}{r}\right)P_j = \epsilon_j\int drQ_kQ_j + \sum_{i\neq j}\epsilon_{ij}\delta_{\kappa_i,\kappa_j}\int drQ_kQ_i$$

Let's evaluate (1) + (2) - (3) - (4). Using the facts that $\int drP_j\nu_{0i}P_k = \int drP_k\nu_{0i}P_j$ and $\int drP_j\nu_{lki}P_k = \int drP_k\nu_{lki}P_j$, we see that the first term contracts and the rest on the left hand side becomes

$$c\int dr\left[P_j\left(\frac{d}{dr}-\frac{\kappa}{r}P_k\right) - Q_j\left(\frac{d}{dr}+\frac{\kappa}{r}\right)P_k - P_k\left(\frac{d}{dr}-\frac{\kappa}{r}\right)Q_j + Q_k\left(\frac{d}{dr}+\frac{\kappa}{r}\right)Q_j\right]$$
$$= c\int dr\left[\frac{d}{dr}(P_jQ_k) - \frac{d}{dr}(Q_jP_k)\right] = c(P_jQ_k - Q_jP_k)|_0^\infty = 0 \tag{6.26}$$

And the right hand side is

$$(\epsilon_k-\epsilon_j)\int dr\psi_j^\dagger\psi_k + \sum_{i\neq k}\epsilon_{ik}\delta_{\kappa_i,\kappa_k}\int dr\psi_i^\dagger\psi_j - \sum_{i\neq j}\epsilon_{ij}\delta_{\kappa_i,\kappa_j}\int dr\psi_i^\dagger\psi_k \tag{6.27}$$

The simplest choice here is to take all ϵ_{ij} to be 0. Then we have for $\epsilon_k \neq \epsilon_j$ that

$$(\epsilon_k-\epsilon_j)\int dr\psi_j^\dagger\psi_k = 0 \tag{6.28}$$

which implies the orthogonality on ψ_j and ψ_k.

Multiplying equations 6.25 with P_i and Q_i respectively, summing them up and integrating, the following expression is obtained.

$$\langle\psi_k|h+V_{HF}|\psi_k\rangle = \epsilon_k \tag{6.29}$$

The full energy is

$$E_{\psi_1\ldots\psi_N} = \sum_i[j_i]\left(h_{ii} + \frac{1}{2}\sum_j[j_j]\left(R^0_{ijij} - \sum_l\Lambda_{ijl}R^l_{ijji}\right)\right) =$$
$$\sum_k[j_k]\langle\psi_k|h+\frac{1}{2}V_{HF}|\psi_k\rangle = \sum_k[j_k]\langle\psi_k|\epsilon_k - \frac{1}{2}V_{HF}|\psi_k\rangle \tag{6.30}$$

Examples of DHF equations for closed shells atoms are those for helium

$$(V_{nuc}+c^2+\nu_{01s})P_{1s} + c\left(\frac{d}{dr}-\frac{\kappa}{r}\right)Q_{1s} = \epsilon_{1s}P_{1s}$$
$$(V_{nuc}-c^2+\nu_{01s})Q_{1s} - c\left(\frac{d}{dr}+\frac{\kappa}{r}\right)P_{1s} = \epsilon_{1s}Q_{1s} \tag{6.31}$$

and for beryllium

$$(V_{nuc} + c^2 + \nu_{0,1s} + 2\nu_{0,2s})P_{1s} + c\left(\frac{d}{dr} - \frac{\kappa}{r}\right)Q_{1s} - \nu_{0,1s,2s}P_{2s} = \epsilon_{1s}P_{1s}$$

$$(V_{nuc} - c^2 + \nu_{0,1s} + 2\nu_{0,2s})Q_{1s} - c\left(\frac{d}{dr} + \frac{\kappa}{r}\right)P_{1s} - \nu_{0,1s,2s}Q_{2s} = \epsilon_{1s}Q_{1s} \tag{6.32}$$

$$(V_{nuc} + c^2 + 2\nu_{0,1s} + \nu_{0,2s})P_{2s} + c\left(\frac{d}{dr} - \frac{\kappa}{r}\right)Q_{2s} - \nu_{0,1s,2s}P_{1s} = \epsilon_{2s}P_{2s}$$

$$(V_{nuc} - c^2 + 2\nu_{0,1s} + \nu_{0,2s})Q_{2s} - c\left(\frac{d}{dr} + \frac{\kappa}{r}\right)P_{2s} - \nu_{0,1s,2s}Q_{1s} = \epsilon_{2s}Q_{2s} \tag{6.33}$$

Example of DHF solutions for a heavy atom is plotted in the Figure 7.

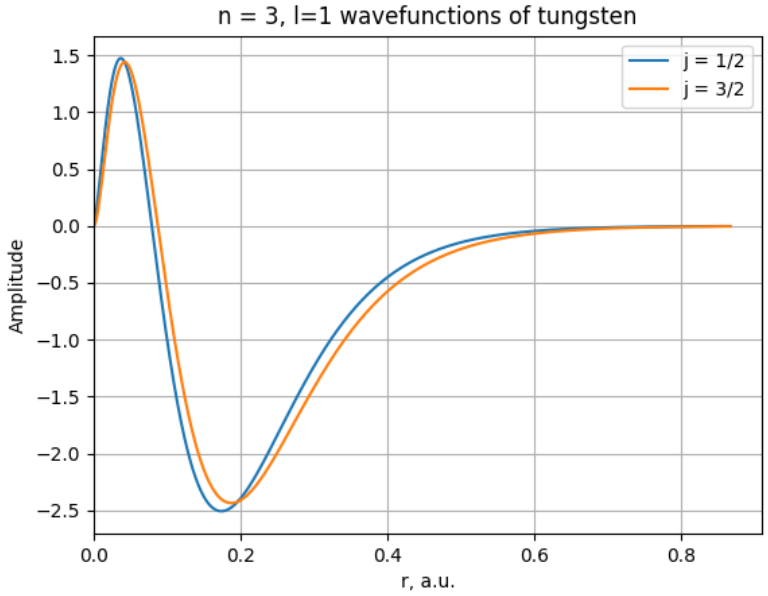

Figure 7: DHF solutions for $M_{2,3}$ shells of Tungsten clearly shows relativistic splitting between orbitals with the same PQN and angular momentum (of a big component)

6.2 Open shell equations

Equations derived above are only valid for closed shells. The physical reason for this is that Coulomb repulsion operator does not commute with operators of one electron angular momenta l_i, but only with an operator of full angular momentum L and hence with J. As a result we should evaluate the matrix element $\langle j_1 m_1 ... j_N m_N JM|H|j_1 m_1 ... j_N m_N JM\rangle$ instead of the one electron one.

6.2.1 One valence electron

In case of one valence electron we can still use closed-shell DHF equations. This can be seen directly from the fact that in such a state still has only one possible value of the full J. It can also be traced through the derivation of closed shells equations that all the diagrams involved include at most one valence electron. Hence if we first choose to sum over a closed shell, no steps are affected except for the fact that $[j_v] = 1$. The full energy is then

$$E_{full} = E_{closed} + E_v = E_{closed} + \langle \psi_v | h + V_{HF} | \psi_v \rangle \tag{6.34}$$

If instead of one valence electron there is a hole, these considerations are still fair. We only need to subtract corresponding matrix elements instead of adding them.

$$E_{full} = E_{closed} - E_h = E_{closed} - \langle \psi_h | h + V_{HF} | \psi_h \rangle \tag{6.35}$$

This shows that the removal energy of one electron, i.e. ionization energy of the closed shell atom, is

$$E_{ionisation} = E_{atom} - E_{ion} = \langle \psi_h | h + V_{HF} | \psi_h \rangle \tag{6.36}$$

This statement is known as Koopman's theorem. However, results obtained with its help are generally in a poor agreement with experiment. The problem is an implicit assumption made that matrix elements of both atom and ion are evaluated in the same basis ψ_i, i.e., the same self-consistent field. However, wavefunctions obtained from the DHF system for atom and ion are different, which leads to the necessity to solve DHF equations twice. Changes in the basis wavefunctions caused by a removal of an electron are called *relaxation*. More detailed discussion of the relaxation and its connection to the perturbation theory will be given later.

6.2.2 Two valence electrons

When we have two valence electrons we should adjust our calculations of the DHF energy. We can separate the energy contributions in three parts

$E_{full} = E_{closed-closed} + E_{closed-open} + E_{open-open}$.

$E_{closed-closed}$ and $E_{closed-open}$ can be evaluated as above, so the correction comes from the electrons on the open shells. The energy is different in different coupled states $|j_1 m_1 j_2 m_2 JM\rangle$. We need to compute the action of the Coulomb operator on the coupled states

$$\langle (j_1 m_1 j_2 m_2) JM | r_{12}^{-1} | (j_3 m_3 j_2 m_2) JM \rangle = \sum_{\substack{m_1, m_2 \\ m_3, m_2}} \langle j_1 m_1 j_2 m_2 |$$

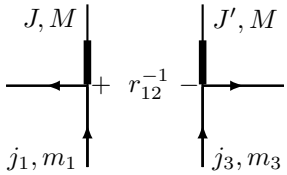

$$| j_3 m_3 j_2 m_2 \rangle$$

Direct term is

$$\sum_{l=0}^{\infty}(-1)^l X^l_{1212}$$

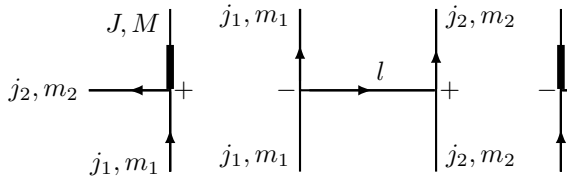

$$=$$

$$\sum_{l=0}^{\infty} X^l_{1212}$$

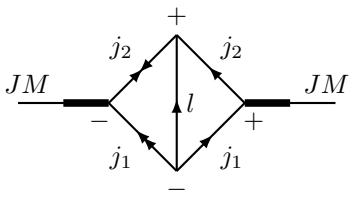

$$= \sum_{l=0}^{\infty} X^l_{1212}(-1)^{2j_1}$$

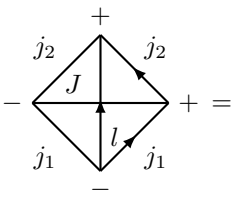

$$+ =$$

$$\sum_{l=0}^{\infty} X^l_{1212}(-1)^{2j_1}(-1)^{2j_2}(-1)^{2j_1}(-1)^{j_2+l+j_2}(-1)^{j_2+j_1+J}$$

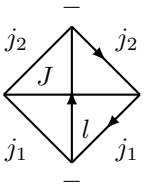

$$+ =$$

$$\sum_{l=0}^{\infty} X^l_{1212}(-1)^{l+j_1+j_2+J} \begin{Bmatrix} j_2 & j_1 & J \\ j_1 & j_2 & l \end{Bmatrix} = \sum_{l=0}^{\infty} X^l_{1212}(-1)^{l+j_1+j_2+J} \begin{Bmatrix} j_1 & j_1 & l \\ j_2 & j_2 & J \end{Bmatrix} \tag{6.37}$$

And for the exchange the derivation is similar, we only need to exchange j_1 with j_2 on the one pair of legs on the Coulomb diagram. The result is

$$\sum_{l=0}^{\infty} X^l_{1221}(-1)^{l+j_1+j_2+1} \begin{Bmatrix} j_1 & j_2 & l \\ j_1 & j_2 & J \end{Bmatrix} \tag{6.38}$$

So

$$E_{dir} - E_{exc} = \sum l \left(X^l_{1212}(-1)^{l+j_1+j_2+J} \begin{Bmatrix} j_1 & j_1 & l \\ j_2 & j_2 & J \end{Bmatrix} + X^l_{1221}(-1)^{l+j_1+j_2} \begin{Bmatrix} j_1 & j_2 & l \\ j_1 & j_2 & J \end{Bmatrix} \right) \tag{6.39}$$

As an example we can write the expressions for the carbon atom

$$\begin{aligned}
&1s^2_{1/2}2s^2_{1/2}2p^2_{1/2}[J=0] && E = F^0 \\
&1s^2_{1/2}2s^2_{1/2}2p_{1/2}2p_{3/2}[J=1] && E = F^0 - \frac{5}{25}G^2_{1/2,3/2} \\
&1s^2_{1/2}2s^2_{1/2}2p_{1/2}2p_{3/2}[J=2] && E = F^0 - \frac{1}{25}G^2_{1/2,3/2} \\
&1s^2_{1/2}2s^2_{1/2}2p^2_{3/2}[J=0] && E = F^0 + \frac{5}{25}G^2_{3/2,3/2}
\end{aligned}$$

$$1s^2_{1/2}2s^2_{1/2}2p^2_{3/2}[J=2] \qquad E = F^0 - \frac{3}{25}G^2_{3/2,3/2} \tag{6.40}$$

Where $F^l_{12} = R^l_{1212}$ and $G^l_{12} = R^l_{1221}$
There is of no surprise, that $2p^2_{1/2}$ state comes without any correction beyond the regular DHF energy, as this state for the relativistic case is a closed shell. It is interesting to compare these results with a non-relativistic case. It is known, that for light atoms spin-orbital interaction is negligible and LS coupling is a good representation of atomic states. In LS coupling carbon has three terms ^1S,^3P,^1D and their energies are

$$\begin{aligned} 1s^2 2s^2 2p^2[^1S] &= F^0_{2p2p} + \frac{10}{25}F^2_{2p2p} \\ 1s^2 2s^2 2p^2[^1D] &= F^0_{2p2p} + \frac{1}{25}F^2_{2p2p} \\ 1s^2 2s^2 2p^2[^3P] &= F^0_{2p2p} - \frac{5}{25}F^2_{2p2p} \end{aligned} \tag{6.41}$$

In both cases we have 15 magnetic substates and if we compute an average energy for a magnetic substate and take into account that in a non-relativistic case $p_{1/2}$ and $p_{3/2}$ are the same state p and $G^l_{11} = F^l_{11}$, then

$$E_{av} = F^0 + \frac{1}{15}(-3\frac{5}{25} - 5\frac{1}{25} + 1\frac{5}{25} - 5\frac{3}{25})F^2 = F^0 - \frac{2}{25}F^2 \tag{6.42}$$

in relativistic case and

$$F^0 + \frac{1}{15}(1\frac{10}{25} + 5\frac{1}{25} - 9\frac{5}{25})F^2 = F^0 - \frac{2}{25}F^2 = F^0 - \frac{2}{25}F^2 \tag{6.43}$$

They turn out to be the same. As expected, average energy does not depend on the coupling scheme.

6.2.3 Three and more valence electrons

When we deal with more than two valence electrons situation complicates even further. For three electron couplings, we need to introduce so-called coefficients of fractional parentage (or grandparentage) in order to achieve the antisymmetrization of the final states. Calculations of all possible atomic states become very cumbersome. Besides, valence structure of atoms is often strongly affected by the chemical bonds, so the computations of the coupled states must be performed taking this fact into account. Moreover, they are actually not needed, as we expect that valence electrons do not affect a lot inner shells, so for the inner shell spectroscopy we do not need to worry about all the details of the atomic states. This is why another approach is followed in the current work.

6.2.4 Average configuration energy

We saw that the average configuration energy does not depend on the way of computing it. Then it does not depend on which basis we are computing it, so we can go from coupled states to the "configuration" state of uncoupled electrons. So instead of computing the

average energy in atomic states, we can compute the average interaction energy between electrons on the open shells.

Average interaction energy between two open shells
From the derivation of the DHF energy we know the full interaction energy between two shells. We assume that interaction energy between any two electrons is identical. So if we have on the q_1 electrons of $[j_1]$ possible on the first shell and q_2 electrons of $[j_2]$ possible on the second shell, then they have $q_1 q_2$ electron interactions. The amount of interactions between electrons two closed shells is $[j_1][j_2]$. Then the average interaction energy between this two shells is

$$E_{av} = \frac{q_1 q_2}{[j_1][j_2]} E_{closed}. \tag{6.44}$$

Average interaction energy of electrons on the same open shell
The closed shell j contains $\frac{[j]([j]-1)}{2}$ interactions between electrons. In case if there are q electrons on this shell, energy of their interaction is then

$$E_{av} = \frac{q(q-1)}{[j]([j]-1)} E_{closed} \tag{6.45}$$

6.3 Continuum wavefunction

To obtain accurate cross-sections, it is crucial to compute continuum wavefunctions in the field of a relaxed ion. As soon as we have wavefunctions, obtained in a self-consistent field of an ion, we can find a continuum wavefunction from the equations

$$(V_{nuc} + c^2 + V_{HF})P_\epsilon + c\left(\frac{d}{dr} - \frac{\kappa}{r}\right)Q_\epsilon = \epsilon_\epsilon P_\epsilon \tag{6.46}$$

$$(V_{nuc} - c^2 + V_{HF})Q_\epsilon - c\left(\frac{d}{dr} + \frac{\kappa}{r}\right)P_\epsilon = \epsilon_\epsilon Q_\epsilon \tag{6.47}$$

To illustrate why the relaxation is important, atomic and ionic wavefunctions for the same shells of Tungsten are plotted in the Figure 6.3. It is noticeable that an M_5 wavefunction almost does not change after the ionization. The reason can be understood with the help of following considerations. M_5 is a deep shell for Tungsten, which means that it feels most of nuclear charge unscreened (say, $\sim 50e$). Then, removing an electron from a shell below (in this case from the same shell) only changes the attractive potential by several percent. In contrast, for a valence electron, which is O_4 shell for Tungsten, the nucleus charge is almost completely screened. The O_4 electron feels a charge of order ~ 1. This is why removing one electron from an inner shell affects strongly the shape of valence wavefunctions. This discussion leads to the conclusion, that major corrections to the cross sections occur due to the change of valence electron wavefunctions. In principle, outer wavefunctions are not sensitive to what electron was removed from inner shells. The most important correction is a change in the total charge felt by outer electrons. For this reason it is possible to use instead of the full relaxation the so-called $Z + 1$ approximation, when instead of removing an electron from, one additional proton is added to the nucleus. It will be shown in the Appendix 5 that results, obtained in this approximation, are close to results, obtained from

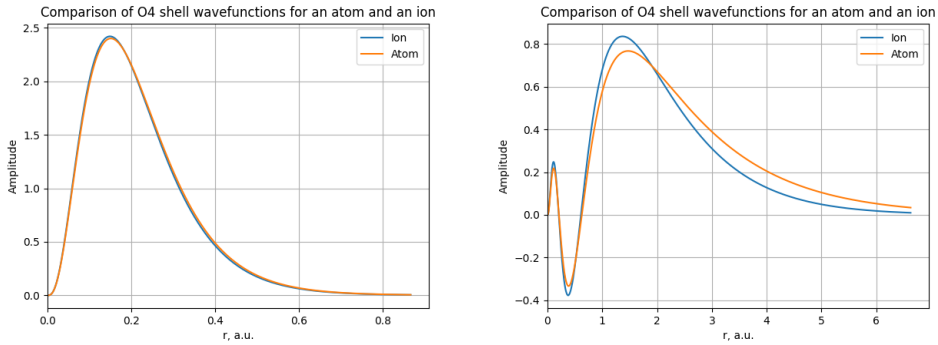

Figure 8: Comparison of M_5 and O_4 shells for an atom and an ion of Tungsten. Ion misses one M_3 electron

the fully consistent relaxation.

In principle, the continuum equation should be solved self-consistently with DHF equations for bound states. It is especially important for small energies, where a slow electron can polarize the core. However, these calculations also require to solve the whole DHF system for every continuum wave separately. Assuming, that we need to compute energy loss for 50 energy points for 11 values of κ, we need to solve the DHF system roughly 600 times for a single element. For heavy elements such as Tungsten, a single DHF system takes several minutes to be solved in AMBiT. Solving all the equations self-consistently it would take more than a day, to get the results for a single shell of Tungsten. In practice, this is unfeasible except for, may be, calculations on clusters or GPU. However, it would be interesting to obtain self-consistent solutions for several energy points and several elements, to check how much the result is affected by a back reaction of an ionized electron. In the current work such calculations were not performed. This is a known limitation of our results. However, the overall cross section shape for the case of an ionized electron which escapes the atom is not affected, even though small changes at low energies of the outgoing electron are possible.

It can be shown (Appendix 4) that for outgoing waves to be normalized on the energy scale

$$\int [P_\epsilon(r)P'_\epsilon(r) + Q_\epsilon(r)Q'_\epsilon(r)]dr = \delta(\epsilon' - \epsilon) \tag{6.48}$$

we should take the amplitude of a free wave at infinity to be

$$A_\epsilon = \sqrt{\frac{k_\epsilon}{\pi\epsilon}} \tag{6.49}$$

6.4 Nucleus model

The density distribution inside the nucleus was approximated by a Fermi model

$$\rho(r) = \frac{\rho_0(r)}{1 + exp(B(r - r_0))} \tag{6.50}$$

where $B = \frac{4log3}{T}$, T is a nuclear thickness, taken to be a constant equal $2.3fm$ and r_0 is defined in terms of atomic mass as

$$r_0 = 0.836 * A + 0.57 \tag{6.51}$$

Comparison of results for different nuclear models can be found, for example, in [23].

We provide a following table for a comparison between our computations those of [11]. Small difference in energies for a $1s_{1/2}$ subshell are, most probably, due to the fact that in [11] a more sophisticated nuclear potential is used.

	Intelicato	Computed
$1s_{1/2}$	88498.39	88492.35
$2p_{3/2}$	13079.67	13079.59
$K\alpha$	75418.73	75412.67

Table 2: Ionization and transition energies for lead, Z = 82.

Another comparison with [23] is done for the full energy of an atom. The table also illustrates the difference between point nucleus and Fermi models.

	Vesscher	Computed
Point charge	20919.61	20919.67
Fermi model	20913.67	20913.18

Table 3: Full DHF energy of an atom for lead, Z = 82. Energies are expressed in Hartree.

Fineally, the following table compares results from [11] and [18] for computations with a Breit interaction, divided into magnetic and retardation ones, included.

	Intelicato	Mann
Coulomb	88498.39	88502.49
Magnetig	-355.02	-344.75
Retardation	33.3	21.69
Total	88176.7	88179.4

Table 4: Contributions for the ionization energy for $1s_{1/2}$ level, Z = 82.

Correspondence of calculated energies and those in literature was used to validate the correctness of our DHF calculations. Nevertheless, in cross section calculations experimental energies [20], [1], [21] are used to improve the results [2].

7 Inelastic scattering

7.1 Cross section

If we have an incoming flux of particles with a momentum k and some localized potential V, then define a scattering cross section on this potential as

$$d\sigma_{\alpha\beta}(\rho) = \frac{dN_{scattered}(\rho)}{dN_{incoming}(\rho)/dS} \tag{7.1}$$

where ρ is a point in the plane perpendicular to the momenta of incoming particles and

$$\begin{aligned} \frac{dN_{incoming}}{dS} &= \int dt \Phi(\rho, t) \\ dN_{scattered} &= \int dt \omega_\rho(\alpha \to \beta) \Phi(\rho, t) \end{aligned} \tag{7.2}$$

Here $\omega_\rho(\alpha \to \beta)$ is a probability for the particle to scatter from a state α to a state β. We can only measure $\sigma_{\alpha\beta}$ averaged over some area S

$$\sigma_{\alpha\beta} = S \frac{\int dt \int d^2\rho \omega_\rho(\alpha \to \beta)(t) \Phi_\alpha(\rho, t)}{\int dt \int d^2\rho \Phi_\alpha(\rho, t)} \tag{7.3}$$

If we now assume that probabilities and the incoming flux do not depend on time and also that later does not depend on ρ, then we can simplify and get

$$\sigma_{\alpha\beta} = \int d^2\rho \omega_\rho(\alpha \to \beta) \tag{7.4}$$

In quantum mechanics, however, the number of incoming particles is not a very well defined notion, so additional considerations should be taken into account.

7.2 The S-matrix

Suppose we have a Hamiltonian

$$H = H_0 + V_{int} \tag{7.5}$$

where H_0 is a Hamiltonian of the free particle and V_{int} describes its interaction with a scattering centre. We want to consider the evolution of the particle from its initial state $|i\rangle$ to the final state $|f\rangle$. In the Schrodinger picture it is done by the evolution operator

$$|\psi_S\rangle_t = U(t, t_0)|\psi_S\rangle_{t_0} = Te^{-i\int_{t_0}^{t} H(t)dt}|\psi_S\rangle_{t_0} \tag{7.6}$$

The scattering task is, however, solved conveniently in another basis - so-called Dirac or interaction picture. The transformation is

$$|\psi_D\rangle = e^{iH_0 t}|\psi_S\rangle \tag{7.7}$$

Then Schrodinger equation transforms as

$$i\frac{\partial}{\partial t}|\psi_D\rangle = i\frac{\partial}{\partial t}(e^{iH_0t}|\psi_S\rangle) = -H_0e^{iH_0t}|\psi_S\rangle + e^{iH_0t}(H_0+V)|\psi_S\rangle = e^{iH_0t}|\psi_S\rangle = V_D|\psi_D\rangle \tag{7.8}$$

which shows that in Dirac picture only the interaction Hamiltonian determines the evolution of the state. It immediately leads to the following expression for the evolution operator

$$|\psi_D\rangle_t = U(t,t_0)|\psi_D\rangle_{t_0} = Te^{-i\int_{t_0}^{t}V(t)dt}|\psi_D\rangle_{t_0} = 1 - i\int_{t_0}^{t}dt'V(t') - \int_{t_0}^{t}dt'V(t')\int_{t_0}^{t'}dt''V(t'') + ... \tag{7.9}$$

For the scattering task we are interested in the transformation of the state $|i\rangle$ at $t=-\infty$ to the state $|f\rangle$ at $t=+\infty$. The corresponding operator is called S-matrix [13].

$$S = U(\infty,-\infty) \tag{7.10}$$

If we cut the series for S at the first term then

$$\langle f|S|i\rangle = \delta(f-i) - i\lim_{t\to\infty}\left[\lim_{\epsilon\to 0}\int_{-\infty}^{t}dt'e^{i\omega_{fi}t'+\epsilon t'}\langle f|V|i\rangle\right] = \delta(f-i) - 2\pi i\delta(E_f-E_i)\langle f|V|i\rangle \tag{7.11}$$

where the limits are taken in a way to ensure that $U(-\infty,-\infty)=1$. We also implicitly assumed here that initial and final states have a well-defined energy. In case of wave packets we will have to integrate as shown in the next section.

This approximation is equivalent to the Lippman-Swinger equation or the Born row at the first order. It can be shown that it works better with the increase in the energy of incoming particles. In the work we consider the beam of relativistically fast electrons and consider the approximation to be sufficient.

The first δ-function in the expression describes a propagation of the incoming wave without scattering, so we will from now consider only the second term with the notation $T_{\beta\alpha} = \langle\beta|V|\alpha\rangle$ the expression for the probability of the transition becomes

$$\omega(\alpha\to\beta) = |\langle\beta|V|\alpha\rangle|^2\delta^2(E_\beta - E_\alpha) \tag{7.12}$$

The scattering cross section in the following chapters is worked out in the formalism of non-relativistic Schrodinger solutions but with a relativistic dispersion relation as it is tricky to work with Dirac spinors out of the field theory context. It can be shown that a strict QED derivation gives the same result in a low energy limit.

7.3 Wave packets scattering

A most natural choice for the $|i\rangle$ and $|f\rangle$ can be thought to be plane waves. However, plane waves are not square integrable, so they do not represent particles and formulas for the cross section must be adjusted. States that naturally adopt the classical treatment are wave packets centered around some p_0 and normalized by unity [25]. We will denote with α the rest of the quantum numbers of the wave packet independent of $\boldsymbol{p}$ (such as spin or full momenta). For a wave packet $|\varphi_\rho\rangle = \int d^3\boldsymbol{p} e^{-i\rho p_\perp}\varphi(\boldsymbol{p})|\boldsymbol{p},\alpha\rangle$ scattered to a state $|p,\beta\rangle$, where we should integrate over all the possible p, we can write

$$\int d^2\rho\omega(\varphi_\rho \to \beta) = 4\pi^2 \int d^3p\langle\beta,p|V|\varphi_\rho\rangle\langle\varphi_\rho|V|\beta,p\rangle =$$
$$\int d^2\rho \int d^3\boldsymbol{p}\int d^3\boldsymbol{p'}\delta(E_{\boldsymbol{p},\beta} - E_{\boldsymbol{p'},\alpha})e^{-i\boldsymbol{\rho}\boldsymbol{p'}_\perp}\varphi(\boldsymbol{p'})\langle\boldsymbol{p},\beta|V|\boldsymbol{p'},\alpha\rangle\times$$
$$\times \int d^3\boldsymbol{p''}\delta(E_{\boldsymbol{p},\beta} - E_{\boldsymbol{p''},\alpha})e^{i\boldsymbol{\rho}\boldsymbol{p''}_\perp}\varphi(\boldsymbol{p''})\langle\boldsymbol{p''},\alpha|V|\boldsymbol{p},\beta\rangle \tag{7.13}$$

Using the definition of the delta function $\int d^2\rho e^{i\boldsymbol{\rho}(\boldsymbol{p'}_\perp - \boldsymbol{p''}_\perp)} = (2\pi)^2\delta^2(\boldsymbol{p'}_\perp - \boldsymbol{p''}_\perp)$. With this fact in mind we can also write $\delta(E'_p - E''_p) = \delta(E'_p(p'_\parallel) - E''_p(p''_\parallel))$. Relativistic dispersion relation is $E = \sqrt{p^2c^2 + m^2c^4} = \sqrt{p_\perp^2c^2 + p_\parallel^2c^2 + m^2c^4}$, so $\delta(E'_p - E''_p) = \frac{E'_p}{p_\parallel c^2}\delta(p'_\parallel - p''_\parallel) = \frac{1}{v_\parallel}\delta(p'_\parallel - p''_\parallel)$. The result is

$$\sigma = (2\pi)^4 \int d^3p \int d^3p'\delta(E_{\beta,p} - E_{\alpha,p'})\frac{1}{v_\parallel}|\varphi(p')|^2|\langle\beta,p|V|\alpha,p'\rangle|^2 \tag{7.14}$$

7.4 Plane-wave solution

The solution can also be obtained differently, via plane waves. Delta function normalization of the plane waves leads to an infinite probability of scattering if it is expressed through S-matrix due to the square of the delta function. Moreover it is not clear how to count incoming particles in case of the infinite plane wave. To account for these issues, we will rewrite the cross section in terms of the incoming and scattering probabilities [13].

$$\sigma_{\beta\alpha} = \frac{\omega_{scattered}}{\omega_{incoming}}S = \frac{d\omega_{scatteed}/dt}{d\omega_{incoming}/dt}S \tag{7.15}$$

$d\omega_{incoming}/dt = \int d^2\rho j(\boldsymbol{\rho},t)$ where $j(\boldsymbol{\rho},t)$ is a probability flux through the ρ plane. If the flux is independent of $\boldsymbol{\rho}$ or averaged, the expression for the cross section becomes

$$\sigma_{\beta\alpha} = \frac{d\omega_{scattered}/dtS}{jS} = \frac{d\omega_{scattered}/dt}{j} \tag{7.16}$$

To deal with plane waves, we will use the box normalization. We can express the probability of scattering in the unit of time from 7.11 and 7.12 to obtain after the differentiation and taking the limits

$$\frac{d\sigma_{\beta\alpha}}{dt} = 2\pi|\langle f|V|i\rangle|^2\delta(E_f - E_i) \tag{7.17}$$

The fact that the scattering per a unit of time does not depend on time justifies the expression, as delta on the right emerges as a result of the integration on time. As we normalize waves in the box with a length L, $|f\rangle$ and $|i\rangle$ are discrete states. To get rid of the delta function we need to integrate over the all possible final states $|f\rangle$. To do this we need to know the density of states in the continuum. From the relation

$$E_n = c\sqrt{m^2c^2 + \boldsymbol{k}'^2} = c\sqrt{m^2c^2 + \left(\frac{2\pi}{L}\right)^2 |\boldsymbol{n}|^2} \tag{7.18}$$

it follows that

$$\rho(E)d\Omega = \frac{\Delta n}{\Delta E}d\Omega = \frac{Ep}{c^2}\left(\frac{L}{2\pi}\right)^3 \delta\Omega \tag{7.19}$$

and so the integration over all the final states gives

$$\frac{d\omega_{scattered}}{dt} = \frac{Ep}{c^2}\frac{L^3}{(2\pi)^2}\int d\Omega |\langle f|V|i\rangle|^2 \tag{7.20}$$

The probability current for the plane wave is $\boldsymbol{j} = \frac{\boldsymbol{v}}{L^3}$, so the result for the cross-section in the box is

$$\sigma = \frac{1}{v_\parallel}\frac{Ep}{c^2}\left(\frac{L^3}{2\pi}\right)^2 \int d\Omega |\langle f|V|i\rangle|^2 \tag{7.21}$$

Now we can go from the box to the continuum using the connection

$$|k\rangle_{continuum} = \sqrt{\frac{L^3}{(2\pi)^3}}|k\rangle_{discrete} \tag{7.22}$$

and obtain the final result for the plane wave scattering

$$\sigma = (2\pi)^4 \frac{1}{v_\parallel}\frac{Ep}{c^2}\int d\Omega |\langle f|V|i\rangle|^2 \tag{7.23}$$

We can now compare it with 7.14. If we add an integral over the momentum to the 7.23 as $\int dp'\delta(p-p')$ and transform the delta function to the delta function over the energy $\delta(E_p - E'_p) = \frac{E_p}{p_\parallel c^2}$, the expression is

$$\begin{aligned}(2\pi)^4 \int dp' p'^2 \delta(E_p - E'_p)\frac{1}{v_\parallel}\int d\Omega |\langle f|V|i\rangle|^2 &= (2\pi)^4 \int d^3\boldsymbol{p'}\frac{1}{v_\parallel}\delta(E_p - E'_p)|\langle f|V|i\rangle|^2 \\ &= \frac{1}{v_\parallel}(2\pi)^4 \int d^3\boldsymbol{p}\delta(E'_p - E_p)|\langle \beta, p|V|\alpha, p'\rangle|^2 \end{aligned} \tag{7.24}$$

The last equality is just to make notation as in 7.14. The results are the same except for the distribution over initial states. This means that if we now take an initial state to be a wave packet as in the previous chapter and substitute it in 7.23 we will get precisely 7.14. Two formulas agree as expected.

7.5 Electron impact ionization of the atom

Now we can obtain the expression for the ionization of the atom.

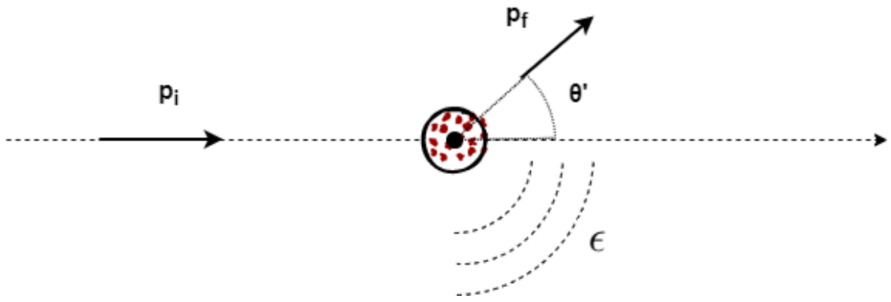

Figure 9: Inelastic scattering. Ejected electron is taken as a spherical wave.

We will denote matrix element in 7.24 as T_{fi}. Our initial state is $|\Psi_{atom}\rangle|p_i\rangle$ and the final state is $|\Psi_{ion}\rangle|\epsilon, \kappa_\epsilon, m_\epsilon\rangle|\psi_f\rangle$. Delta function becomes $\delta(E_{atom} + E_i - E_{ion} - E_f - \epsilon)$. In general formulas in the previous chapters we assumed β to be some particular set of quantum numbers. Now, we are only interested in the differential cross section with respect to the energy of the E_{loss} or, the same, ϵ. So our cross section includes the sum over all the rest atomic numbers of outgoing electron.

$$d\sigma = d\epsilon(2\pi)^4 \sum_{\kappa_\epsilon, m\epsilon} \frac{1}{v_i} \frac{E_f p_f}{c^2} \int d\Omega |T_{fi}|^2 = d\epsilon(2\pi)^4 \sum_{\kappa_\epsilon, m\epsilon} \frac{E_i p_i}{c^2} \frac{E_f p_f}{c^2} \int d\Omega |T_{fi}|^2 \tag{7.25}$$

7.6 One electron approximation

It remains to find the transition matrix elements. Interaction potential between the electron and the atom is

$$V = V_{nuc}(\boldsymbol{r}) + \sum_{i=1}^{N} \frac{1}{|\boldsymbol{r} - \boldsymbol{r}_i|} \tag{7.26}$$

where $\boldsymbol{r}$ is a coordinate of the incoming electron and $\boldsymbol{r}_i$ are coordinates of atomic ones. Then transition matrix elements are

$$T_{\beta\alpha} = \frac{1}{(2\pi)^3} \int d^3\boldsymbol{r} e^{i\boldsymbol{q}\boldsymbol{r}} \int d^3\boldsymbol{r}_1 ... d^3\boldsymbol{r}_N \Psi_{ion+\epsilon} \left[V_{nuc}(\boldsymbol{r}) + \sum_{i=1}^{N} \frac{1}{|\boldsymbol{r} - \boldsymbol{r}_i|} \right] \Psi_{atom} \tag{7.27}$$

with $\boldsymbol{q} = \boldsymbol{p}_f - \boldsymbol{p}_i$. Here the approximation of Schrodinger plane waves was made. It is possible to show that fair calculations with Dirac spinors introduces corrections to the square of the matrix element proportional to $\frac{q}{c^2}$, which are very small, until q is very large. Moreover, these corrections only capture part of full QED corrections, which were neglected.

At small momentum transfers main relativistic corrections come from a different from non-relativistic energy-momentum exchange during the collision, i.e., from kinematics. Let's first Fourier transform the potential, i.e, perform the first integral over $\boldsymbol{r}$.

$$\int d^3\boldsymbol{x}\frac{e^{i\boldsymbol{q}\boldsymbol{x}}}{x}$$

diverges, but using a standard trick of taking it equals to the limit

$$\lim_{\epsilon\to 0}\int d^3\boldsymbol{x}\frac{e^{i\boldsymbol{q}\boldsymbol{x}}}{x}e^{-\epsilon r}=\frac{4\pi}{q^2} \tag{7.28}$$

we arrive to

$$T_{\beta\alpha}=\frac{1}{2\pi^2}\int d^3\boldsymbol{r}_1...d^3\boldsymbol{r}_N\Psi_{ion}\left[\hat{V}_{nuc}(q)+\sum_{i=1}^{N}\frac{e^{i\boldsymbol{q}\boldsymbol{r}_i}}{q^2}\right]\Psi_{atom} \tag{7.29}$$

We will now assume that wavefunctions of ion are orthonormal with those of an atom and that continuum wavefunction of an ionized electron is orthogonal to atomic ones. Then according to properties of matrix operators between determinantal wavefunctions, nuclear potential does not give any contribution to the ionization process. In case of non-orthogonal bases it will not be the case. The whole expression reduces to the matrix element between the final and initial states of an ionized electron.

$$\frac{1}{2\pi^2}\int d^3\boldsymbol{r}_i\psi_{\epsilon l' j' m'}\frac{e^{i\boldsymbol{q}\boldsymbol{r}_i}}{q^2}\psi_{nljm} \tag{7.30}$$

We expand the exponent

$$e^{i\boldsymbol{q}\boldsymbol{r}}=\sum_{\lambda=0}^{\infty}i^{\lambda}(2\lambda+1)j_n\lambda(qr)P_{\lambda}(cos(\theta)) \tag{7.31}$$

where j_λ are spherical Bessel functions. Then using

$$Y_{\lambda 0}=\sqrt{\frac{2\lambda+1}{4\pi}}P_{\lambda}(cos(\theta))$$

the following expression is obtained

$$T_{\beta\alpha}=\frac{1}{2\pi^2}\frac{1}{q^2}\sum_{\lambda=0}^{\infty}i^{\lambda}\sqrt{4\pi(2\lambda+1)}\int dr\int\left[P_{\epsilon\kappa'}P_{n\kappa}+Q_{\epsilon\kappa'}Q_{n\kappa}\right]j_{\lambda}(qr)d\Omega Y_{\lambda 0}\Omega^{+}_{\kappa' m'}\Omega_{\kappa m} \tag{7.32}$$

and applying the Wigner-Eckart theorem

$$T_{\beta\alpha}=\frac{1}{2\pi^2}\frac{1}{q^2}\sum_{\lambda=0}^{\infty}i^{\lambda}(-1)^{m'+1/2}(2\lambda+1)\sqrt{[j'][j]}\int dr\left[P_{\epsilon\kappa'}P_{n\kappa}+Q_{\epsilon\kappa'}Q_{n\kappa}\right]j_{\lambda}(qr)$$

$$\begin{pmatrix} j' & \lambda & j \\ -m' & 0 & m \end{pmatrix} \begin{pmatrix} j' & j & \lambda \\ -1/2 & 1/2 & 0 \end{pmatrix} \prod(l' + \lambda + l) \quad (7.33)$$

From this expression it follows that Coulomb interaction does not change the projection of momenta of the ionized electron.
A short notation for the radial integral is $\langle j_\lambda(qr)\rangle = \int dr\,[P_{\epsilon\kappa'}P_{n\kappa} + Q_{\epsilon\kappa'}Q_{n\kappa}]\,j_\lambda(qr)$
To obtain the full cross section we must sum $T_{\beta\alpha}$ over the momenta projections. In case if we have an open shell we should in principle multiply the result with the $n_{occupied}/n_{maximum}$ but for inner shells this is never the case. The expression is then

$$\sum_m |T_{\beta\alpha}|^2 = \frac{1}{4\pi^4}\frac{1}{q^4}\sum_{\lambda=0}^{\infty}\sum_{\lambda'=0}^{\infty} i^{\lambda-\lambda'}(-1)^{2m+1}(2\lambda+1)(2\lambda'+1)[j'][j]\langle j_\lambda(qr)\rangle\langle j_{\lambda'}(qr)\rangle$$
$$\begin{pmatrix} j' & j & \lambda \\ -1/2 & 1/2 & 0 \end{pmatrix} \begin{pmatrix} j' & j & \lambda' \\ -1/2 & 1/2 & 0 \end{pmatrix} \prod(l' + \lambda + l) \prod(l' + \lambda' + l) \sum_m \begin{pmatrix} j' & \lambda & j \\ -m' & 0 & m \end{pmatrix} \begin{pmatrix} j' & \lambda' & j \\ -m' & 0 & m \end{pmatrix}$$
$$= \frac{1}{4\pi^4}\frac{1}{q^4}[j][j']\sum_{\lambda=0}^{\infty}(2\lambda+1)\langle j_\lambda(qr)\rangle \begin{pmatrix} j' & j & \lambda \\ -1/2 & 1/2 & 0 \end{pmatrix}^2 \prod(l' + \lambda + l) \quad (7.34)$$

where the orthogonality relation for 3j symbols was used.

7.7 Many-electron effects in the relaxation picture

The solution in the one electron picture takes the effect of relaxation into account only partially. Though the continuum wave is calculated in the field of an ion, it should be orthogonalized with respect to atomic states. In this picture no many-electron effects naturally arise. We can obtain the corrections by involving the perturbation theory, but we also can also use the general formula for non-orthogonal matrix elements, obtained in the Chapter 6 to go from 7.29 to

$$T_{\alpha\beta} = \frac{1}{2\pi^2}\left[\hat{V}_{nuq}(q) + \frac{1}{q^2}\sum_{i,j=1}^{N}(-1)^{j+i}\langle\psi_i'(i)|e^{i\mathbf{q}\cdot\mathbf{x}_i}|\psi_j(i)\rangle S^{ij}\right] \quad (7.35)$$

where

$$S^{ij} = \begin{vmatrix} \langle 1'|1\rangle & . & . & \langle 1'|j-1\rangle & \langle 1'|j+1\rangle & . & . & \langle 1'|N\rangle \\ . & & & . & & & & . \\ . & & & & . & & & . \\ \langle i-1'|1\rangle & . & . & \langle i-1'|j-1\rangle & \langle i-1'|j+1\rangle & . & . & \langle i-1'|N\rangle \\ \langle i+1'|1\rangle & . & . & \langle i+1'|j-1\rangle & \langle i+1'|j+1\rangle & . & . & \langle i+1'|N\rangle \\ . & & & & . & & & . \\ . & & & & & & . & . \\ \langle N'|1\rangle & . & . & \langle N'|j-1\rangle & \langle N'|j+1\rangle & . & . & \langle N'|N\rangle \end{vmatrix}$$

is a determinant of wavefunctions overlaps as in 5.31.

We can separate this sum into three pieces with different physical meaning. We suppose

that the ionized electron before the ionization is $|\psi_k\rangle$ and after is $|\psi'_k\rangle = |\chi\rangle$.
Then firstly, we have a single term

$$T_{\alpha\beta} = \frac{1}{2\pi^2}\frac{1}{q^2}\langle\psi'_k|e^{i\mathbf{q}\cdot\mathbf{x}}|\psi_k\rangle S^{ij} = \frac{1}{2\pi^2}\frac{1}{q^2}\langle\chi|e^{i\mathbf{q}\cdot\mathbf{x}}|\psi_k\rangle S^{ij}$$

which is up to a scaling S^{kk} corresponds to the matrix element we obtain in the one electron approximation.
Secondly, we can ionize another orbital.

$$T_{\alpha\beta} = \frac{1}{2\pi^2}\frac{1}{q^2}\sum_{j\neq k}(-1)^{j+k}\langle\psi'_1|e^{i\mathbf{q}\cdot\mathbf{x}}|\psi_j\rangle S^{kj} = \frac{1}{2\pi^2}\frac{1}{q^2}\sum_{j\neq k}(-1)^{j+k}\langle\chi|e^{i\mathbf{q}\cdot\mathbf{x}}|\psi_j\rangle S^{kj}$$

This terms describe processes, in which electron j is kicked to the continuum and then replaced by an electron from the "first" orbital (i.e, orbital of interest).
Finally, rest of the terms

$$T_{\alpha\beta} = \frac{1}{2\pi^2}\frac{1}{q^2}\sum_{i,j\neq k}(-1)^{j+i}\langle\psi'_i|e^{i\mathbf{q}\cdot\mathbf{x}}|\psi_j\rangle S^{ij}$$

describe the process of autoionization (as S^{ij} contains $\langle\chi|\psi_j\rangle$) , followed by the rearrangement of the rest of electrons.
We will expand the exponent up to the linear term. $e^{i\boldsymbol{qx}} = 1 + i\boldsymbol{qx}$ (monopole + dipole contributions). Monopole terms deserve especial attention. The main contribution to the determinant comes from the product of its diagonal terms $\prod_i\langle\psi_{i'}|\psi_i\rangle = S_0\langle\chi|\psi_k\rangle$, where $S_0 \sim 1$ so at the first order $T_{\beta\alpha} \propto N\langle\chi|\psi_k$. This is a huge value, which can not be neglected. However, it is easy to show that they are cancelled out by a nuclear potential. Indeed, if we have a point nucleus with a potential $-\frac{Z}{r}$, then its integration with the incoming electron gives $-\frac{Z}{q^2}$. The rest of the electrons contribute $\langle\Psi_{ion+\epsilon}|\Psi_{atom}\rangle = S$. On the other hand

$$\sum_{i,j}(-1)^{j+i}\langle\psi'_i|e^{i\mathbf{q}\cdot\mathbf{x}}|\psi_j\rangle S^{ij} = \sum_j S = NS = ZS$$

In principle, nuclear potential is not necessary that of the point nucleus. But it is different from the point one in such a small area of space, that the difference is negligible while integrating the potential over the whole space. For this reason in this work it is assumed, that monopole and nuclear contributions are exactly cancelled.

Analytical formula for the C-K crossection in the dipole approximation is the following

$$|T_{\beta\alpha}|^2 = \frac{1}{2\pi^4}\frac{1}{q^4}\left[\langle 1s'|1s\rangle\langle 2s'|2s\rangle^2\langle 2p'|2p\rangle^2\right]\left[\langle\epsilon' p|\boldsymbol{qr}|1s\rangle - \langle 2p|\boldsymbol{qr}|1s\rangle\frac{\langle\epsilon' p|2p\rangle}{\langle 2p'|2p\rangle} - \langle\epsilon' p|\boldsymbol{qr}|2s\rangle\frac{\langle 2s'|1s\rangle}{\langle 2s'|2s\rangle}\right]^2 \tag{7.36}$$

where again non-relativistic approximation $2p_{3/2} = 2p_{1/2} = 2p$ was made.

8 Perturbation theory

We have considered, how good ionization energies can be obtained through the variation in the self-consistent field due to the vacancy. This method requires to solve Dirac-Hartree-Fock equations twice. [11, 2, 12] Expressions for matrix elements between non-orthogonal Slater determinant states contain all kinds of overlaps between non-orthogonal wavefunctions. These terms can be seen as multi electron processes, leading to the formation of the hole on a level i and the continuum wave ϵ. Another way to calculate the multi electron processes is to use the perturbation theory. Non-orthogonality of initial and final wavefunctions can therefore be seen as corrections due to the perturbative potential. In this chapter perturbative corrections are obtained up to the second order (and partially of higher orders through the RPA equations). Afterwards, two approaches are compared.

8.1 Rayleigh-Schrodinger Perturbation Theory

Rayleigh-Schrodinger Perturbation Theory is a formalism of the perturbation theory, suitable for treatment of degenerate levels [12]. Suppose that we know a solution to the task

$$H_0|\Psi_0^a\rangle = E_0^a|\Psi_0^a\rangle \tag{8.1}$$

where $|\Psi_0^a\rangle$ are so-called model wavefunctions, which form a model subspace. Subspace orthogonal to a model subspace is called an orthogonal subspace. We want to find a solution of the task

$$H|\Psi^a\rangle = E^a|\Psi^a\rangle \tag{8.2}$$

The wave operator Ω is defined through

$$|\Psi^a\rangle = \Omega|\Psi_0^a\rangle \tag{8.3}$$

and operators P and Q are projection operators on the model and orthogonal subspaces

$$\begin{aligned} P|\Psi^a\rangle &= |\Psi_0^a\rangle \\ Q|\Psi^a\rangle = |\Psi^a\rangle - |\Psi_0^a\rangle &= |\Delta\Psi^a\rangle \end{aligned} \tag{8.4}$$

We will also introduce the correlation operator χ

$$\Omega = 1 + \chi \tag{8.5}$$

and it follows

$$\chi|\Psi_0^a\rangle = Q|\Psi^a\rangle \tag{8.6}$$

We can derive equations for wave and correlation operators from a Schrodinger (or Dirac) equation. In this work we will assume that model space is completely degenerate (in particular, if we have a single model wavefunction, such as a Slater determinant for a closed shell). Separating $H = H_0 + V$, we can rewrite it as

$$(E - H_0)|\Psi^a\rangle = V|\Psi^a\rangle \tag{8.7}$$

and acting with P on both sides

$$(E - H_0)|\Psi_0^a\rangle = PV|\Psi^a\rangle \tag{8.8}$$

Acting then with Q we get

$$E|\Psi^a\rangle - \Omega H_0|\Psi_0^a\rangle = \Omega PV\Omega|\Psi_0^a\rangle \tag{8.9}$$

And subtracting this from the Schrodinger equation we arrive to

$$[\Omega, H_0]|\Psi_0^a\rangle = (V\Omega - \Omega PV\Omega)|\Psi_0^a\rangle \tag{8.10}$$

or in the operator form

$$\begin{aligned} [\Omega, H_0]P = V\Omega P - \Omega PV\Omega P \qquad & \text{or equivalent} \\ (E_0 - H_0)\Omega P = V\Omega P - \Omega PV\Omega P \qquad & \end{aligned} \tag{8.11}$$

This equation is called a generalized Bloch equation. Now we can expand Ω in powers of the perturbation potential V

$$\Omega = 1 + \Omega^{(1)} + \Omega^{(2)} + ...$$

To obtain the system

$$\begin{aligned} &(E_0 - H_0)P = 0 \\ &(E_0 - H_0)\Omega^{(1)}P = QVP \\ &(E_0 - H_0)\Omega^{(2)}P = QV\Omega^{(1)}P - \Omega^{(1)}PVP \end{aligned} \tag{8.12}$$

We will introduce resolvent as an operator

$$R(E_0 - H_0) = Q, \qquad RQ = R \tag{8.13}$$

and we can write its spectral decomposition as

$$R = \sum_b \frac{|\Psi^b\rangle\langle\Psi^b|}{E_0 - E_0^b} \tag{8.14}$$

Acting on both sides of 8.12 we obtain

$$\begin{aligned} &QP = 0 \qquad \text{which is always true} \\ &Q\Omega^{(1)}P = \sum_b \frac{|\Psi^b\rangle\langle\Psi^b|VP}{E_0 - E_0^b} \\ &Q\Omega^{(2)}P = \sum_{bc} \frac{|\Psi^c\rangle\langle\Psi^c|V|\Psi^b\rangle\langle\Psi^b|VP}{(E_0 - E_0^c)(E_0 - E_0^b)} - \sum_b \frac{|\Psi^b\rangle\langle\Psi^b|VPVP}{(E_0 - E_0^b)^2} \end{aligned} \tag{8.15}$$

As $\Omega^{(n)}|\Psi_0\rangle = |\Psi_a^n\rangle$, corrections to the wavefunctions are

$$|\Psi_0^1\rangle = \sum_b \frac{|\Psi^b\rangle\langle\Psi^b|V|\Psi_0^a\rangle}{E_0 - E_0^b}$$

$$|\Psi_0^2\rangle = \sum_{bc} \frac{|\Psi^c\rangle\langle\Psi^c|V|\Psi^b\rangle\langle\Psi^b|V|\Psi_0\rangle}{(E_0 - E_0^c)(E_0 - E_0^b)} - \sum_{ab} \frac{|\Psi^b\rangle\langle\Psi^b|V|\Psi^a\rangle\langle\Psi^a|V|\Psi_0\rangle}{(E_0 - E_0^b)^2} \tag{8.16}$$

where indices b, c indicates summation over all the basis function from orthogonal subspace and a over the wavefunctions from the model subspace.

We can also introduce the so-called effective Hamiltonian, that is an operator acting like

$$H_{eff}|\Psi_0^a\rangle = E|\Psi^a\rangle \tag{8.17}$$

It can be easily obtained, by acting on both sides of the Schrodinger equation with P

$$H_{eff} = PH\Omega = PH\Omega P \tag{8.18}$$

where the last equality holds on the model subspace. We can use the obtained expansion for Ω to expand the Hamiltonian in orders of V and get corrections to the energy

$$\begin{aligned} E^{(1)} &= \langle\Psi_0|H_{eff}^{(1)}|\Psi_0\rangle = \langle\Psi_0|V|\Psi_0\rangle \\ E^{(2)} &= \langle\Psi_0|H_{eff}^{(2)}|\Psi_0\rangle = \sum_b \frac{\langle\Psi_0|V|\Psi^b\rangle\langle\Psi^b|V|\Psi_0\rangle}{(E_0 - E_0^b)} \end{aligned} \tag{8.19}$$

This expression is different from the one obtained in a more standard Brillouin-Wigner perturbation theory in the respect, that it only includes the summation over the orthogonal subspace and hence applicable to degenerate levels.

8.2 Quantization of the Hamiltonian

Perturbation expansions are obtained naturally in the second quantization picture. Introducing as usual creation and annihilation operators $a\dagger_k$ and a_k for the electron on the energy level ϵ_k, we can quantize our Hamiltonian 5.1 to obtain

$$\begin{aligned} H &= H_0 + V \\ H_0 &= \sum_{\epsilon_k} a_k^\dagger a_k \\ V &= \sum_{ij} U_{ij} a_i^\dagger a_j + \frac{1}{2}\sum_{ijkl} g_{ijkl} a_i^\dagger a_j^\dagger a_k a_l \\ U_{ij} &= \int d^3\boldsymbol{x}\psi_i^\dagger((x))U(\boldsymbol{x})\psi_j((x)) \\ g_{ijkl} &= \int d^3\boldsymbol{x_1} d^3\boldsymbol{x_2}\psi_i^\dagger(\boldsymbol{x}_1)\psi_j^\dagger(\boldsymbol{x}_2)\frac{1}{|\boldsymbol{x}_1 - \boldsymbol{x}_2|}\psi_k(\boldsymbol{x}_1)\psi_l(\boldsymbol{x}_2) \end{aligned} \tag{8.20}$$

Here U is some good approximation for the central field of an atom. It can be direct Hartree-Fock energy or some effective potential like Thomas-Fermi. It is introduced to make the perturbation theory applicable to the difference $V_{HF} - U$, as Hartree-Fock potential is itself too big to be treated perturbatively. ϵ_k are one electron eigenvalues, obtained in a field $V_{nuc} + U$.

It is convenient to define a vacuum state of an atom to be $|0_c\rangle = a_N^\dagger ... a_1^\dagger|0\rangle$, where $|0\rangle$

is a real vacuum, i.e., state with 0 particles. Vacuum state represents some particular configuration of atomic electrons, which is assumed to be a closed shell. We will then define normal ordering of operators to be

$$\begin{aligned} &: a_m^\dagger a_n^\dagger := - : a_n a_M^\dagger := a_m^\dagger a_n \qquad \text{for n, m being excited orbitals} \\ &: a_a^\dagger a_b := - : a_b a_a^\dagger := -a_b a_a^\dagger \qquad \text{for a, b being core orbitals} \end{aligned} \tag{8.21}$$

Normally ordered operator is hence that that annihilates the ground state

$$\langle 0_c| : a_i ... a_j a_l^\dagger ... a_m^\dagger : |0_c\rangle = 0 \tag{8.22}$$

As shown in Apendix ?? we can rewrite Hamiltonian through normally ordered operators as

$$\begin{aligned} H_{no} &= H_0 + V \\ H_0 &= E_0 + \sum_k \epsilon_k : a_k^\dagger a_k : \\ V &= V_0 + V_1 + V_2 \\ E_0 &= \sum_a \epsilon_a \\ V_0 &= \sum_a \left[\frac{1}{2} (V^{HF})_{aa} - U_{aa} \right] \\ V_1 &= \sum_{ij} \left[V_{ij}^{HF} - U_{ij} \right] : a_i^\dagger a_j := \sum_{ij} \nu_{ij} : a_i^\dagger a_j \\ V_2 &= \frac{1}{2} \sum_{ijkl} g_{ijkl} : a_i^\dagger a_j^\dagger a_l a_k : \end{aligned} \tag{8.23}$$

As can be easily seen,

$$\langle 0_c | H_{no} | 0_c \rangle = E_0 + V_0 = E_{HF} \tag{8.24}$$

8.3 Perturbative corrections to the atomic energy levels

We can now combine the formalism of the last to chapters to obtain corrections to the atomic energies and wavefunctions for the closed shell atoms (or for any state, determined by a single Slater determinant). It is in principle possible to substitute a non-quantized Coulomb Hamiltonian to the first and the second order corrections obtained in the previous chapter, but even at the second order calculations become very confusing. It is a common approach to quantize the wave operator in the Generalized Bloch equation and then use the Wick's theorem [14, 12] to simplify expressions with creation and annihilation operators.

We will take our unperturbed atomic wavefunction to be $|0_c\rangle$ and take the Hamiltonian to be in its normal form. Then we write

$$[\Omega^{(1)}, H_0] P = QVP$$

and separate our potential $V = V_0 + V_1 + V_2$. V_0 part is just a constant, so $QV_0P = 0$. We will also assume that we chose $U = V^{HF}$, so that $V_1 = 0$. Then we obtain

$$[\Omega^{(1)}, H_0]P = QV_2P = Q\frac{1}{2}\sum_{ijkl} g_{ijkl} : a_i^\dagger a_j^\dagger a_l a_k : P = Q\frac{1}{2}\sum_{mnab} g_{mnab} : a_m^\dagger a_n^\dagger a_b a_a : P \quad (8.25)$$

where mn denotes excited orbitals and ab the core ones. On the other hand we can write

$$\Omega^{(1)} = \frac{1}{2}\sum_{mnab} a_m^\dagger a_n^\dagger a_b a_a x_{ab}^{mn} \quad (8.26)$$

with x_{ab}^{mn} being some unknown constants. In such a form it is clear that

$$[\Omega^{(1)}, H_0]|0_c\rangle = \frac{1}{2}\sum_{mnab} (\epsilon_a + \epsilon_b - \epsilon_m - \epsilon_n)|0_c\rangle \quad (8.27)$$

and hence

$$\Omega^{(1)} = \frac{1}{2}\sum_{mnab} a_m^\dagger a_n^\dagger a_b a_a \frac{g_{mnab}}{(\epsilon_a + \epsilon_b - \epsilon_m - \epsilon_n)} \quad (8.28)$$

The first order for the energy is trivial

$$E^{(1)} = \langle 0_c|V|0_c\rangle = \langle 0_c|V_0|0_c\rangle = V_0 \quad (8.29)$$

From this follows that $E^{(0)} + E^{(1)} = E_{HF}$.

In the second order

$$\begin{aligned}[H_0, \Omega^{(2)}]P &= QV\Omega^{(1)}P - \Omega^{(1)}PVP = QV\Omega^{(1)}P - \Omega^{(1)}|0_c\rangle\langle 0_c|V|0_c\rangle\langle 0_c| \\ &= Q(V_0 + V_2)\Omega^{(1)}P - (P+Q)V_0\Omega^{(1)}P = Q(V_2)\Omega^{(1)}P \end{aligned} \quad (8.30)$$

where it was used that $P\Omega^{(1)}P = 0$. Then

$$[\Omega^{(2)}, H_0]P = Q\frac{1}{4}\sum_{ijkl} : a_i^\dagger a_j^\dagger a_l a_k : g_{ijkl} \sum_{mnab} a_m^\dagger a_n^\dagger a_b a_a \frac{g_{mnab}}{\epsilon_a + \epsilon_b - \epsilon_m - \epsilon_n} P \quad (8.31)$$

Wick's theorem states that $: A :: B :=: AB : + : \overbrace{AB} :$, where $\overbrace{AB}$ denotes all possible contractions between two operators. With its help we get that

$$: a_i^\dagger a_j^\dagger a_l a_k : a_m^\dagger a_n^\dagger a_b a_a =: \cdots : + (\delta_{ia}\delta_{jb} - \delta_{ib}\delta_{ja})(\delta_{km}\delta_{ln} - \delta_{kn}\delta_{lm}) \quad (8.32)$$

$: \cdots :$ term represents a sum some partially contracted products of the operators. To obtain the full expression for the second order wave operator, we would have to compute them all, and then calculate the commutator up to the 4-particle excitation (as a fully-non contracted term contains 4 creation and annihilation operators). In this work we will only be interested in RPA, which only requires first order corrections to the wavefunction, so we will not write here explicit expressions. The expression for energy, in contrast, only requires a fully contracted term, which can be seen from the

$$E^{(2)} = \langle 0_c|H_{eff}^{(2)}|0_c\rangle = \langle 0_c|V\Omega^{(1)}|0_c\rangle = \frac{1}{2}\sum_{mnab} \frac{(g_{abmn} - g_{abnm})g_{mnab}}{\epsilon_a + \epsilon_b - \epsilon_m - \epsilon_n} \quad (8.33)$$

where the equality $g_{mnab} = g_{nmba}$ was used.

In principle these expressions for corrections are only valid for the closed shell atom or atoms with a one valence electron. It is possible to work out more complicated formulas to correct for all the possible couplings. But, as before, we are interested in the average configuration energy, so we will assume that any our state can be represented by a single Slater determinant, so these formulas are applicable, for example, for the electron-hole states.

8.4 Random Phase Approximation

Now we can obtain the correction to a transition matrix element $\langle F|O|I\rangle$. Corrections to wavefunctions implies that we can expand the element as

$$\begin{aligned} O^{(1)} &= \langle F^{(0)}|O|I^{(0)}\rangle \\ O^{(2)} &= \langle F^{(0)}|O|I^{(1)}\rangle + \langle F^{(1)}|O|I^{(0)}\rangle \\ O^{(3)} &= \langle F^{(2)}|O|I^{(0)}\rangle + \langle F^{(1)}|O|I^{(1)}\rangle + \langle F^{(0)}|O|I^{(2)}\rangle \end{aligned} \tag{8.34}$$

We will treat O as a general one particle operator $O = \sum_{ij} O_{ij} : a_i^\dagger a_j :$. We will always assume that it is normally ordered and hence sometimes omit ::. Also, as our initial and final states are orthogonal, constant will drop out. Let's find transition matrix elements between initial state to be vacuum state, and final state to have one electron ionized to the continuum.

$$O^{(1)}_{a\epsilon} = \langle 0_c|a_a^\dagger a_\epsilon \sum_{ij} a_i^\dagger O_{ij} a_j|0_c\rangle = \langle 0_c| \sum_{ij} O_{ij}\delta_{ai}\delta_{\epsilon j}|0_c\rangle = O_{a\epsilon} \tag{8.35}$$

So at the first order transition matrix element is just a one electron matrix element, obtain before in the first quantization. At the second order

$$O^{(2)}_{a\epsilon} = \langle 0_c|a_a^\dagger a_\epsilon \sum_{ij} O_{ij} a_i^\dagger a_j \Omega^{(1)}|0_c\rangle + \langle 0_c|a_a^\dagger a_\epsilon (\Omega^{(1)})^\dagger \sum_{ij} O_{ij} a_i^\dagger a_j|0_c\rangle$$

Let's work out the first terms. With a wave operator given as 8.28 it contains a product of operators

$$: a^\dagger a_\epsilon :: a_i^\dagger a_j :: a_m^\dagger a_n^\dagger a^c a^d =: \cdots : +(\delta_{ac}\delta_{id} - \delta_{ad}\delta_{ic})(\delta_{\epsilon m}\delta_{jn} - \delta_{\epsilon n}\delta_{jm})$$

which must be fully contracted to give a non-zero contribution between vacuum states. So, the first term is, after some algebra,

$$\sum_{mc} \frac{O_{mc}(g_{\epsilon mac} - g_{\epsilon mca})}{\epsilon_c - \epsilon_m - \epsilon + \epsilon_a} \tag{8.36}$$

The second one is obtained in the same way, and $O^{(2)}_{a\epsilon}$ becomes

$$O^{(2)}_{a\epsilon} = \sum_{mc} \frac{O_{mc}(g_{\epsilon mac} - g_{\epsilon mca})}{\epsilon_c - \epsilon_m + \epsilon + \epsilon_a} + \sum_{mc} \frac{O_{cm}(g_{\epsilon cam} - g_{\epsilon cma})}{\epsilon_c - \epsilon_m + \epsilon - \epsilon_a} \tag{8.37}$$

RPA approximation consists in substituting O_{cm} on the right hand side of this equation [14], with the corrected value of the operator from the left hand side. In this way we arrive to the system of self-consistent equations for matrix elements

$$O^{RPA}_{a\epsilon} = O_{a\epsilon} + \sum_{mc} \frac{O^{RPA}_{mc}(g_{\epsilon mac} - g_{\epsilon mca})}{\epsilon_c - \epsilon_m + \epsilon + \epsilon_a} + \sum_{mc} \frac{O^{RPA}_{cm}(g_{\epsilon cam} - g_{\epsilon cma})}{\epsilon_c - \epsilon_m + \epsilon + \epsilon_a} \tag{8.38}$$

In this way we can capture some terms of the perturbation theory up to the infinite order. However, the precision of the method is limited, as there are much more elements that are not included in the RPA.

8.5 Correspondence between perturbation and variational approaches

A natural question, which arises, is how perturbative and variational pictures correspond to each other [2]. To see it we can write DHF equations for an atom and an ion, denoting DHF potential of the atom as H_{HF} and a potential of a hole (a perturbation) as W.

$$H_{HF}|n,\kappa\rangle = \epsilon|n,\kappa\rangle$$
$$(H_{HF} + W)|n,\kappa\rangle_{ion} = \epsilon_{ion}|n,\kappa\rangle_{ion}$$

Multiplying the second equations with the $|n',\kappa'\rangle$, taking into account that result is 0 $\kappa \neq \kappa'$ and changing n on n' at the first equation, if we obtain

$$H_{HF}|n',\kappa\rangle = \epsilon'|n',\kappa\rangle$$
$$\langle n'\kappa|(H_{HF} + W)|n,\kappa\rangle_{ion} = \epsilon_{ion}\langle n'\kappa|n,\kappa\rangle_{ion}$$

H is Hermitian, so we can express the overlap as

$$\langle n'\kappa|n,\kappa\rangle_{ion} = \frac{\langle n'\kappa|W|n,\kappa\rangle_{ion}}{\epsilon_{ion} - \epsilon'} \tag{8.39}$$

We will assume for the applicability of the perturbation theory that $|a\rangle$ and $|c\rangle$ represent different one electron states. Denoting for brevity $|n,\kappa\rangle = |a\rangle$, $|n',\kappa\rangle_{ion} = |\tilde{c}\rangle$, we rewrite it

$$\langle a|\tilde{c}\rangle = \frac{\langle a|W|\tilde{c}\rangle}{\epsilon_{\tilde{c}} - \epsilon_a}$$

And using that W is a potential of a hole $|b\rangle$

$$\langle \tilde{c}|W|a\rangle = -\int d\boldsymbol{r}\int d\boldsymbol{r'}\tilde{\psi}_c(\boldsymbol{r})\psi_b(\boldsymbol{r'})\frac{1}{|\boldsymbol{r}-\boldsymbol{r'}|}(\psi_b(r')\psi_a(r) - \psi_b(r)\psi_a(r')) = g_{\tilde{c}bab} - g_{\tilde{c}bba} \tag{8.40}$$

So in a analogy with a previous chapter

$$\langle a|\tilde{c}\rangle = \frac{g_{\tilde{c}bab} - g_{\tilde{c}bba}}{\epsilon_{\tilde{c}} - \epsilon_a}$$

We can expand $|\tilde{c}\rangle$ in an old basis as

$$|\tilde{c}\rangle = \sum_k |k\rangle\langle k|\tilde{c}\rangle = |c\rangle\langle c|\tilde{c}\rangle + \sum_{k\neq c}\frac{g_{\tilde{c}bkb} - g_{\tilde{c}bbk}}{\epsilon_{\tilde{c}} - \epsilon_k}|k\rangle \tag{8.41}$$

And the normalization condition for a wavefunction gives us

$$|\langle c|\tilde{c}\rangle|^2 = 1 - \sum_{k\neq c} \frac{|g_{\tilde{c}bkb} - g_{\tilde{c}bbk}|^2}{(\epsilon_{\tilde{c}} - \epsilon_k)^2} \tag{8.42}$$

From this expression it follows that to the first order $\langle c|\tilde{c}\rangle = 1$. Then at the first order of corrections

$$\langle \tilde{c}|O|a\rangle = O_{\tilde{c}a} = O_{ca} + \sum_{k\neq c} \frac{g_{cbkb} - g_{cbbk}}{\epsilon_c - \epsilon_k} O_{ka} \tag{8.43}$$

This expression contains terms, which represent transitions between of an electron to another occupied state. It either represents a process, where electron goes to an occupied orbital (which is impossible due to Pauli principle) and then is pushed to the continuum or it demands hole to interact with the electron before interaction with the beam (i.e., before its creation). From the general expressions of perturbation theory, obtained earlier, we could see that only transitions from bound to occupied states enter results for all the corrections. It means that we should rewrite the last equation as

$$\langle \tilde{v}|O|a\rangle = O_{\tilde{v}a} = O_{va} + \sum_{m\neq v} \frac{g_{vbmb} - g_{vbbm}}{\epsilon_v - \epsilon_m} O_{va} + \sum_{d\neq v} \frac{g_{vbdb} - g_{vbbd}}{\epsilon_v - \epsilon_d} O_{da} \tag{8.44}$$

and we expect the last term to be cancelled by some other contributions. To see it explicitly, we will use the expression obtained for the dipole ionization of C-K shell 7.36

$$|T_{\beta\alpha}|^2 = \frac{1}{2\pi^4}\frac{1}{q^4}\left[\langle 1s'|1s\rangle\langle 2s'|2s\rangle^2\langle 2p'|2p\rangle^2\right]\left[\langle \epsilon' p|\boldsymbol{qr}|1s\rangle - \langle 2p|\boldsymbol{qr}|1s\rangle\frac{\langle \epsilon' p|2p\rangle}{\langle 2p'|2p\rangle} - \langle \epsilon' p|\boldsymbol{qr}|2s\rangle\frac{\langle 2s'|1s\rangle}{\langle 2s'|2s\rangle}\right]^2$$

Expanding the terms in brackets

$$\langle \epsilon' p|\boldsymbol{qr}|1s\rangle = \langle \epsilon p|\boldsymbol{qr}|1s\rangle + \langle 2p|\boldsymbol{qr}|qs\rangle\langle \epsilon' p|2p\rangle + \sum_{n>2}\langle np|\boldsymbol{qr}|ns\rangle\langle \epsilon' p|np\rangle$$

$$= \langle \epsilon p|\boldsymbol{qr}|1s\rangle + \langle 2p|\boldsymbol{qr}|qs\rangle\frac{\langle \epsilon p|W|2p\rangle}{\epsilon_p - \epsilon_{2p}} + \sum_{n>2}\langle np|W|ns\rangle\frac{\langle \epsilon p|\boldsymbol{qr}|np\rangle}{\epsilon_p - \epsilon_{np}} + ...[1]$$

$$\langle 2p|\boldsymbol{qr}|1s\rangle\frac{\langle \epsilon' p|2p\rangle}{\langle 2p'|2p\rangle} = \langle 2p|\boldsymbol{qr}|1s\rangle\frac{\langle \epsilon p|W|2p\rangle}{\epsilon_p - \epsilon_{2p}} + ... \qquad [2]$$

$$\langle \epsilon' p|\boldsymbol{qr}|2s\rangle\frac{\langle 2s'|1s\rangle}{\langle 2s'|2s\rangle} = \langle \epsilon p|\boldsymbol{qr}|2s\rangle\frac{\langle 2s|W|1s\rangle}{\epsilon_{2s} - \epsilon_{1s}} + ... \qquad [3]$$

We see that the second term in [1] cancels [2], so in such a way nonphysical terms are eliminated. The third term is identically zero in the first order as $\langle 2s|W|1s\rangle = g_{2s1s1s1s} - g_{2s1s1s1s} = 0$.

As it was mentioned above, the alternative solution to the computation of full non-orthogonal

matrix elements is an orthoganalization of the continuum wave w.r.t. bound states of a neutral atom.

$$|\epsilon_o p\rangle = |\epsilon' p\rangle - \langle 2p|\epsilon' p\rangle |2p\rangle = |\epsilon p\rangle + \sum_{n>2} \langle np|\epsilon' p\rangle |np\rangle \tag{8.45}$$

This expression substituted to the matrix element gives a result that is identical to the first order from that obtained from non-orthogonal matrix elements. In the second order it is not the case, as orthogonalization of the continuum wave removes [2], while second order nonphysical corrections from [1] partially remains. However, identical first order explains, why expected deviations from the full elements are very small, especially for inner shells, where energy denominators are large.

Considering a matrix element for an ionized electron, which neutral state was denoted b through this chapter

$$\langle \epsilon'|O|b\rangle = \langle \epsilon|O|b\rangle + \sum_k O_{kb} \frac{g_{\epsilon' bkb} - g_{\epsilon' bbk}}{\epsilon - \epsilon_k} \tag{8.46}$$

We notice, that it coincides with the first term in the RPA expression for the particular case $m = b$, $c = k$. It follows, that non-orthogonal matrix elements approach takes into account a part of RPA correction. In principle, these are different contributions, though. RPA takes into account the deviation from a spherically symmetric picture, with corrections to electrons of an atom and an ion in the same central field. Corrections are taken into account up to the first, and partially, higher orders. Relaxation, in contrast, takes into account all the possible corrections due to the different spherical fields. Taking into account non-spherical corrections to the spherical fields in the relaxation picture one should in principle obtain the same result, as taking higher order perturbative corrections to the spherical field of a neutral atom.

9 Results

9.1 Results from a one electron approximation

In this section we compare theoretical predictions, obtained from our computations, with those, obtained from a DFT model [17] and experimental data (provided by ThermoFisher Scientific). Experimental spectra, presented below, are first processed with a background subtraction and then deconvolved with low-loss spectra in order to extract the corresponding electron-atom inelastic scattering data.

The following figure shows a correspondence between experimental and theoretically calculated EELS spectra for an M shell of Tungsten.

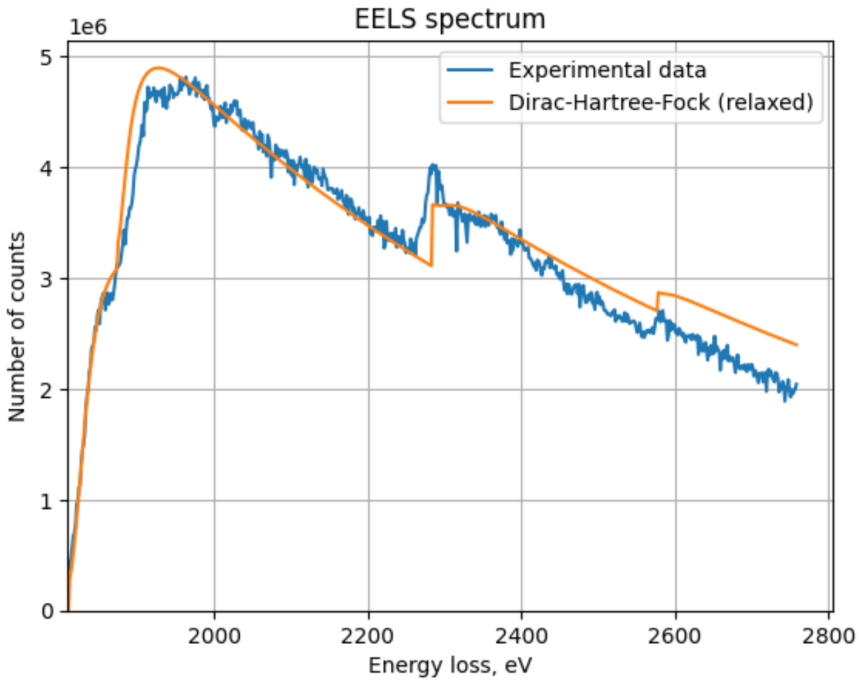

Figure 10: Theoretical and experimental EELS spectra for W-M shell. Beam energy: 200 keV, maximum collection angle: 100 mrad (Data provided by ThermoFisher Scientific).

Theoretical shape is in good correspondence with the experiment for M_4 and M_5 subshells. The slope coincides with the experiment before and after the peak. The only discrepancy in the region till 2300 ev is right at the peak, where we expect to have the biggest experimental noise. Significant difference in amplitude right at the M_3 peak might have several possible reasons. The peak shape indicates that it can be a discrete transition of an electron to some unoccupied band state, for example, 6s. Finally, divergence of experimental and theoretical slopes at high energies is most probably due to errors caused by the limited

range of validity of the extrapolation of the effective power law background model. This typically happens if background is subtracted with the same parameters over a broad region.

Then next figure illustrates the comparison between DHF and effective models.

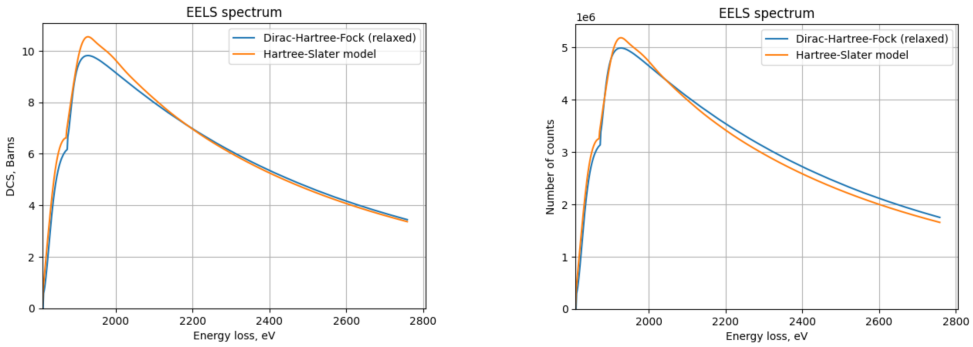

Figure 11: Comparison between a Dirac-Hartree-Fock and an effective model from [17] for Tungsten Ru-M shell. Left: absolute differential cross sections expressed in Barns. Right: cross sections times parameter k, chosen to fit the best experimental data from 10. $k_{DHF} = 498559$, $k_{eff} = 476268$

M_2 and M_3 are not plotted due to their absence for effective models in open sources. Looking on $M-4$ - $M-5$ peak, we see that an effective model gives a higher peak than DHF. This leads to the fact, that while fitted to the experiment that peak turns out to be steeper then one from DHF calculations. It means that its peek is going to be higher then DHF one, and at the same time its slope at high energies is going to be lower then predicted by DHF. As DHF peak seems to be a bit higher than the experiment, while a slope matches the data well, it is clear, that an effective model shows incorrect behaviour in the region where DHF seems to work well.

Though absolute quantification gives only a difference between k_{DHF} and k_{eff} of order 5%, which can be considered insignificant as it is most certainly smaller than error obtained from other factors, shape variations are of greater importance. When superimposed several close peaks are analyzed t mistakes arising from background subtraction and deconvolution, wrong shape can lead to totally different results.

Another M-shell element, Ruthenium, shows a very good match between theoretical ab initio calculations and experiment. The major peak seems to coincide with theoretical predictions both in width and amplitude. Asymptotic behaviour at high energies seems to be correct as well. In fact, the theoretical model seems to be within small experimental noise almost over the whole region of comparison. The only areas, where disagreement is observed, are near the edge areas, and it will be shown in the following subsection that such disagreement is expected.

Ruthenium is an example of elements, for which effective models show especially big deviations from the DHF model and the data.

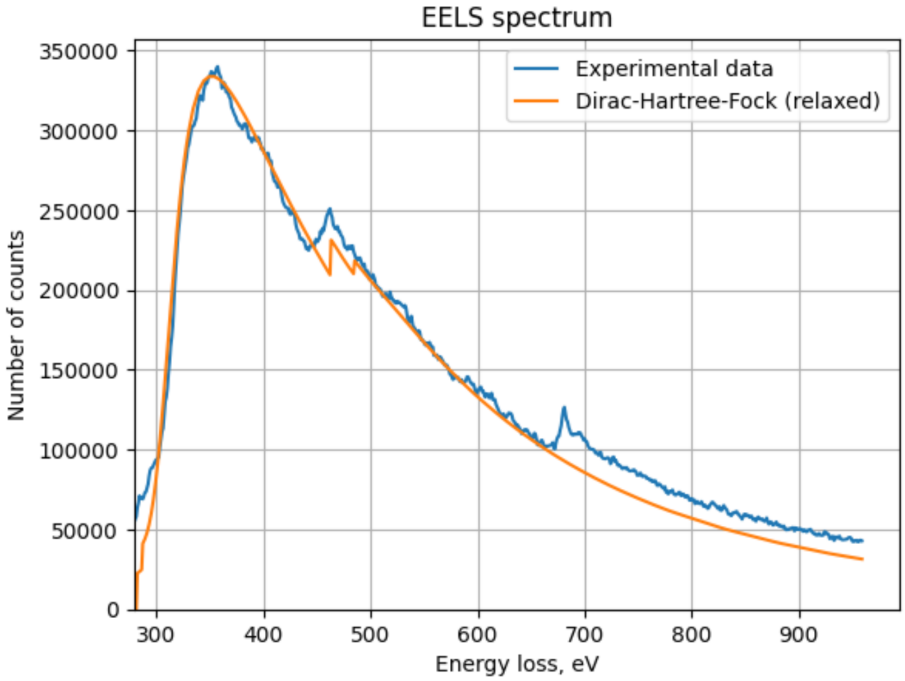

Figure 12: Theoretical and experimental EELS spectra for Ru-M shell. Beam energy: 200 keV, maximum collection angle: 40 mrad. Last experimental peak does not belong to a Ruthenium family.

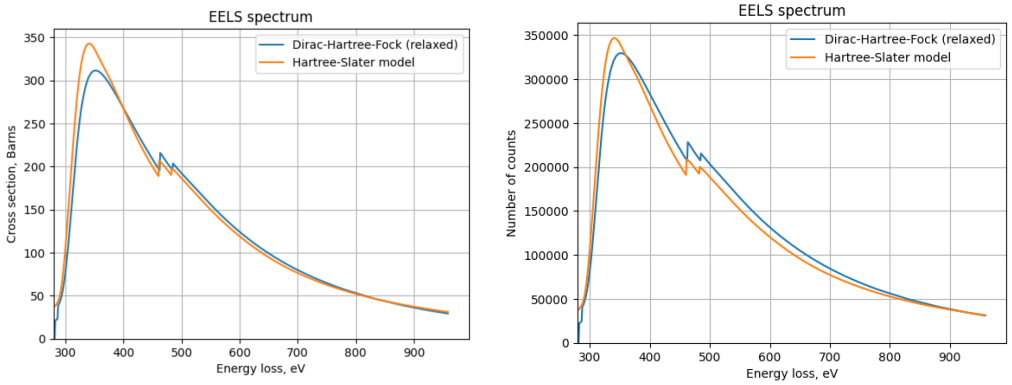

Figure 13: Comparison between a Dirac-Hartree-Fock and an effective model from [17] for Ruthenium Ru-M shell. Left: absolute differential cross sections expressed in Barns. Right: cross sections times parameter k, chosen to fit the best experimental data from 12. $k_{DHF} = 1086$, $k_{eff} = 1053$

Not only an effective model peak turns out to be significantly higher than DHF one, but it is also shifted to the right. This means that besides factors described above, another practical issues can appear. It may happen with high probability that an experimental spectrum is obtained on an imprecisely calibrated spectrometer. This will lead to the shift of all the ionization energies on some constant value, relatively to their theoretical value. These, for instance, happened with both Tungsten and Ruthenium spectra, described in this work. If a theoretical model has proper slopes and a major peak position, then it is not a problem to adjust the fitting with respect to the shift. However, if a theoretical model predicts the position of the major peak wrongly, and smaller peaks are small or overlapped with peaks from other elements, it is not clear, how to determine the shift. Least squares fitting, for example, will put the theoretical peak on top of the experimental one, what will bring error to the whole quantification processes.

9.2 Multi-electron corrections

As it was discussed in previous chapters, we can use full non-orthogonal matrix elements to capture the remaining corrections due to relaxation. We expect these corrections to occur only in relatively shallow "intermediate" shells. This follows from the fact that the deviations from orthogonalized matrix elements only appear at the second order of perturbation theory. Hence, they are of order $\frac{1}{E^2}$, where E is shell electron binding energy, and decrease fast with atomic number. Another theoretical prediction [19] is that these corrections are expected to become a constant factor at sufficiently high ejected electron energies. This constant is equal to $\prod_{i \neq i_{ionized}} \langle \psi_i' | \psi_i \rangle$ (See chapters 7,8). Indeed, calculations for Tungsten, though very long, do not show any difference between one- and multi-electron cross sections except for a constant decrease in amplitude (not plotted here). In contrast, for Ruthenium and Carbon cross sections change in correspondence with predictions. NR-HS: Non relativistic DCS

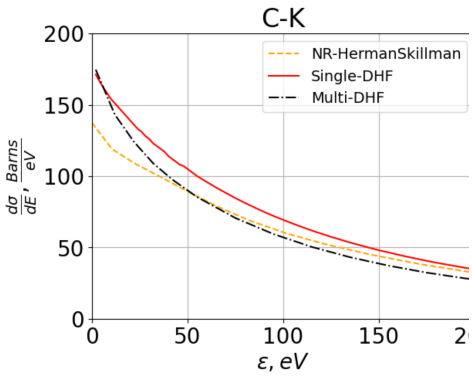

Figure 14: C-K

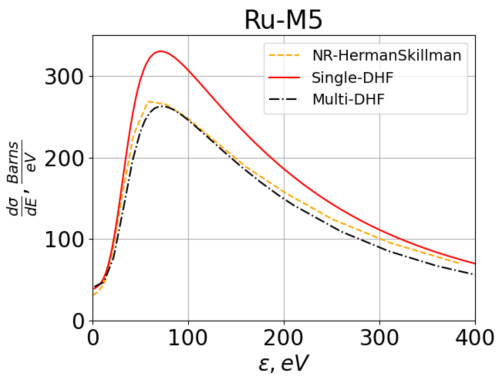

Figure 15: Ti-K

with Herman-Skillman wavefunctions where the electron-electron interaction in the atom is approximated by an effective spherical Fermi potential [17]. Single/Multi-DHF: relativistic DCS for fully relaxed DHF wavefunctions with orthogonalized and non-orthogonal final states respectively.
Beam energy: C-K, - $300keV$ Ru-M_5 - $80keV$, Scattering angle: $0.1rads$

10 Summary and outlook

The calculation of the inelastic electron-atom differential cross section takes into account the relativistic nature of the incoming electrons, the ionization of the atom by the incoming electrons due to their electromagnetic interaction and the many body effects in the atomic structure description. Those effects include the electron-electron Coulobm and exchange interaction and the relaxation of the atom and charge transfer due to the creation of a core hole in an inner shell. The numerical results for challenging cases of ionization of high angular momenta shells show remarkable agreement with the experiment. As a result, the numerical calculation of the cross sections will be continued for all the subshells of all the elements in the periodic table which appear within the typical energy ranges of EELS spectra.

Many body corrections seem to reflect, at least qualitatively, those regions, where the agreement between one-electron cross section is broken. However, not all theoretically predicted corrections are now taken into account. The continuum wave solution is decoupled from the bound atomic electrons during the iterative computation. This means that polarization of the atomic core due to its interaction with an ionized electron is neglected, though it can be significant at low energies. These can significantly influence corrections obtained from multi-electron cross sections or introduce new of the same order. These points require further investigation.

Another type of corrections, that are not included in this work, is corrections, arising while considering full QED cross sections for the scattering process. These are corrections due to exchange of transverse photons, i.e. appearance of transverse degrees of freedom in calculations. Similar type of corrections also occur within the electron-electron interaction in the atom. This is typically included within the Breit-Wigner approximation [14]. This one was also neglected during the computations because it is not major for intermediate elements. It increase calculations by an order of magnitude, while arising corrections play some small role only for very deep atomic shells that are typically experimentally unachievable within this framework.

A Appendix

A.1 Atomic units

All formulas and plots in this work are provided in Hartree atomic units, if not stated the opposite. They are related to SI units as following:

1 mass atomic unit $= m_e$

1 charge atomic unit $= \dfrac{|e|}{\sqrt{4\pi\epsilon_0}}$

1 action atomic unit $= \hbar$

1 energy atomic unit $= 1$ Hartree $= \dfrac{me^4}{(4\pi\epsilon_0\hbar)^2} = 27.2114$ eV

$c = 137.036$ velocity atomic units, where c is speed of light

$\alpha = \dfrac{e^2}{4\pi\epsilon_0\hbar c} = \dfrac{1}{137.036}$

That is, electron mass, elementary charge and Plank constant are taken to be unity.

A.2 Auxiliary relations

Lemma: Dirac Hamiltonian commutes with full momentum $\boldsymbol{J} = \boldsymbol{L} + \boldsymbol{S}$
Proof: It is clear, that the only term in Dirac Hamiltonian, which acts on the same subspace as a momentum operator, is a kinetic term. Let's consider one component of momentum.

$$[J_x, \boldsymbol{\alpha} \cdot \boldsymbol{r}] = \sigma_x[L_x, \frac{x}{r}] + \sigma_y[L_x, \frac{y}{r}] + \sigma_z[L_x, \frac{z}{r}] + \frac{1}{2}\frac{x}{r}[\sigma_x, \sigma_x] + \frac{1}{2}\frac{y}{r}[\sigma_x, \sigma_y] + \frac{1}{2}\frac{z}{r}[\sigma_x, \sigma_z] \tag{A.1}$$

$L_x = yp_z - zp_y$
$[L_x, \frac{y}{r}] = iz, \qquad [L_x, \frac{z}{r}] = -iy, \qquad [L_x, \frac{x}{r}] = 0$

$[\sigma_x, \sigma_x] = 0, \qquad [\sigma_x, \sigma_y] = i2\sigma_z, \qquad [\sigma_x, \sigma_z] = -i2\sigma_y$

Combined, this leads to

$$[J_x, \boldsymbol{\alpha r}] = i\sigma_y z - i\sigma_z y + iy\sigma_z - iz\sigma_y = 0$$

Same holds for two other components.
Lemma:

$$\boldsymbol{\sigma} \cdot \boldsymbol{a} \quad \boldsymbol{\sigma} \cdot \boldsymbol{b} = \boldsymbol{a} \cdot \boldsymbol{b} + i\sigma[\boldsymbol{a}, \boldsymbol{b}] \tag{A.2}$$

Proof:

$$(\sigma_x a_x)(\sigma_x b_x + \sigma_y b_y + \sigma_z b_z) = a_x b_x + i a_x(\sigma_z b_y - \sigma_y b_z) \tag{A.3}$$

Same for two others component. Combined, it results in the desired relation.
Lemma:

$$\boldsymbol{\sigma} \cdot \boldsymbol{p} = -i\boldsymbol{\sigma} \cdot \hat{\boldsymbol{r}} \left(i\hat{\boldsymbol{r}} \cdot \boldsymbol{p} - \frac{\boldsymbol{\sigma}[\boldsymbol{r} \times \boldsymbol{p}]}{r} \right) = -i\boldsymbol{\sigma} \cdot \hat{\boldsymbol{r}} \left(i\hat{\boldsymbol{r}} \cdot \boldsymbol{p} - \frac{\boldsymbol{\sigma} \cdot \boldsymbol{L}}{r} \right) \tag{A.4}$$

Proof: from the previous lemma it follows, that $\boldsymbol{\sigma} \cdot \hat{\boldsymbol{r}} \quad \boldsymbol{\sigma} \cdot \hat{\boldsymbol{r}} = 1$. Then,

$$\boldsymbol{\sigma} \cdot \hat{\boldsymbol{p}} = \boldsymbol{\sigma} \cdot \hat{\boldsymbol{r}} \quad \boldsymbol{\sigma} \cdot \hat{\boldsymbol{r}} \quad \boldsymbol{\sigma} \cdot \hat{\boldsymbol{p}} = -i\boldsymbol{\sigma} \cdot \hat{\boldsymbol{r}}(i\boldsymbol{\sigma} \cdot \hat{\boldsymbol{r}} \quad \boldsymbol{\sigma} \cdot \hat{\boldsymbol{p}}) = -i\boldsymbol{\sigma} \cdot \hat{\boldsymbol{r}} \left(i\hat{\boldsymbol{r}} \cdot \boldsymbol{p} - \frac{\boldsymbol{\sigma} \cdot \boldsymbol{L}}{r} \right) \tag{A.5}$$

Lemma:

$$\boldsymbol{s} \cdot \hat{\boldsymbol{r}} \Omega_{\kappa m} = -\Omega_{-\kappa m} \tag{A.6}$$

Proof: The statement following from the fact that $s \cdot \hat{r}$ commutes with an operator of angular momentum and hence leaves it unchanged. However, $\boldsymbol{s} \cdot \hat{\boldsymbol{r}}$ has a parity -1, which means that value of l should change under the action of such an operator. Then $\boldsymbol{s} \cdot \hat{\boldsymbol{r}} \sim cos\theta \sim Y_{10}$, so the operator does not affect the angular momenta projection. From these conditions it follows $\boldsymbol{s} \cdot \hat{\boldsymbol{r}} \Omega_{\kappa m} = A\Omega_{-\kappa m}$. Finally, $\boldsymbol{s} \cdot \hat{\boldsymbol{r}} \boldsymbol{s} \cdot \hat{\boldsymbol{r}} = 1$. So $a = \pm 1$. Evaluating the expression at $\theta = 0$ gives a value -1.

Lemma:

$$\langle \Omega_{\kappa_i m_i} || C^l || \Omega_{\kappa_j m_j} \rangle = (-1)^{j_i+1/2} \sqrt{[j_i][j_j]} \begin{pmatrix} j_i & j_j & l \\ -1/2 & 1/2 & 0 \end{pmatrix} \prod (l_i + l_j + l) \tag{A.7}$$

Proof: Let's find a value of $\langle l_1 m_1 || C^l || l_2 m_2 \rangle$. Wigner-Eckart's theorem gives

$$\langle l_1 m_1 | C^l_q | l_2 m_2 \rangle = (-1)^{l_1 - m_1} \begin{pmatrix} l_1 & k & l_2 \\ -m1qm_2 & \langle & l \end{pmatrix}_1 m_1 || C^l || l_2 m_2 \rangle \tag{A.8}$$

And we can expand a product of two angular wavefunctions as

$$Y_{kq} Y_{l_2 m_2} = \sum_{lm} A_{lm} Y_{lm} \tag{A.9}$$

Then matrix element is

$$\langle l_1 m_1 | C^l_q | l_2 m_2 \rangle = \sum_{lm} A_{lm} \sqrt{\frac{4\pi}{2l+1}} \int_0^\infty d\Omega Y_{l_1, m_1} Y l, m = A_{l_1 m_1} \sqrt{\frac{4\pi}{2l+1}} \tag{A.10}$$

Which gives, when compared to the former expression,

$$A_{lm} = \sqrt{\frac{2k+1}{4\pi}} (-1)^{l-m} \begin{pmatrix} l & k & l_2 \\ -m & q & m_2 \end{pmatrix} \langle l || C^k || l_2 \rangle \tag{A.11}$$

Using the orthogonality relation

$$\sum_{m_2 q} \begin{pmatrix} l_1 & k & l_2 \\ -m_1 & q & m_2 \end{pmatrix} \sum_{lm} \sqrt{\frac{2k+1}{4\pi}} (-1)^{l-m} \begin{pmatrix} l & k & l_2 \\ -m & q & m_2 \end{pmatrix} \langle l || C^k || l_2 \rangle Y_{lm} = \sqrt{\frac{2k+1}{4\pi}} \frac{(-1)^{l_1 - m_1}}{2l_1 + 1} \langle l_1 || C^k || l_2 \rangle Y_{l_1, m_1} \tag{A.12}$$

Evaluating the expression at $\theta = 0$ and with the help of $Y_{l,0} = \sqrt{\frac{2l+1}{4\pi}}$, we get the following expression for the matrix element

$$\langle l_1 || C^k || l_2 \rangle = (-1)^{l_1} \sqrt{[l_1][l_2]} \begin{pmatrix} l_1 & k & l_2 \\ 0 & 0 & 0 \end{pmatrix} \tag{A.13}$$

From this equation the definition of spherical harmonics, the statement of the lemma follows trivially.

Lemma:

$$\langle \Psi_f | \sum_{i=1}^N f(i) | \Psi_i \rangle = \sqrt{N!} \langle \psi'_1(1) ... \psi'_N(N) | \sum_{i=1}^N f(i) | \Psi_f \rangle \tag{A.14}$$

where $\Psi_i = \{\psi_1(1) ... \psi_N(N)\}$

Proof: Let's give an explicit derivation for two electrons. Normalization factors are omitted for brevity.

$$\langle \psi'_1(1)\psi'_2(2) - \psi'_1(2)\psi'_2(1) | f(1) + f(2) | \psi_1(1)\psi_2(2) - \psi_1(2)\psi_2(1) \rangle =$$

$$\langle\psi_1'(1)\psi_2'(2)|f(1)+f(2)|\psi_1(1)\psi_2(2)-\psi_1(2)\psi_2(1)\rangle-$$
$$\langle\psi_1'(2)\psi_2'(1)|f(1)+f(2)|\psi_1(1)\psi_2(2)-\psi_1(2)\psi_2(1)\rangle$$

Now we can change radial labeling in the second term: $2 \longleftrightarrow 1$ and it becomes

$$\begin{aligned}
&-\langle\psi_1'(2)\psi_2'(1)|f(1)+f(2)|\psi_1(1)\psi_2(2)-\psi_1(2)\psi_2(1)\rangle \\
&=-\langle\psi_1'(1)\psi_2'(2)|f(2)+f(1)|\psi_1(2)\psi_2(1)-\psi_1(1)\psi_2(2)\rangle \\
&=\langle\psi_1'(1)\psi_2'(2)|f(1)+f(2)|\psi_1(1)\psi_2(2)-\psi_1(2)\psi_2(1)\rangle
\end{aligned}$$

So, the second term is equal to the first. In general, this is fair for any permutation, so we can substitute the first term with N! copies of the tensor product of one electron wavefunctions. Restoring the normalization, we obtain the desired result.

Q.E.D

A.3 Confluent Hypergeometric Functions

Confluent hypergeomntric functions [8] are solutions of the confluent hypergeometric equation

$$xy''(x) + (b - x)y'(x) - ay(x) = 0 \tag{A.15}$$

Solutions, regular at origin are called confluent hypergeomentric functions of the first type. They can be expressed through the series

$$F_1(a, b, x) = M(a, b, x) = 1 + \frac{a}{b}\frac{x}{1!} + \frac{a(a+1)}{b(b+1)}\frac{x^2}{2!} + \ldots, \quad b \neq 0, -1, -2, \ldots \tag{A.16}$$

Differentiation gives

$$M'(a, b, x) = \frac{a}{b} + \frac{a(a+1)}{b(b+1)}\frac{x}{1} + ... + \frac{a(a+1)}{b(b+1)} \ldots \frac{a+n-1}{b+n-1}\frac{x^(n-1)}{(n-1)!} = \frac{a}{b}M(a+1, b+1, x) \tag{A.17}$$

Introducing Pochhammer symbols $(a)_n = a(a+1)...(a+n-1)$, we can write

$$M(a, b, x) = \sum_{n=0}^{\infty} \frac{(a)_n}{(c)_n}\frac{x^n}{n!} \tag{A.18}$$

Let's justify the following formula, encountered while solving Dirac equation

$$x\frac{dM(a, b, x)}{dx} + aM(a, b, x) = aM(a+1, b, x) \tag{A.19}$$

Substituting an expression for the derivative, we obtain

$$x\frac{a}{c}\sum_{n=0}^{\infty} \frac{(a+1)_n}{(c+1)_n}\frac{x^n}{n!} + a\sum_{n=0}^{\infty} \frac{(a)_n}{(c)_n}\frac{x^n}{n!} = a\left[1 + \sum_{n=1}^{\infty} \frac{1}{c}\frac{(a+1)_{n-1}}{(c+1)_{n-1}}\frac{x^n}{(n-1)!} + \frac{(a)_n}{(c)_n}\frac{1}{n!}\right] =$$
$$= a\left[1 + \sum_{n=1}^{\infty} \frac{x^n}{n!}\frac{n(a+1)_{n-1} + (a)_n}{(c)_n}\right] = \sum_{n=0}^{\infty} \frac{(a+1)_n}{(c)_n}\frac{x^n}{n!} = M(a+1, b, x) \tag{A.20}$$

A.4 Normalization of Dirac free waves

Asymptotic of the continuum wave function at infinity for the Coulomb field, as can be shown by expansion of positive energy Dirac solutions, have a form

$$\begin{aligned} &P_{E\kappa}(r)\tilde{A}_E sin(k_E r - l\frac{\pi}{2} - \eta_E ln(2k_E r)) \\ &Q_{E\kappa}(r)\tilde{A}_E\sqrt{\frac{E}{E+2m_e c^2}} sin(k_E r - l\frac{\pi}{2} - \eta_E ln(2k_E r)) \end{aligned} \tag{A.21}$$

If the field is Coulomb asymptotically, which must be true for any ionic potential, solutions gain some phase shift d_E due to the deviation of the field from Coulomb near the nucleus.

$$\begin{aligned} &P_{E\kappa}(r)\tilde{A}_E sin(k_E r - l\frac{\pi}{2} - \eta_E ln(2k_E r) + d_E) \\ &Q_{E\kappa}(r)\tilde{A}_E\sqrt{\frac{E}{E+2m_e c^2}} sin(k_E r - l\frac{\pi}{2} - \eta_E ln(2k_E r) + d_E) \end{aligned} \tag{A.22}$$

We want to determine a normalisation of Dirac free waves. The derivation in this appendix follows [22] with some deviations. Writing out radial equations for components

$$\begin{aligned} P'_{E\kappa} + \frac{\kappa}{r}P_{E\kappa} &= \frac{E-V+2c^2}{c}Q_{E\kappa} \\ Q'_{E\kappa} - \frac{\kappa}{r}Q_{E\kappa} &= -\frac{E-V}{c}P_{E\kappa} \end{aligned} \tag{A.23}$$

We can Multiply them with Q'_E and P'_E to obtain

$$\begin{aligned} Q_{E'\kappa}P'_{E\kappa} + \frac{\kappa}{r}Q_{E'\kappa}P_{E\kappa} &= Q_{E'\kappa}\frac{E-V+2c^2}{c}Q_{E'\kappa}Q_{E\kappa} \\ P_{E'\kappa}Q'_{E\kappa} - \frac{\kappa}{r}Q_{E\kappa} &= -P_{E'\kappa}\frac{E-V}{c}P_{E\kappa} \end{aligned}$$

If we subtract from this equations same equations with $E' \longleftrightarrow E$, we arrive to

$$\begin{aligned} &Q_{E'\kappa}P'_{E\kappa} - Q_{E\kappa}P'_{E'\kappa} + \frac{\kappa}{r}(Q_{E'\kappa}P_{E\kappa} - Q_{E\kappa}P_{E'\kappa}) = \frac{E-E'}{c}Q_{E'\kappa}Q_{E\kappa} + Q_{E\kappa}\frac{V}{c}Q_{E'\kappa} - Q_{E'\kappa}\frac{V}{c}Q_{E\kappa} \\ &P_{E'\kappa}Q'_{E\kappa} - P_{E\kappa}Q'_{E'\kappa} - \frac{\kappa}{r}(P_{E'\kappa}Q_{E\kappa} - P_{E\kappa}Q_{E\kappa}) = \frac{E'-E}{c}P_{E'\kappa}P_{E\kappa} + P_{E'\kappa}\frac{V}{c}P_{E\kappa} - P_{E\kappa}\frac{V}{c}P_{E'\kappa} \end{aligned}$$

The potential part vanishes for any local potential, but non necessarily for non-local. In case of exchange potential $\sum_{b\in bound}\int_0^\infty dr' \frac{r_<^l}{r_>^{l+1}}(P_b P_{E'\kappa}(r') + Q_b Q_{E'\kappa})P_{E\kappa}(r)P_b(r)$ is different from $\sum_{b\in bound}\int_0^\infty dr' \frac{r_<^l}{r_>^{l+1}}(P_b P_{E\kappa}(r') + Q_b Q_{E\kappa})P_{E'\kappa}(r)P_b(r)$. In further calculations κ will be omitted everywhere for brevity. Subtracting the second equation from the first and integrating from 0 to R, we obtain

$$\begin{aligned} &\frac{E-E'}{c}\int_0^R [P_E P_{E'} + Q_E Q_{E'}]dr + \sum_b \Bigg[\int_0^R dr(P_E(r)P_b + Q_E Q_b(r))\int_0^\infty dr' \frac{r_<^l}{r_>^{l+1}}(P_{E'}(r')P_b(r') + Q_{E'}Q_b(r')) \\ &- \int_0^R dr(P_{E'}(r)P_b + Q_{E'}Q_b(r))\int_0^\infty dr' \frac{r_<^l}{r_>^{l+1}}(P_E(r')P_b(r') + Q_E Q_b(r'))\Bigg] = Q_E(R)P_{E'}(R) - P_E(R)Q_{E'}(R) \end{aligned} \tag{A.24}$$

We see, that in the limit $R \to \infty$ the second term from the right vanishes even for the exchange potential. Then we are left with

$$\int_0^R [P_E P_{E'} + Q_E Q_{E'}]dr = \frac{c}{E - E'}(Q_E(R)P_{E'}(R) - P_E(R)Q_{E'}(R)) \tag{A.25}$$

In the same limit left hand side becomes just an inner product between ψ_E and $\psi_{E'}$. The right hand side should give us a normalisation but requires some elaboration. We will express P and Q through their asymptotic expansions in the area of big R. This gives

$$\frac{c}{E - E'} A_E A_{E'} \left[\sqrt{\frac{E}{E + 2c^2}} cos\varphi_E sin\varphi_{E'} - \sqrt{\frac{E'}{E' + 2c^2}} cos\varphi'_E sin\varphi_E \right] \tag{A.26}$$

φ_E is the whole phase of the wave as above

$$k_E R - l\frac{\pi}{2} - \eta_E ln(2k_E R) - d_E \tag{A.27}$$

To deal with the whole expression in brackets we use expansion formulas for product of sin and cos

$$sin\alpha cos\beta = \frac{sin(\alpha + \beta) + sin(\alpha - \beta)}{2} \tag{A.28}$$

and arrive to

$$\sqrt{\frac{E}{E + 2c^2}} cos\varphi_E sin\varphi_{E'} - \sqrt{\frac{E'}{E' + 2c^2}} cos\varphi_{E'} sin\varphi_E =$$
$$\frac{1}{2}\left[\sqrt{\frac{E}{E + 2c^2}} (sin(\varphi_E + \varphi_{E'}) + sin(\varphi_{E'} - \varphi_E)) - \sqrt{\frac{E'}{E' + 2c^2}} (sin(\varphi_E + \varphi_{E'}) + sin(\varphi_E - \varphi_{E'})) \right] \tag{A.29}$$

We want our states to be normalized as

$$\int_0^\infty [P_E P_{E'} + Q_E Q_{E'}]dr = \delta(E - E') \tag{A.30}$$

which implies

$$\int_0^\infty dE \int_0^\infty [P_E P_{E'} + Q_E Q_{E'}]dr = 1 \tag{A.31}$$

Due to the presence of the $k_E R$ term in sines, in case of $E \neq E'$ integration of A.29 over energies gives 0 due to infinitely fast oscillations at big R. Exploration of the case $E = E'$ requires a careful limiting procedure due to the presence of $E - E'$ in denominator of the right hand side. In a limit $E \to E'$ we take square roots to be the same and obtain at the first order of expansion in E)

$$\lim_{R \to \infty} \frac{c}{E - E'} \frac{E}{E + 2c^2} sin[(k_E - k_{E'})R - \eta'_E(E' - E)ln(2k'_E R) + \eta_E ln(k_{E'}/k_E) - d'_E(E - E')] \tag{A.32}$$

which can be transformed to

$$\frac{c}{E-E'}\frac{E}{E+2c^2}\frac{c(k_E-k_{E'})}{E-E'}\lim_{R\to\infty}\frac{sin((k-k')(R+\alpha lnR+\beta)}{k-k'} \tag{A.33}$$

The limit evaluates to $\pi\delta(k-k')$ and with some algebra we arrive to the result

$$\int_0^R [P_E P_{E'}+Q_E Q_{E'}]dr = \frac{c}{E-E'}(Q_E(R)P_{E'}(R)-P_E(R)Q_{E'}(R)) = A_E^2\frac{\pi E}{k_E}\delta(E-E') \tag{A.34}$$

Hence normalisation constant must be taken to be

$$A_E = \sqrt{\frac{k_e}{\pi E}} \tag{A.35}$$

A.5 Z+1 approximation

This appendix illustrates the fact, that Z+1 approximation, though may look nonphysical, gives results very close to the actual relaxation, especially for inner shells.

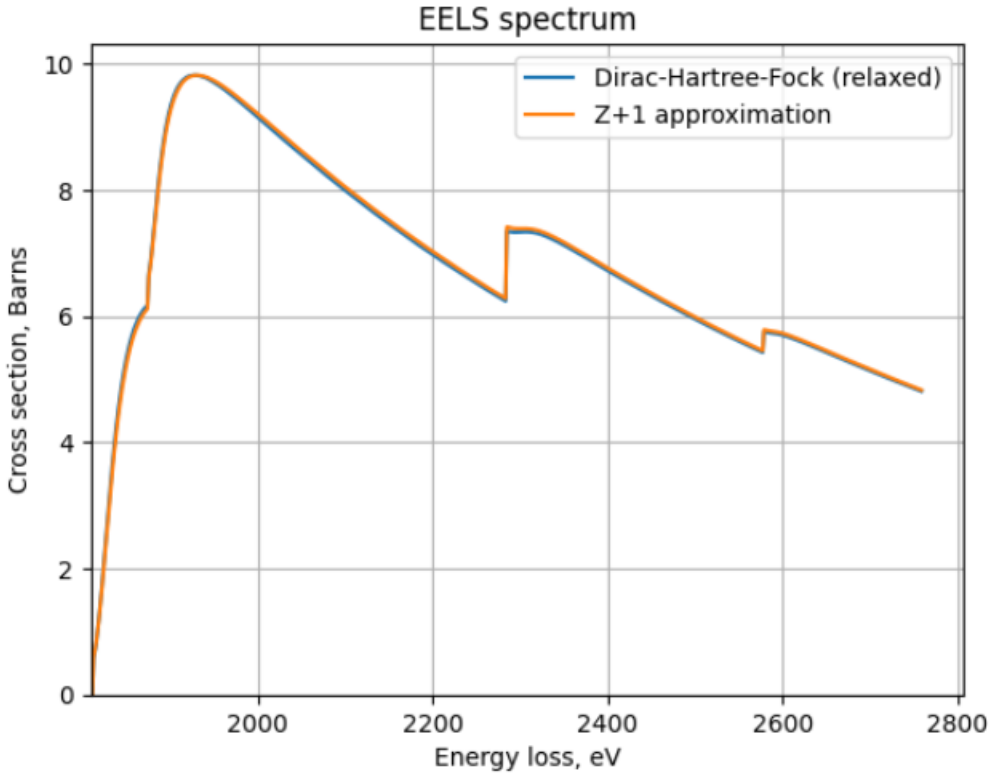

Figure 16: Comparison of DCS obtained within a DHF relaxation picture and a Z + 1 approximation.

A.6 Numerical Dirac-Hartree-Fock solution algorithm

This appendix provides a sketch of an algorithm, used to solve Dirac-Hartree-Fock equations. Details can be found in [14], [3] and [24]. DHF equations have a form

$$(V_{nuc} + c^2 + V_{HF})P_k + c\left(\frac{d}{dr} - \frac{\kappa}{r}\right)Q_k = \epsilon_k P_k \tag{A.36}$$

$$(V_{nuc} - c^2 + V_{HF})Q_k - c\left(\frac{d}{dr} + \frac{\kappa}{r}\right)P_k = \epsilon_k Q_k \tag{A.37}$$

To obtain solutions we should be able to solve the following Sturm-Liouville task

$$\begin{aligned}\frac{dP}{dr} &= [A(r) + \epsilon]P(r) + B(r)Q(r)\\ \frac{dQ}{dr} &= C(r)P(r) + [\epsilon + D(r)]Q(r)\end{aligned} \tag{A.38}$$

They can be integrated numerically starting from boundaries, using, for example, Adams-Moulton multi-point integration formulas. Solutions on the boundaries can be obtained using asymptotic expressions for the potential (and hence coefficients A, B, C, D) and asymptotic expansions for P and Q. Then P can be integrated from zero and infinity, and can always be scaled to match at an intermediate point a_c. However, corresponding Q values at a_c will be different from left and right, except for a particular value of ϵ, which is a eigenvalue of the system. This allows to find ϵ iteratively

$$\epsilon^{(n)} = \epsilon^{(n-1)} + \frac{cP(a_c)(Q_{right} - Q_{left})}{\int_0^\infty (P^2 + Q^2)} \tag{A.39}$$

As soon as we are able to solve A.38, we can find an initial approximation for DHF wavefunctions by substituting V_{HF} with some effective central potential $U(r)$ and rewriting A.36 as

$$\begin{aligned}\frac{d}{dr}Q_k &= \frac{1}{c}\left[\epsilon_k - (U - V_{nuc} - c^2 + \frac{\kappa}{r})\right]\\ \frac{d}{dr}P_k &= \frac{1}{c}\left[-\epsilon_k + (U + V_{nuc} - c^2 - \frac{\kappa}{r})\right]\end{aligned} \tag{A.40}$$

if $U(r)$ is taken to be a direct potential or any other effective potential, that depends on P and Q, than we can solve this system iteratively. We can put to the right side $U(P^{(n-1)}, Q^{(n-1)}$ to solve the equation and obtain $P^{(n)}$ and $Q^{(n)}$, which are used to obtain $U(P^{(n)}, Q^{(n)}$. We repeat the procedure until self-consistency is obtained, i.e. $|P^{(n)}(r) - P^{(n-1)}(r)| < \delta$. In fact, at this moment algorithm solves Hartree-Slater and all other effective potentials, introduced in the Chapter 5.

After we obtained solutions for homogeneous equations A.41, we can begin the Hartree-Fock procedure. We can restore DHF equations in a following form

$$\begin{aligned}\frac{d}{dr}Q_k - \frac{1}{c}\left[\epsilon_k - (U - V_{nuc} - c^2 + \frac{\kappa}{r})\right] &= -(V_{HF} - U)Q_k\\ \frac{d}{dr}P_k - \frac{1}{c}\left[-\epsilon_k + (U + V_{nuc} - c^2 - \frac{\kappa}{r})\right] &= (V_{HF} - U)P_k\end{aligned} \tag{A.41}$$

This system can also be solved iteratively either in the same scheme as before, i.e. maintaining on both sides P^n, or choosing to have $P^{(n)}$ on the left and $P^{(n-1)}$ on the right. The second approach requires an additional subroutine to solve an inhomogeneous equation. However, it is used in practice due to better convergence properties.

Bibliography

[1] A. F. Burr A. Bearden. Reevaluation of x-ray atomic energy levels. *Rev. Mod. Phys.*, pages 125–142, 1967.

[2] M. Ya. Amusia. *Atomic photoeffect*. Plenum Press, New York, 1990.

[3] Per Jonsson Charlotte Froese Fischer, Tomas Brage. *Computational Atomic Structure. An MCHF Approach*. IOP Publishing Ltd, 1997.

[4] Robert D. Cowan. *The theory of atomic structure and spectra*. University of California press, 1981.

[5] C. Barry Carter David B. Williams. *Transmission Electron Microscopy. A Textbook for Materials Science*. Springer Science + Business Media, third edition, 2009.

[6] J. I. Goldstein D.C. Joy, A. D. Roming. *Principles of Analytical Electron Microscopy*. Springer, 1986.

[7] R.F. Egerton. *Electron Energy-Loss Spectroscopy in the Electron microscope*. Springer New York Dordrecht Heidelberg London, third edition, 2011.

[8] Frank E. Harris George B. Arfken, Hans J. Weber. *MATHEMATICAL METHODS FOR PHYSICISTS*. Elsevier inc, 2013.

[9] I.P. Grant. *Relativistic Quantum Theory of Atoms and Molecules*. Springer Science + Business Media, LLC, 2007.

[10] D.R. Hartree. The calculation of atomic structures. *J. Willey, New York*, 1957.

[11] P. Indelicato and E. Lindroth. Relativistic effects, correlation, and qed corrections on $\kappa\alpha$ transitions in medium to very heavy atoms. *Physical Review A*, 46(5):2426–2436, 1992.

[12] John Morrison Ingvar Lindgren. *Atomic Many-Body Theory*. Springer-Verlag Berlin Heidelberg New York, 1986.

[13] Jim Napolitano J.J. Sakurai. *Modern quantum mechanincs*. Cambridge University press, third edition, 2021.

[14] Walter R. Johnson. *Atomic Structure Theory*. Springer Berlin Heidelberg New York, 2007.

[15] W. Kohn and L. J. Sham. Self-consistent equations including exchange and correlation effects. *Phys. Rev.*, 140:A1133–A1138, Nov 1965.

[16] Lifshitz E.M. Landau L. D. *Quantum mechanics. Non-relativistic Theory*, volume 3. Pergamon, third edition, 1991.

[17] R. D. Leapman, P. Rez, and D. F. Mayers. K, L, and M shell generalized oscillator strengths and ionization cross sections for fast electron collisions. *The Journal of Chemical Physics*, 72(2):1232–1243, 07 2008.

[18] Joseph B. Mann and Walter R. Johnson. Breit interaction in multielectron atoms. *Physical Review A*, 4(1):41–51, Jul 1971.

[19] R. L. Martin and D. A. Shirley. Theory of core-level photoemission correlation state spectra. *The Journal of Chemical Physics*, 64(9):3685–3689, 08 2008.

[20] Charlotte E. Moore. *Atomic energy levels*, volume 1-3. National Bureau of Standards, 1949 - 1958.

[21] https://physics.nist.gov/PhysRefData/XrayTrans/Html/search.html.

[22] Francesc Salvat and Jos´e M. Fern´andez-Varea. radial: a fortran subroutine package for the solution of the radial schr¨odinger and dirac wave equations. *Diagonal 645, E-08028 Barcelona, Catalonia*, 2019.

[23] L. Visscher and K.G. Dyall. Dirac–fock atomic electronic structure calculations using different nuclear charge distributions. *Atomic Data and Nuclear Data Tables*, 67(2):207–224, 1997.

[24] S. A. Teukolsky W. H. Press, B. P. Flannery and W. T. Vetterling. *Numreical Recipies: the art of scientific computing*. Cambridge University Press, 1989.

[25] Steven Weinberg. *Lectures on Quantum Mechanics*. Plenum Press, New York, 1990.